JOINT TRANSPORTATION
RESEARCH PROGRAM
INDIANA DEPARTMENT OF TRANSPORTATION
AND PURDUE UNIVERSITY

Field Trials of Rapid-Setting Repair Materials

Prashant V. Ram, Jan Olek, Jitendra Jain

SPR-3019 • Report Number: FHWA/IN/JTRP-2013/02 • DOI: 10.5703/1288284315185

RECOMMENDED CITATION

Ram, P. V., J. Olek, and J. Jain. *Field Trials of Rapid-Setting Repair Materials.* Publication FHWA/IN/JTRP-2013/02. Joint Transportation Research Program, Indiana Department of Transportation and Purdue University, West Lafayette, Indiana, 2013. doi: 10.5703/1288284315185.

AUTHORS

Prashant V. Ram
Graduate Research Assistant
Lyles School of Civil Engineering
Purdue University

Jan Olek, PhD, PE
Professor of Civil Engineering
Lyles School of Civil Engineering
Purdue University
(765) 464-5015
olek@purdue.edu
Corresponding Author

Jitendra Jain, PhD
Postdoctoral Research Assistant
Lyles School of Civil Engineering
Purdue University

JOINT TRANSPORTATION RESEARCH PROGRAM

The Joint Transportation Research Program serves as a vehicle for INDOT collaboration with higher education institutions and industry in Indiana to facilitate innovation that results in continuous improvement in the planning, design, construction, operation, management and economic efficiency of the Indiana transportation infrastructure. https://engineering.purdue.edu/JTRP/index_html

Published reports of the Joint Transportation Research Program are available at: http://docs.lib.purdue.edu/jtrp/

NOTICE

TECHNICAL REPORT STANDARD TITLE PAGE

1. Report No.	2. Government Accession No.	3. Recipient's Catalog No.
FHWA/IN/JTRP-2013/02		

4. Title and Subtitle	5. Report Date
Field Trials of Rapid-Setting Repair Materials	June 2013
	6. Performing Organization Code

7. Author(s)	8. Performing Organization Report No.
Prashant V. Ram, Jan Olek, Jitendra Jain	FHWA/IN/JTRP-2013/02

9. Performing Organization Name and Address	10. Work Unit No.
Joint Transportation Research Program Purdue University 550 Stadium Mall Drive West Lafayette, IN 47907-2051	
	11. Contract or Grant No. SPR-3019

12. Sponsoring Agency Name and Address	13. Type of Report and Period Covered
Indiana Department of Transportation State Office Building 100 North Senate Avenue Indianapolis, IN 46204	Final Report
	14. Sponsoring Agency Code

15. Supplementary Notes

Prepared in cooperation with the Indiana Department of Transportation and Federal Highway Administration.

16. Abstract

The primary objective of the present study was to identify the critical properties (based on the laboratory tests) that could be correlated to the field performance of the rapid setting repair materials.

The first phase of the project involved laboratory evaluation of six commercial rapid-setting repair materials (RMs). When tested in the laboratory, all but two exhibited acceptable rates of strength gain and three RMs displayed relatively poor freeze-thaw resistance. All the RMs exhibited acceptable values for free-shrinkage, high resistance to cracking and good bond to substrate concrete. The resistance to chloride ion penetration of one of the RMs was very poor.

The second phase of the project involved field installation and performance evaluation of the RMs. It was seen that while, in most cases, the controlled laboratory conditions yielded consistent mixes and acceptable performance, the properties of mixes produced on site were more variable. This variability was the result of somewhat uncontrolled changes in the amount of aggregate extension used, moisture content of the aggregates, amount water added and ambient temperature conditions. Follow-up inspection of the repair patches indicated that all the patches except one underwent premature failures (primarily cracking and edge de-bonding). The ambient temperature during the repairs was around 10°C and this led to an extended set-time for all the materials. The 12-hr compressive strengths values of the specimens from the field-mixes were in some cases lower than the 4-hr compressive strength values of laboratory mixes. Since the repairs were open to traffic after approximately 4 hours after placement, the low early age strengths could be a potential reason for premature failures of some of the patches.

In general, several materials were found to be very sensitive to excess water added during mixing resulted in a significant impact on the durability properties – especially the freeze-thaw resistance. In the field, for most of the materials, the consistency of the mixes varied from batch to batch – this can be attributed to the variations in the aggregate extension adopted, mix-water added and also the moisture content of the aggregates used. Construction related issues (consolidation and finishing) also played an important role in the performance of the repair patches.

17. Key Words	18. Distribution Statement
rapid setting repair materials, field performance, mechanical properties, durability, shrinkage, SPR-3019	No restrictions. This document is available to the public through the National Technical Information Service, Springfield, VA 22161.

19. Security Classif. (of this report)	20. Security Classif. (of this page)	21. No. of Pages	22. Price
Unclassified	Unclassified	96	

Form DOT F 1700.7 (8-69)

EXECUTIVE SUMMARY

FIELD TRIALS OF RAPID-SETTING REPAIR MATERIALS

Introduction

Repairs performed under high traffic volumes and aggressive environmental conditions require materials that will cure rapidly while providing adequate strength and durability. The ability to rapidly repair and rehabilitate deteriorated bridge decks and highway pavements minimizes interference with traffic in heavily traveled areas, travel delays, and construction costs. As a result, rapid-setting repair materials are being routinely used in such applications.

The main factors which cause premature failure of repairs include exposure to freezing and thawing cycles, aggressive chemical exposure, mechanical abrasion, loss of bond between existing concrete and repair material, and dimensional stability of the repair material (elastic modulus, shrinkage, expansion, etc.). While some of the problems associated with premature deterioration of repairs are due to structural failures, most of the problems are durability and construction related.

The primary objective of the present study was to identify the critical properties of the rapid-setting repair materials (based on the laboratory tests) that could be correlated to their field performance.

Findings

The first phase of the project involved laboratory evaluation of six commercial rapid-setting repair materials (RMs). When tested in the laboratory, all but two exhibited acceptable rates of strength gain and three RMs displayed relatively poor freeze-thaw resistance. All the RMs exhibited acceptable values of free-shrinkage, high resistance to cracking, and good bond to substrate concrete. The resistance to chloride ion penetration of one of the RMs was very poor.

The second phase of the project involved field installation and performance evaluation of the RMs. It was seen that while, in most cases, the controlled laboratory conditions yielded consistent mixes and acceptable performance, the properties of mixes produced on site were more variable. This variability was the result of somewhat uncontrolled changes in the amount of aggregate extension used, varying moisture content of the aggregates, amount of water added, and ambient temperature conditions. Follow-up inspection of the repair patches indicated that all the patches except one underwent premature failures (primarily cracking and edge de-bonding). The ambient temperature during the repairs was around 10°C. This led to an extended set-time for all the materials. The 12-hour compressive strengths values of the specimens from the field-mixes were, in some cases, lower than the 4-hour compressive strength values of laboratory mixes. Since the repairs were open to traffic approximately 4 hours after placement, the low early age strengths could be a potential reason for premature failures of some of the patches.

In general, several materials were found to be very sensitive to excess water added during mixing, a practice which resulted in lowering their freeze-thaw resistance. For most of the materials installed in the field the consistency of the mixes varied from batch to batch—this can be attributed to the variations in the aggregate extension adopted, mix-water added and also the moisture content of the aggregates used. Construction related issues (consolidation and finishing) also played an important role in determining the field performance of the repair patches.

Implementation

Based upon laboratory and field results, modifications to the current INDOT performance specifications for rapid-setting repair materials have been suggested. In particular, several recommendations for improvements in quality control measures of field-mixes and construction related issues have been proposed. Future research directions involving the evaluation of the robustness of the repair materials with respect to the uncertainties present on site have also been highlighted.

The implementation process should be coordinated by the maintenance personnel to ensure smooth adoption of the proposed changes in the existing specifications and to eliminate poorly performing materials from the list of approved materials. In addition, INDOT should consider conducting a short training course for the personnel responsible for the patching operations to highlight the importance of the proper quality control and field patch installation practices described, respectively, in sections 8.6.1 and 8.6.2 of this report.

The benefits of this research include the following:

- Generation of the laboratory and field performance data for the range of rapid patching materials formulations.
- Development of the proposed performance criteria as potential basis for modification of specifications and the QC/QA procedures.
- Demonstration of differences between lab and field mixtures and identification of underlying causes for these differences.
- Development of recommendations for improvements to field patch installation procedures.

The implementation of findings from this study will help INDOT to reduce the cost of pavement and bridge deck repairs by eliminating materials identified as poor performers and by increasing the overall quality of the installed patches.

CONTENTS

LIST OF TABLES

LIST OF FIGURES

1. INTRODUCTION

1.1 Background

Concrete repair is a complex process, presenting unique challenges that are different from those associated with new concrete construction. The steps involved in concrete repair, which include condition assessment of the existing structure, selection of appropriate repair materials as related to the exposure conditions and implementation are of such magnitude and complexity so as to require a systematic and a novel approach to the problem at hand. The repair system must successfully integrate new materials with the existing concrete to form a durable composite system which is capable of enduring exposure to service loads, environment and time (*1–3*).

Repairs performed under high traffic volumes and aggressive environmental conditions require materials that will cure rapidly while providing adequate strength and durability. The ability to rapidly repair and rehabilitate deteriorated bridge decks and highway pavements minimizes interference with traffic in heavily traveled areas, travel delays, and construction costs and as a result, rapid-setting repair materials have been in great demand.

The main factors which cause premature failure of repairs include exposure to freezing and thawing cycles, aggressive chemical exposure, mechanical abrasion, loss of bond between existing concrete and repair material, and dimensional stability of the repair material (elastic modulus, shrinkage, expansion, etc.). While some of the problems associated with premature deterioration of repairs are due to structural failures, most of the problems are durability and construction related.

1.2 Problem Statement

Rapid-setting repair materials (RMs) are typically used in dowel-bar retrofitting and partial-depth patching of pavements and bridge decks so that the structure can be opened to traffic at the earliest opportunity. Extensive literature review and field investigations studies of RMs indicate that most of repaired patches undergo premature failures (*4*). This research project is an extension of the laboratory studies SPR-2648 (*5*) and SPR-2789 (*6*) where the mechanical and durability characteristics of a few commercially available rapid-setting repair materials have been evaluated. The results and findings of these reports would be used as a tool in identifying the materials that can potentially perform well in the field. An immediate need exists to verify the field performance of these materials.

1.3 Research Objectives and Study Methodology

The primary tasks of this research project included:

1. Selection of repair materials and mixture proportions based upon recently completed research projects (SPR-2648 and SPR-2784) involving commercial rapid-setting repair materials (CRSMs) and review of existing literature.
2. Detailed analysis of mechanical and durability properties of selected repair materials in the laboratory.
3. Field installations of the selected materials and comparison of their laboratory and field performance to identify the critical properties (based on the laboratory tests) that could be correlated to the field performance of the repair materials.
4. Potential revision of INDOT's specification for rapid-setting repair materials and update of INDOT's list of approved rapid-setting materials for patching and repair based upon laboratory and field findings.
5. Development of recommendations for quality control measures for field mixes.

The study methodology is outlined in Figure 1.1. Phase-I of the study involved literature review on the selection process for the repair materials for the current study and evaluation of the mechanical and durability properties of the selected materials. Phase II involved verification of field performance of the selected materials.

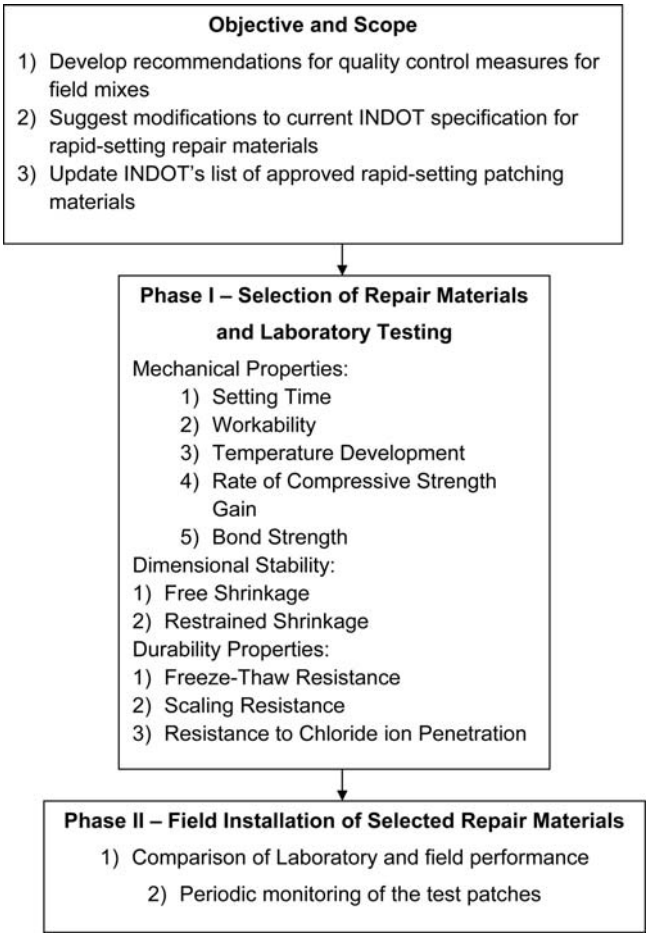

Figure 1.1 Flowchart of study methodology adopted in the study.

1.4 Organization of the Report

This report is divided into eight chapters. Chapter 1 described the problem statement, research objectives and the study methodology adopted.

Chapter 2 presents a review of existing literature on the selection process of a repair material, characteristics of an ideal repair material and the critical material properties to be considered in the selection process of repair materials. The results of the analysis performed on the laboratory test results of SPR-2648 (*5*) and SPR-2789 (*6*) in order to identify the most promising repair materials for the current study are also discussed.

Details and description on the constituent materials, mixture proportions and the laboratory testing protocol are provided in Chapter 3. The test results of Phase I of the study, which involved the laboratory evaluation of mechanical and durability aspects of the RMs are presented in Chapter 4.

The field installation procedures of the repair patches are discussed in Chapter 5. The laboratory testing and experimental results of materials from Grancrete are discussed in Chapter 6 (in preparation for their potential placement during summer 2010 field installations). Chapter 7 describes the laboratory testing of field installations performed during summer of 2010. The overall summary is presented in Chapter 8, which includes conclusions and findings from this research undertaking and suggestions for future research.

Three field inspections were performed for the repair patches (installed during 2007) and discussion of their performances is presented in an Appendix to this report. These were performed after 6 months, and after 2 and 3 winter seasons after initial installation.

2. REVIEW OF LITERATURE

2.1 Introduction

The literature review is divided into two sections. The focus of the first section is on the generic approach to the selection of a repair material, characteristics of an ideal repair material and the critical properties to be considered during the laboratory performance evaluation of rapid-setting repair materials.

The second section presents the results of the data analysis performed on the laboratory test results of SPR-2648 (*5*) and SPR-2789 (*6*), which were the primary sources used for selection of promising materials for further testing and field performance verification covered in this document.

2.2 General Approach to the Selection of a Repair Material

Selection of repair materials is a complex engineering task and requires a systematic and a rational approach. An overview on some important steps to be followed is highlighted in Figure 2.1. First, the condition evaluation of the deteriorated structure must be carried out and the causes for the failure must be ascertained. The next step is to develop the repair strategy, evaluate properties of various repair materials and select a repair material which is most appropriate for the specific repair application. Finally, the repair must be carried out in accordance with the standards and specifications.

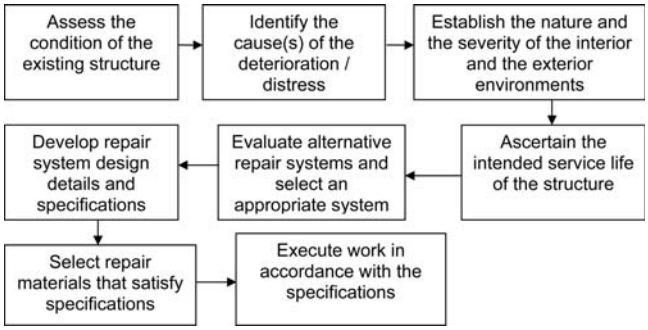

Figure 2.1 Steps to be followed in the selection of a repair material (*3*).

2.3 Characteristics of Suitable Repair Materials

A number of rapid-setting repair materials are available on the market and there are considerable variations in their mechanical properties, durability and the chemical composition. Utmost care must be taken in choosing a repair material for a specific repair application. Before the potential user attempts to select a specific repair material, it is important that he/she identifies the important characteristics of a repair material. Figure 2.2 outlines (broadly) four performance criteria that are required from an ideal repair material.

1. The repair system must be able to meet the structural requirements associated with the load carrying capacity of a given element. In addition, the repair material should have good bond characteristics with the existing concrete, which would enable the repair system to distribute the stresses through the structure.
2. The repair material has to be easy to mix and to place.
3. Another characteristic which would be expected from a rapid-setting material is a fast rate of strength development to minimize the time of closure.
4. The adequate performance of the repair material when subjected to temperature and moisture changes, freeze-thaw cycles and exposure to deicing salts is also required.

One of the greatest factors which govern the performance of a repair material is its compatibility with the existing structure. Table 2.1 provides the summary of the properties required of a patching material for structural compatibility with the existing structure (*8*).

It can be seen from Table 2.1 that the repair material must be at least as strong as the existing concrete to ensure that the composite structure can carry the loads it was originally designed for without causing premature failure of the repair material. It should also be

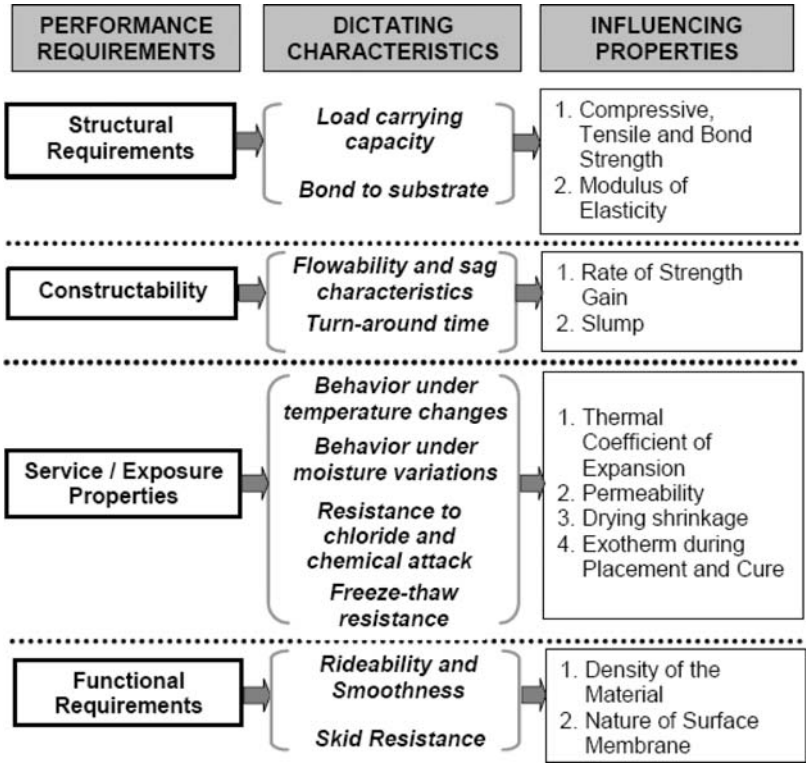

Figure 2.2 Characteristics of an ideal repair material (*7*).

noted that the elastic modulus and the coefficient of thermal expansion of the repair material should be similar to that of the existing concrete to enable proper stress distribution within the structure.

Ideally, a repair material should be able to match the properties of the substrate concrete as such compatibility will ensure close to monolitic behavior of the repaired structure. However, it is highly unlikely that a repair material will perform in exactly the same manner as the existing concrete under different service/exposure conditions. The process of choosing an ideal repair material is a process of compromise and sound engineering judgment is required in selecting the most appropriate material for a specific repair application.

TABLE 2.1
General Requirements of Patch Material for Structural Compatibility (*8*)

Property	Relationship between Repair Material (R) and Substrate Concrete (C)
Strength in compression, tension and flexure	R≥C
Modulus in compression, tension and flexure	R≈C
Coefficient of thermal expansion	R≈C
Adhesion in tension and shear	R≥C
Curing and long-term shrinkage	R≤C
Strain capacity	R≥C
Fatigue performance	R≥C

The following section discusses the critical properties of the repair materials which should be considered while selecting the repair materials.

2.4 Critical Properties to Be Considered in the Repair Material Selection Process

A survey conducted by the Texas state department of highways and public transportation and the departments of transportation of eight other states identified the important characteristics and mechanical properties of rapid-setting repair materials which are to be considered in the selection for patching applications. The listed characteristics included setting time, durability (in general), working time, ease of mixing, placing and finishing, use over a wide temperature range, use in wet weather, cost and similarity to the color of existing concrete. The listed mechanical properties were: bond strength to existing concrete, flexural strength, shrinkage, compressive strength, ductility, wear resistance, coefficient of thermal expansion and modulus of elasticity. It was seen from the rankings that durability and bond strengths ranked among the top characteristics (*9*).

Given the climatic conditions in Indiana, the repair materials will be exposed to a relatively harsh environment of freezing and thawing cycles and de-icing salts. The repair materials should be carefully chosen so that they are dimensionally compatible with the existing substrate and bond well with the existing concrete to form a durable composite system. Sections 2.4.1

through 2.4.5 discuss the most important properties to be considered in the selection of a repair material.

2.4.1 Workability

According to ASTM C 125 (*10*), workability is defined as the property determining the effort required to manipulate a freshly mixed quantity of concrete with minimum loss of homogeneity. Workability is a composite property with two main components:

- Consistency, which describes the ease of flow
- Cohesiveness, which describes the tendency to bleed or segregate

Workability is one of the key properties with respect to field placement. A concrete mixture that cannot be placed easily or compacted fully is not likely to yield the expected strength and durability characteristics (*11*).

Typically, the repair materials used for the partial depth repairs of concrete pavements and bridge decks are not vibrated. It is very important that the repair materials are very workable and are able to flow into the congested areas below the rebars.

2.4.2 Setting Time and Rate of Strength Gain

The main reason for using rapid-setting repair materials is to minimize interference with traffic in heavily traveled areas and travel delays. It is very important that the materials set quickly and gain strength at a rapid rate such that the structure can be re-opened to service in approximately 3 to 6 hours.

2.4.3 Dimensional Compatibility between Repair Material and Substrate Concrete

Dimensional compatibility between the repair material and the substrate concrete is one of the critical factors governing the performance of the repair systems. Dimensional incompatibilities between the repair material and the substrate concrete can result in differential movements which can cause premature cracking in the repair material or de-bonding at the interface because of the inability of the structure to distribute the stresses uniformly. Incompatibilities between repair materials and existing concrete that can affect the durability of the repair include (*12*):

1. Shrinkage of the repair material relative to the concrete substrate
2. Thermal expansion or contraction differences between the repair material and the concrete substrate
3. Differences in stiffness and Poisson's ratio causing unequal load sharing and strains resulting in interface stresses
4. Difference in creep properties of the repair material and the concrete being repaired
5. Relative fatigue performance of the components in the composite repaired structure

A study on the influence of elastic modulus on the stress redistribution and cracking in repair patches on two highway bridges in England was carried out by Mangat and O'Flaherty in 2000 (*12*). Two categories of commercially available repair materials were used: one with elastic modulus less than the concrete substrate and the other with elastic modulus greater than that of the concrete substrate (*12*). In Figure 2.3 through 2.6, the legends 'subs,' 'steel' and 'emb' refer to the strains captured by the strain gages attached to the substrate concrete, steel reinforcement in the repair patch and the repair material respectively.

Figure 2.3 shows the schematic representation of strain distribution with time within a repair patch when the elastic modulus of the repair material (E_{rm}) is greater than that of the substrate concrete (E_{sub}). Three of the tested materials (G2, G3, L1) had their elastic moduli lower than that of the substrate concrete ($E_{rm} < E_{sub}$). The strain time relationships for these three repair systems are shown in Figures 2.4 through 2.6.

In Figure 2.3, zone I refers to the shrinkage transfer stage which occurs between one day after application of the repair and 11 weeks. Materials with $E_{rm} > E_{sub}$ gradually transfer some of their steadily increasing shrinkage strain to the substrate concrete, thereby reducing the shrinkage restraint provided by the substrate which in turn reduces the resulting tension in the repair material. The strains in the steel reinforcement and the repair material at the level of the steel reinforcement also increase linearly in zone 1. Due to the restraint provided by the steel reinforcement and the substrate concrete, the strains are much lower than the free shrinkage of the repair material. The restraint provided by the reinforcement is much greater than the restraint provided by the substrate concrete because the elastic modulus of the steel is much greater than the elastic modulus of the substrate concrete whereas the elastic modulus of the repair material is only marginally greater than that of the substrate concrete. Zone 2 occurring between 11 and 25 weeks is termed as "steady state # 1." In this zone, there is negligible increase in the free shrinkage of the material and hence, there is no strain transfer to the substrate. Zone 3 which occurs between 27 and 47 weeks is the "external load transfer stage" where the externally applied load to the substrate is redistributing to the repair patch. In Zone 4, there is no further redistribution of strains/stresses.

For repair patches with $E_{rm} < E_{sub}$, shown in Figures 2.4 through 2.6, none of strain/stress transfer stages which occur for a repair material with $E_{rm} > E_{sub}$ (shown in Figure 2.3) are present. Hence, Mangat and O'Flaherty (*12*) concluded that materials with elastic modulus lower than substrate concrete ($E_{rm} < E_{sub}$) display no structural interaction and have a higher probability of undergoing a tensile cracking due to restrained shrinkage than repair materials with high stiffness ($E_{rm} > E_{sub}$). According to these authors, the relative stiffness of the repair materials should be the primary design parameter and other parameters, such as strength, are relatively less important (*12*).

Volume change behavior of the repair material is critical to a successful repair. Shrinkage or expansion

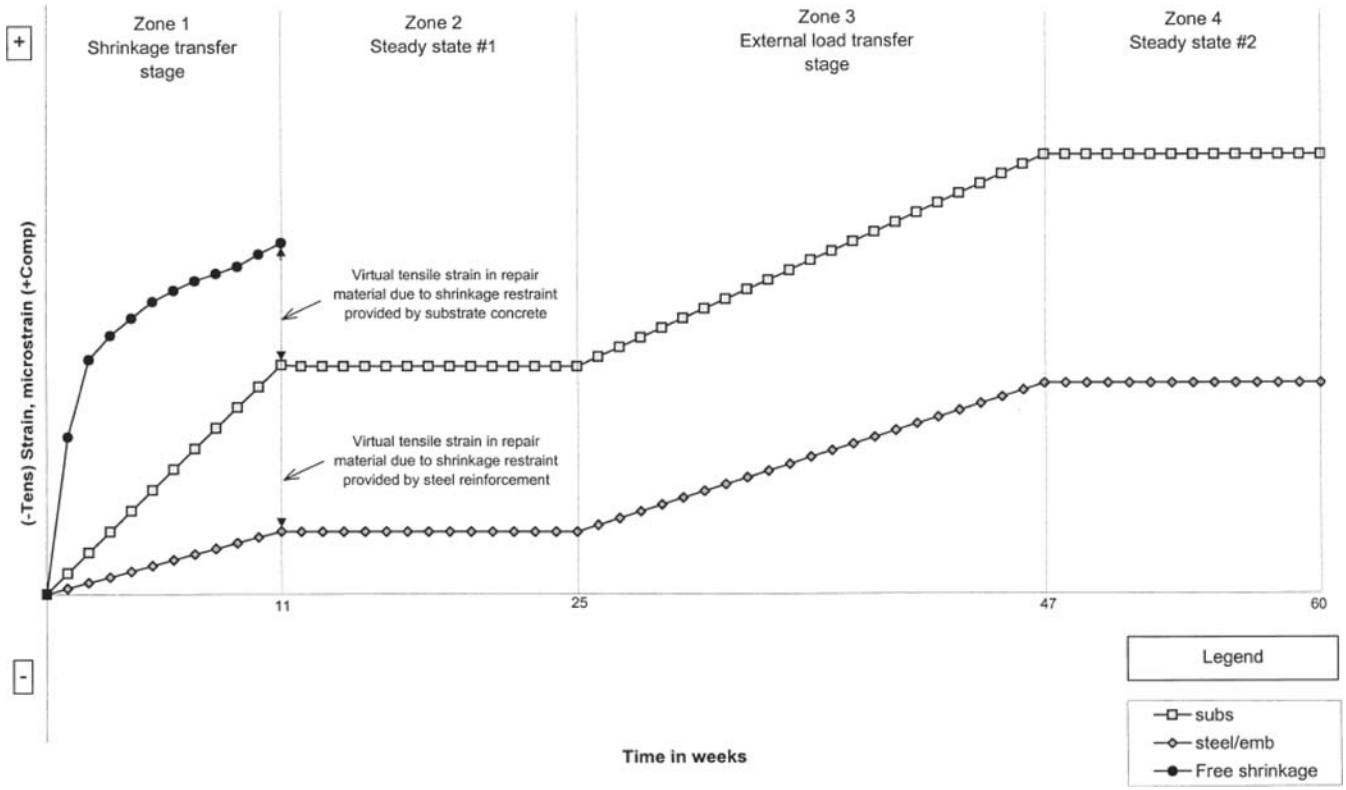

Figure 2.3 Schematic representation of strain distribution with time within a repair patch when $E_{rm}>E_{sub}$ (*12*).

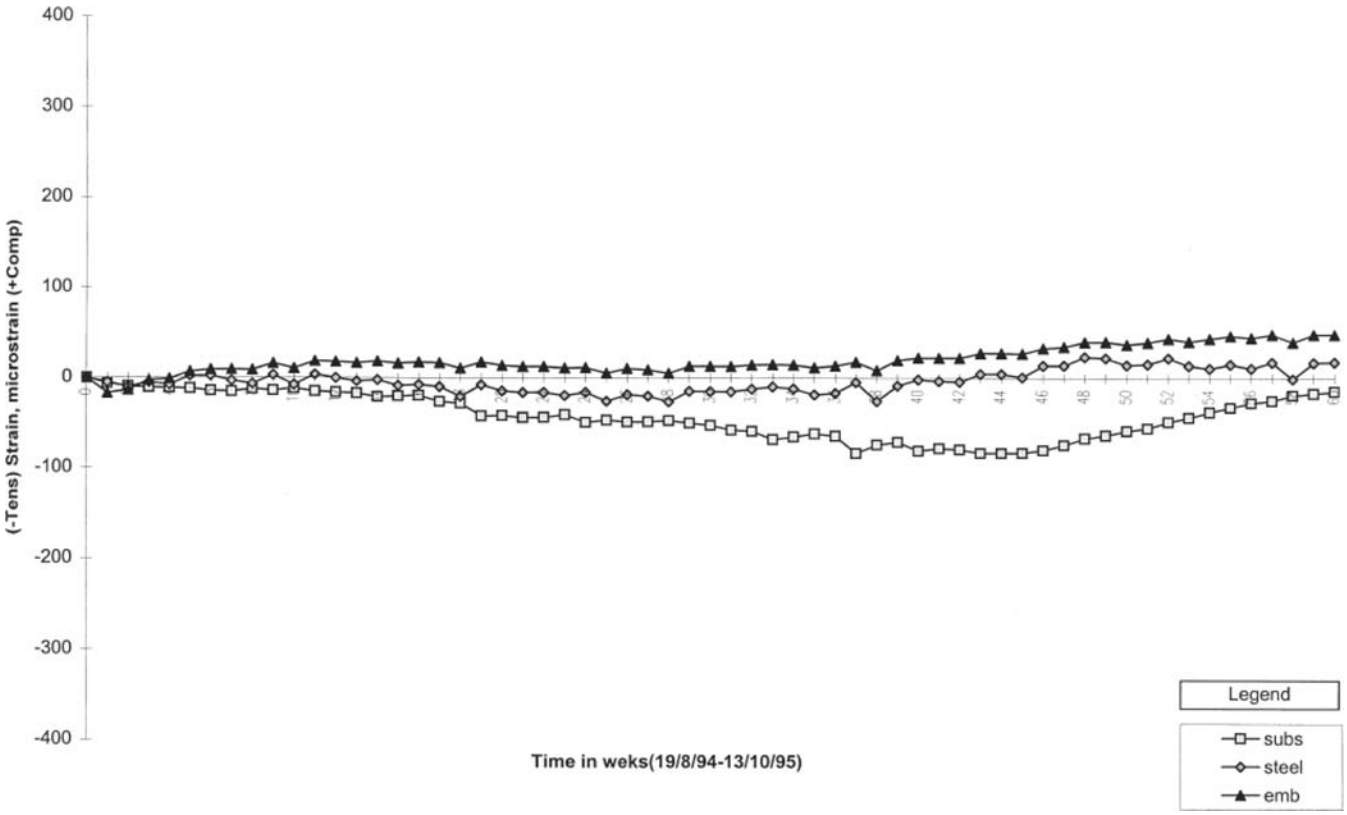

Figure 2.4 Strain-time relationships for repair patch of material G2 (*12*).

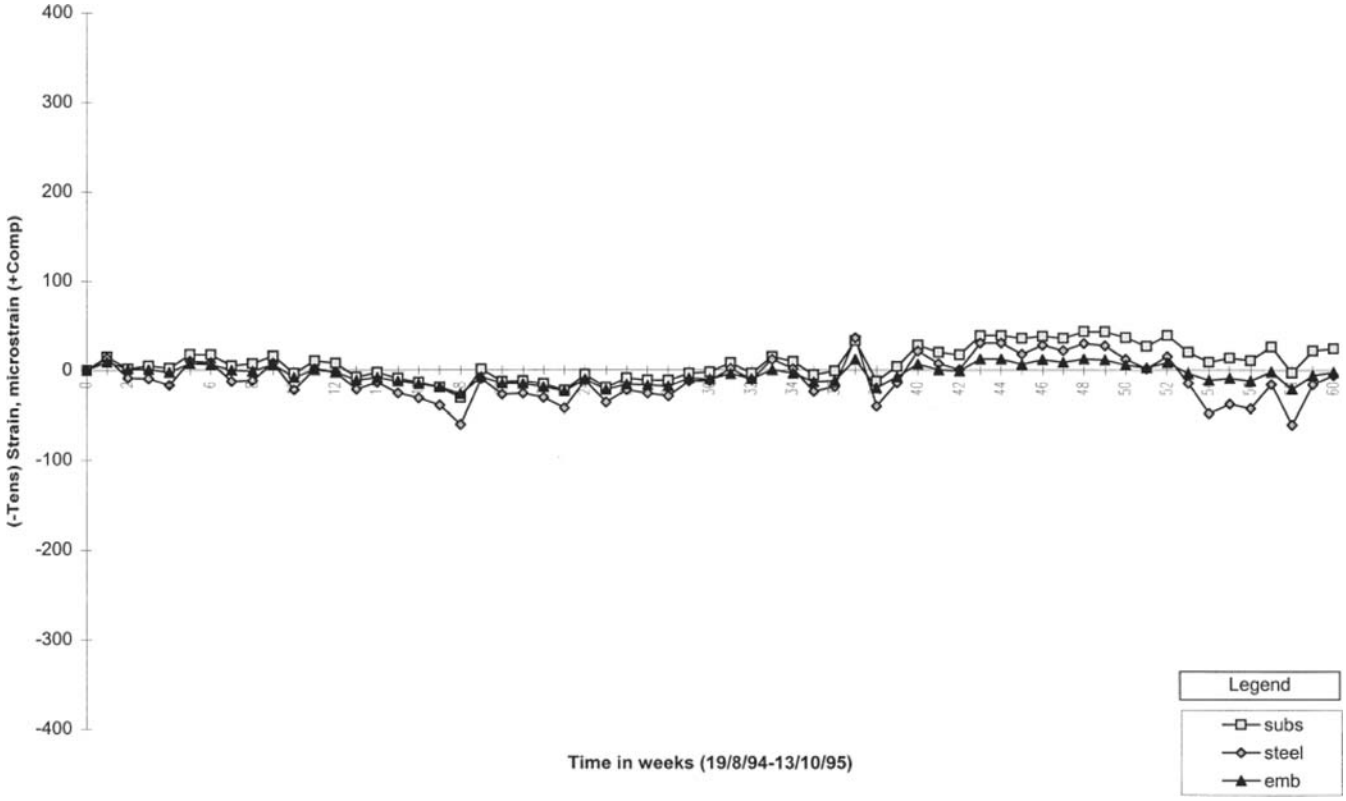

Figure 2.5 Strain-time relationships for repair patch of material G3 (*12*).

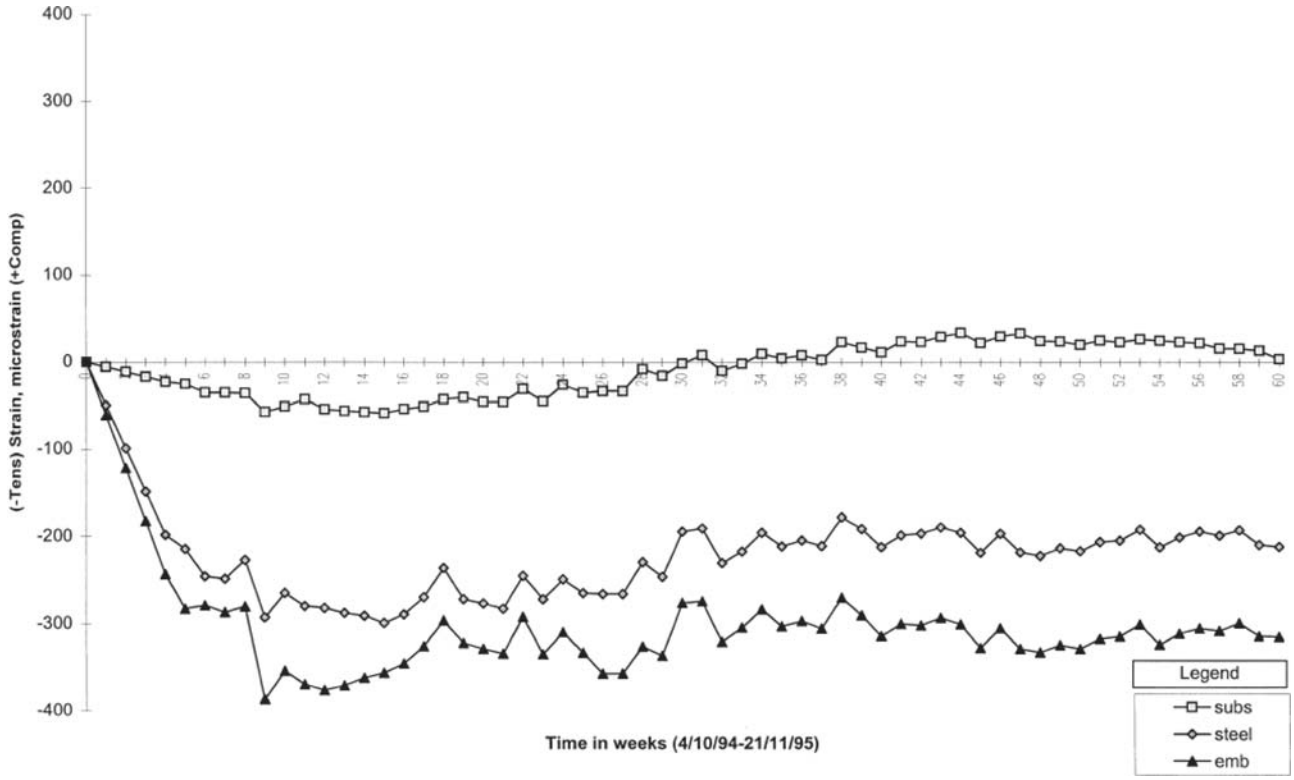

Figure 2.6 Strain-time relationships for repair patch of material L1 (*12*).

may occur as a result of setting or as a result of variations in temperature or moisture conditions. If volume changes of a repair material differ significantly from that of the substrate concrete, loss of bond or cracks may result (*13*).

The repair materials are typically placed over concrete substrate which is substantially aged and therefore does not undergo much of shrinkage. However, as the repair material is drying, it shrinks. As a result of the restraint provided by the substrate at the interface and/or the periphery of an enclosed patch repair, drying shrinkage cannot proceed freely. This results in the development of tensile stress components, which can lead to premature failure of the repaired patch. Free shrinkage measurements are useful to compare different mix proportions, but they do not provide sufficient information to determine if the concrete will crack in service. Shrinkage cracking is a complex process which is a function of many factors such as shrinkage rate and magnitude, material stiffness, extent of stress relaxation and the degree of restraint (*14*).

The primary modes of failure in patch repair due to volume instability (see Figure 2.7) are (*15*):

- Tensile cracking in repair layer
- Delamination of the interface due to peeling and shear stresses

Baluch et al. (*15*) suggest that the 'new generation repair materials' must include a shrinkage compensation action, which may result in a significant initial expansion that might help in reducing the net shrinkage and the magnitude of the restrained stress buildup. Mathematical models to evaluate the risk factors associated with the probability of failure of a patch repair in the three modes discussed have also been developed by these authors.

2.4.4 Bond Strength between Repair Material and the Substrate Concrete

Bond failure is a major cause of deterioration of pavement repairs. Good bond between repair materials and substrate concrete is one of the basic performances required for repair systems. Bond with the substrate concrete is a very important property in concrete pavement repairs, especially when the pavement undergoes freeze-thaw (FT) cycles and is subjected to deicing salts. The prism splitting test was adopted by Li et al. (*16,17*), to study the bond performance of three commonly used rapid-setting repair material with the substrate concrete. The prism splitting test evaluates the bond strength in a state of tension at the interface between the repair material and the substrate concrete. A composite specimen of size 4 x 3 x 16 in. was saw cut into four smaller specimens and the size of the test specimen was 3 x 3 x 4 in, discarding 1 in. at each end before testing. Based upon a finite element analysis, it was observed that there was uniform stress distribution along the bond for smaller specimens as compared to larger ones, so the 3 x 3 x 4 in. specimens were used for the experimental tests. The test setup is shown in Figure 2.8. The test prism is placed in the test machine so that the bond plane is vertical and the two opposing compressive line loadings are applied along the sawed interface.

All the repair materials that were used (A, B and C) were water activated (hydraulic cements/mortars). Along with other proprietary ingredients, material A contained Portland cement, poly-propylene fibers and fine aggregate; material B contained Portland cement and gypsum without any aggregates; and material C contained Portland cement and fine aggregate. The results of their study are summarized in Table 2.2.

The average coefficient of variation (COV) for the splitting tensile strength of the 53 specimens tested was less than 10%. As a result, the splitting prism test was considered to be a good indicator of the tensile bond strength between the repair material and the substrate concrete. It is seen from their results that without FT cycling, the splitting tensile strength increased with age for all the materials tested. It was also seen that specimens which underwent freeze-thaw cycling had lower splitting-tensile strengths when compared to the specimens of the same age which were not subjected to freeze-thaw cycles.

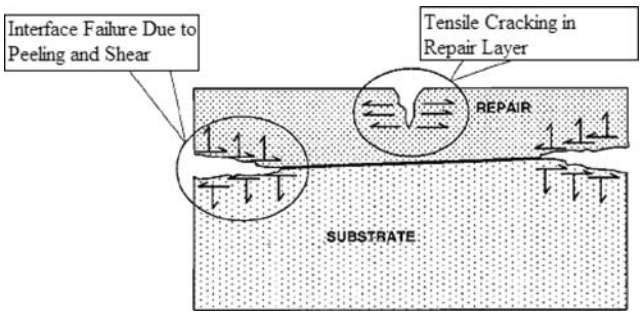

Figure 2.7 Modes of failure in patch repair (*15*).

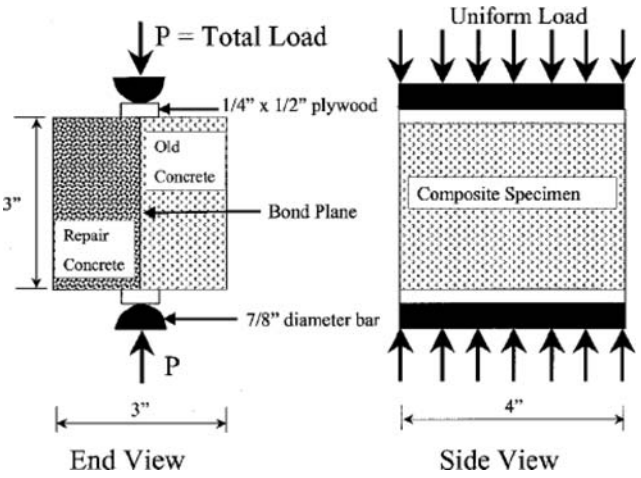

Figure 2.8 Side and end view of the test setup (*16*).

TABLE 2.2
Comparison of Effect of FT Cycles on Bond Strengths (*16*)

Repair Material	Specimen Condition	Splitting Tensile Strength, psi			Surface Scaling with 300 FT Cycles
		Without FT		With 300 FT Cycles	
		7-day	2-month	2-month	
A	Dry old, wet curing	455 (dry)	475 (dry)	465 (dry)	Minimal
B	Wet or damp old, air curing	430 (wet)	550 (wet)	358 (wet), 425 (damp)	Severe
C	Dry or damp old, wet curing	495 (wet)	585 (dry)	455 (dry), 440 (damp)	Severe

NOTE: (dry), (wet), (damp) = initial moisture condition of old concrete.

Momayez et al. (*18,19*) developed a new direct shear test called "the bi-surface shear test." They have also made comparisons between the pull-off test, splitting prism test, slant shear test and the bi-surface shear test for evaluating bond strength between the concrete and repair materials. The test specimens for the different tests studied are shown in Figure 2.9.

According to Momayez et al. (*19*), the most common state of stress encountered in practice is a state of shear at the interface between the concrete substrate and the repair material. In the pull-off and the splitting prism test, there is a state of tension at the interface between the repair material and the substrate concrete while in the slant shear test, the interface is in a state of combined compression and shear stresses. The main advantage of the bi-surface shear test is that the loads are applied symmetrically and that the state of shear stress which is generated along the interface represents the state of stress encountered in most structures, especially pavements and bridge decks. Also, with the bi-surface shear test, the shear strength is measured directly, whereas for the other test methods the shear strength must be calculated from the tensile strength results.

The test matrix used by Momayez et al. (*19*) was composed of six mixtures of repair materials. They tested for seven types of boundary preparations, one of them being a continuous bond composed only of the concrete substrate without any repair material for the purpose of comparison of the test results. Four of the repair materials were sand-cement mortars containing 0, 5, 7 and 10% silica fume. The other two were modified cement-based materials. One of the modified cementitious mortars was prepared by replacing 10% of the cement by a polymer concrete adhesive named K100, while the other was made by replacing 20% of the cement with styrene butadiene resin (SBR). For each of the repair materials, a corresponding mortar bonding agent was applied to the interface. The average thickness of the bonding agent was 3 mm for the cementitious mixes and 1–2 mm. for the polymer-modified mixes. The comparison of the bond strengths obtained from the four test methods for low and high roughness levels of surface preparation are shown in Figure 2.10.

It is seen from Figure 2.10 that the bond strength is greatly dependent on the test method used. The bond tests from slant shear tests were up to eight times higher than those from the pull-off and the splitting prism tests. It is also seen from Figure 2.10 that rough surface preparation leads to a higher bond strength for all the test methods.

The Iowa Shear Test (generally used to evaluate shear bond strengths between asphalt overlays and substrate concrete) is another test method used to determine the shear strength of the bond between new and old concrete. Like in the bi-surface shear test, the interface between the repair material and the concrete substrate in a state of pure shear. The test apparatus consists of a loading jig which can accommodate a 4 in.

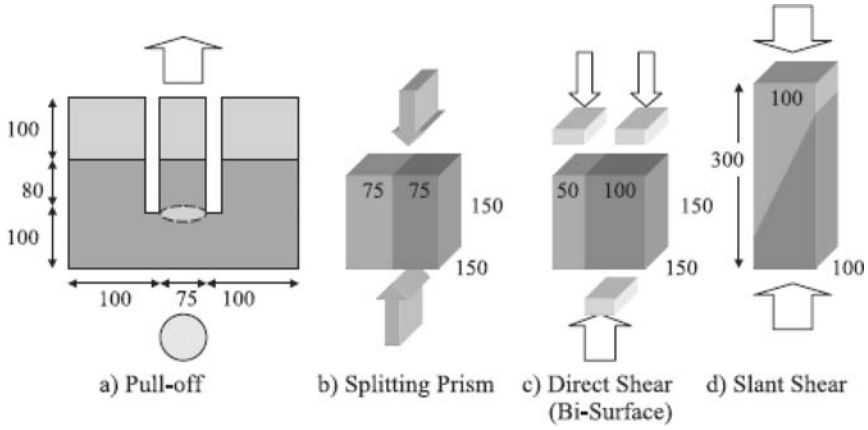

Figure 2.9 Specimens for the bond test methods compared (*19*).

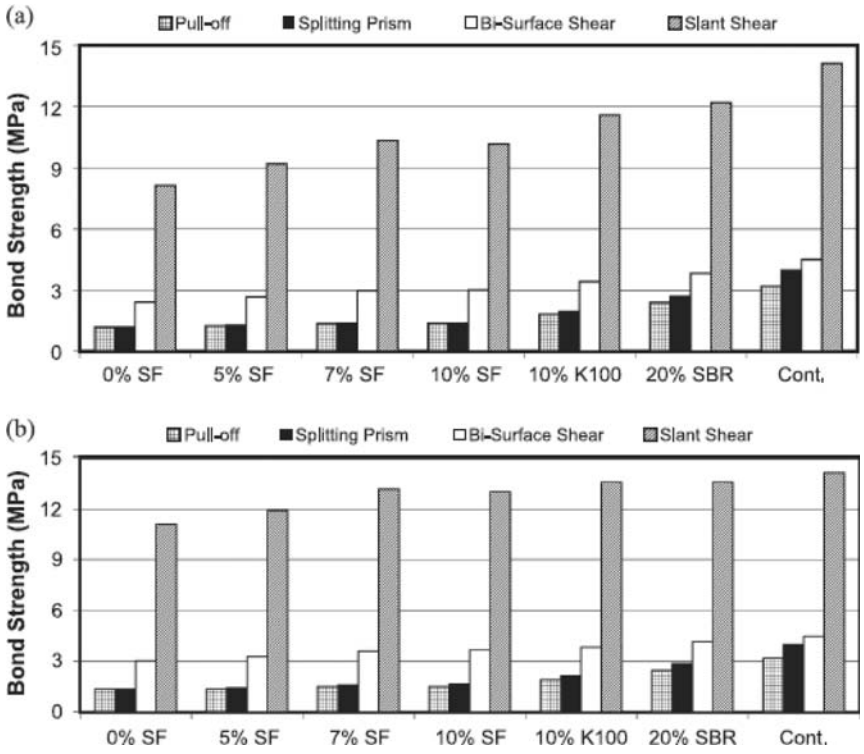

Figure 2.10 Bond strengths by different methods: (a) low roughness (b) high roughness (*19*).

nominal diameter specimen (*20*). The loading is applied using a testing machine capable of applying a smooth and uniform tensile load. Figure 2.11 shows the test setup.

In summary, as already mentioned, the bond strength is one of the most important properties to be considered in the selection processing the repair material. Based upon an extensive review of literature, the shear bond strength between the repair material and the substrate concrete has been identified as the most important bond performance criteria.

Figure 2.11 Test setup for the Iowa shear test.

2.4.5 Freeze-Thaw Durability of Repair Materials

Freeze-thaw cycles and moisture changes have significant impacts on the life and performance of repair patches. In a place like Indiana, where the climatic conditions are relatively harsh and with significant variations in the temperature and moisture conditions, it is important to study the long term durability characteristics of the repair materials in terms of their resistance to freeze-thaw cycles and deicing salts.

A material may exhibit adequate mechanical performance (compressive strength, bond strength etc.), but may display extremely poor durability characteristics. Four commercially available patching materials were studied in SPR-2789 (*6*): SET® 45, Thoroc™ 10-60, American Highway Technology™ Dowel Bar Retrofit Mortar (HDBR) and Five Star® Highway Patch Cement (FSHPC).

Table 2.3 gives details about the air content and spacing factor for the repair materials studied in SPR-2789 (*6*).

TABLE 2.3
Air Content and Spacing Factor for the Repair Materials Studied in SPR-2789 (*6*)

Material	Air Content (%)	Spacing Factor (inch)
SET 45	4.8	0.0221
ThoRoc 10-60	6.2	0.0215
HDBR	3.7	0.0402
FSHPC	1.6	0.1076

From the tests results of SPR-2789 (*6*), it was seen that one of the repair materials, Five Star® Highway Patch Cement, exhibited very good rates of compressive strength gain and good bond-strength but performed extremely poor in the freeze-thaw durability test with the specimens crumbling completely after just 25 cycles of freezing and thawing. This was attributed to the very low air-void content and relatively high air-void spacing factor which is a governing factor in frost resistance of concrete. The good freeze-thaw performance of ThoRoc™10-60 was attributed to the high air content of the fresh material.

2.5 Process of Selection of Repair Materials

Selection of a repair material that is optimal in terms of performance as well as cost is a very difficult task. Hence for this study, the results of the research projects SPR-2648 (*5*) and SPR-2789 (*6*) were adopted as the primary source of information to streamline the selection process.

The different repair materials used in these studies were ranked on the basis of their material properties. Sections 2.5.1 and 2.5.2 summarize the rankings of the materials tested in SPR-2648 (*5*) and SPR-2789 (*6*), respectively. Each material property was relatively ranked on a scale of five, one being the worst and five being the best. Since the two studies performed the experiments under different experimental conditions the ranking scales chosen were different for both of them and are given in detail in Appendices A and B.

The list of the repair materials evaluated in SPR-2648 and SPR-2789 studies, as well as the name of the manufacturer and the specimen labels used in this section, are shown in Table 2.4 and 2.5, respectively.

2.5.1 Ranking of Repair Materials Studied in SPR-2648

In SPR-2648, a total of eleven commercially available repair materials were studied. For the purpose of ranking, the following material properties were taken into consideration:

- Compressive strength at 1, 2, 4, 8, 12, 24 hours, 3 and 7 days
- Flexural strength at 1, 2, 4, 8, 12, 24 hours, 3 and 7 days
- Total shrinkage (autogenous and drying) at 28 days
- Cracking potential at 7 days
- Shear Bond Strength (smooth surface preparation)
- Shear Bond Strength (rough surface preparation)
- Tensile Bond Strength (smooth surface preparation)
- Tensile Bond Strength (rough surface preparation)

The ranking scales adopted for the material properties shown above and the rankings for the materials for each of these properties are presented in this section. The repair materials were relatively ranked in three broad categories:

- Rate of strength gain (compressive and flexural strength)
- Dimensional stability (free and restrained shrinkage)
- Bond strength in shear and tension

The points obtained by each material in each of the categories described above were based on a scale of 100 points. Figure 2.12 shows the ranking for the rate of strength gain. SSRP, FX and DOTP displayed the highest rate of strength gain among all the materials tested.

The rankings for the dimensional stability characteristics are shown in Figure 2.13. It is observed that PPF, EMACO, HPC and THOROC are the worst performing materials with respect to shrinkage characteristics.

From Figure 2.14, it is observed that HPC, FX and PPF are the materials which obtained the highest ranking for the bond strength in tension and shear while SP SET 45 and SET 45 HW obtained the lowest ranking.

2.5.2 Ranking of Repair Materials Studied in SPR-2789

A similar method for ranking of the repair materials as that presented in section 2.5.1 for the SPR-2648 study was adopted here. The following material properties were considered while ranking the materials:

- Workability is terms of spread
- Compressive Strength at 1 or 2, 3 or 4 hours, 1 and 28 days

TABLE 2.4
Repair Materials Used in SPR-2648

Repair Material	Manufacturer	Specimen Label
D.O.T. Patch	Symons Corporation	DOTP
EMACO® T415	ChemRex®	EMACO
FX-928®	Fox Industries, Inc.	FX
High Performance Cement™	US Concrete Products	HPC
POLYPATCH	Symons Corporation	PPF
Rapid Road Repair	QUIKRETE®	QRRR
SET® 45 Regular	ChemRex®	SET 45 R
SET® 45 Hot Weather	ChemRex®	SET 45 HW
Special Patch	Conspec® Marketing and Manufacturing, Inc.	SP
SikaSet® Roadway Patch 2000	Sika Corporation	SSRP
ThoRoc™ 10-60 Rapid Mortar MMortar	ChemRex®	THOROC

TABLE 2.5
Repair Materials Used in SPR-2789

Repair Material	Manufacturer	Specimen Label
SET® 45 Regular	ChemRex®	SET 45 R
SET® 45 Hot Weather	ChemRex®	SET 45 HW
Five Star® Highway Patch Cement	Five Star® Products, Inc.	FSHPC
ThoRoc™ 10-60 Rapid Mortar MMortar	ChemRex®	THOROC

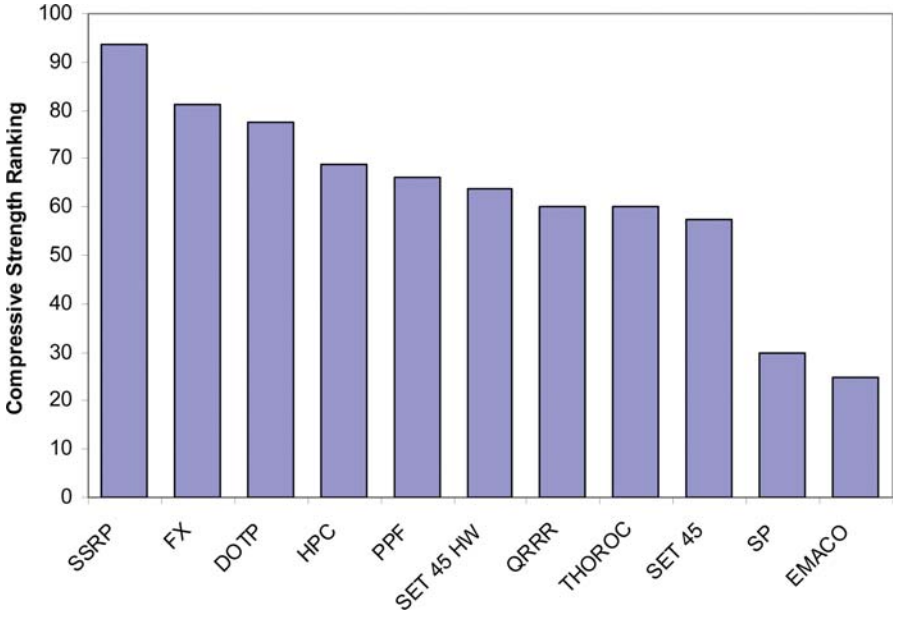

Figure 2.12 Compressive strength ranking.

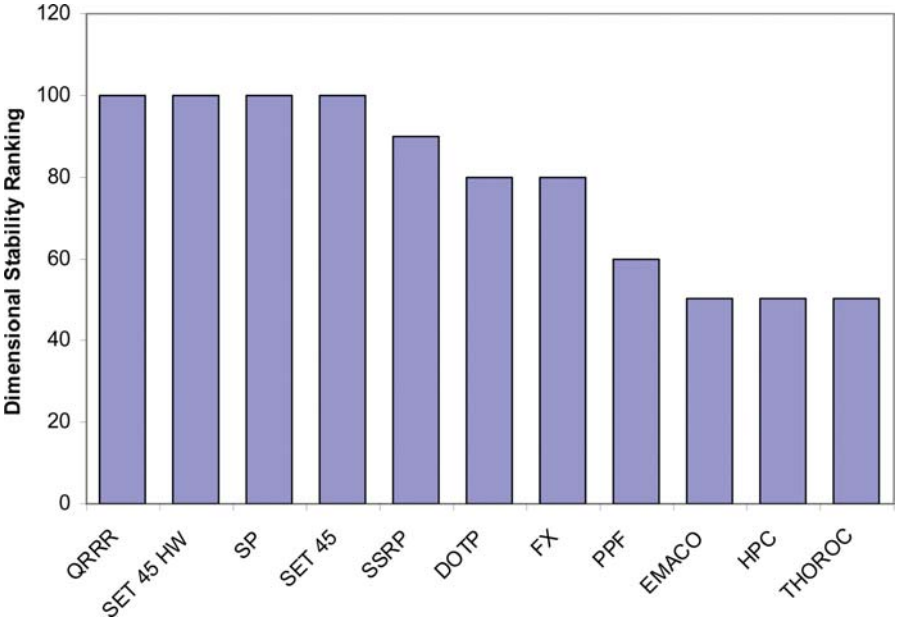

Figure 2.13 Dimensional stability ranking.

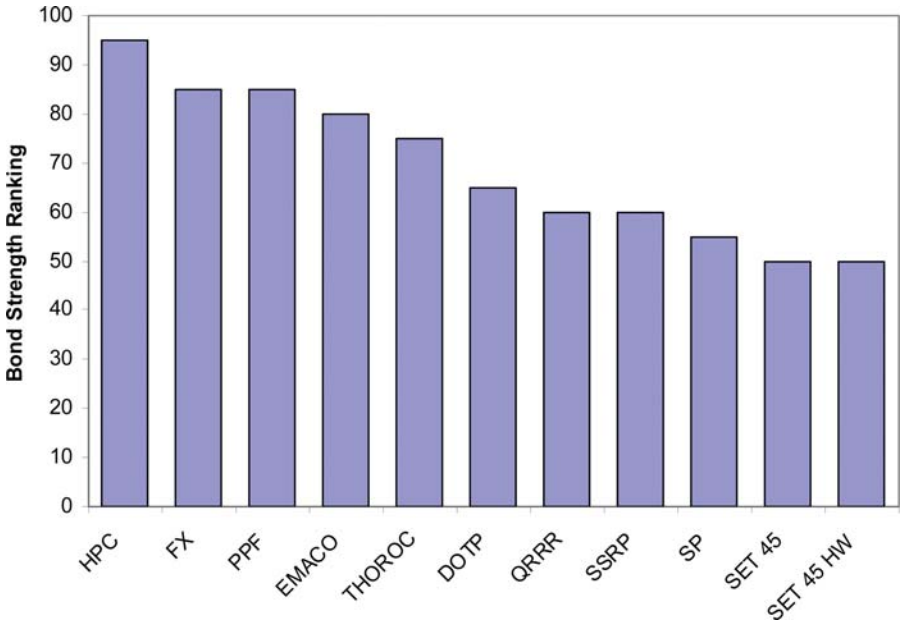

Figure 2.14 Bond strength ranking.

- 28-Day Drying Shrinkage
- Relative Dynamic Modulus after 300 freeze-thaw cycles
- 1- and 7-Day Slant Shear Bond Strength

The material properties were evaluated at three temperature conditions—10, 23 and 40°C. The ranking scales were developed for each of these conditions and are explained in detail in MSCE thesis of P. V. Ram (*21*).

The ranking for the rate of strength gain is shown in Figure 2.15. At 10°C, FSHPC displays the highest rate of strength gain, while at 23 and 40°C, THOROC exhibits the highest rate of strength gain. SET 45 has the lowest rate of strength gain at 23 and 40°C.

Figure 2.16 shows the ranking for the 28-day drying shrinkage. At 10°C, SET 45 had the worst ranking while THOROC and FSHPC displayed lower shrinkage at the same temperature. At 23°C, SET 45 has the highest ranking for the shrinkage and at 40°C; all the materials display comparable shrinkage.

The ranking for the freeze-thaw resistance of the materials is shown in Figure 2.17. THOROC exhibited the best freeze-thaw performance in all temperature conditions and FSHPC displayed the worst freeze-thaw

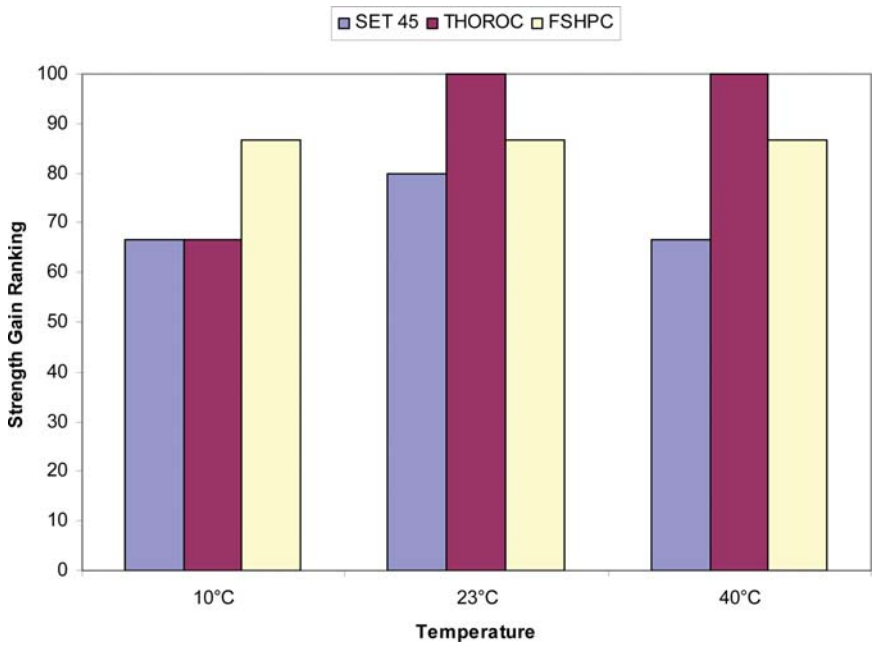

Figure 2.15 Ranking for rate of strength gain (*21*).

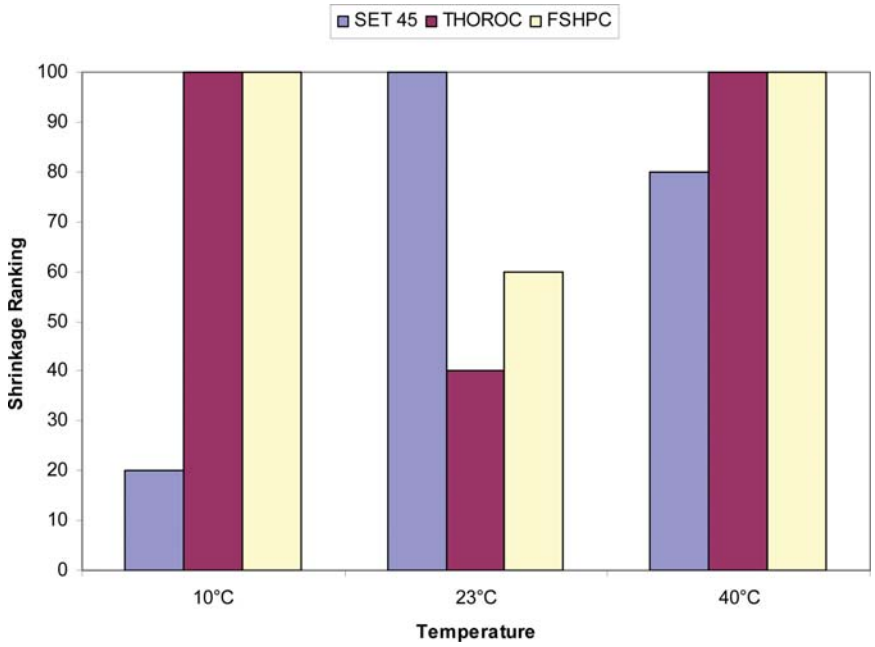

Figure 2.16 28-day free shrinkage ranking (*21*).

performance in all the conditions. The FSHPC freeze-thaw specimens crumbled after just 25 cycles of freezing and thawing and hence, it did not receiving any ranking.

The ranking for the slump/flow characteristics of materials are presented in Figure 2.18. It was observed that THOROC and FSHPC displayed the best performance in all the temperature conditions. SET 45 displayed better flow characteristics at 40°C.

The ranking for the slant-shear bond strength is shown in Figure 2.19. FSHPC displayed the best bond strength in all the temperature conditions. At 10 and 40°C, THOROC displayed slightly better bond strength than SET 45, while at 23°C, THOROC and SET 45 had comparable bond strengths.

2.6 Repair Materials Selected for Current Study

The studies described in Section 2.5 were used to prepare the list of the possible materials for consideration in the present study. These materials are presented in Table 2.6. The materials have been chosen so as to

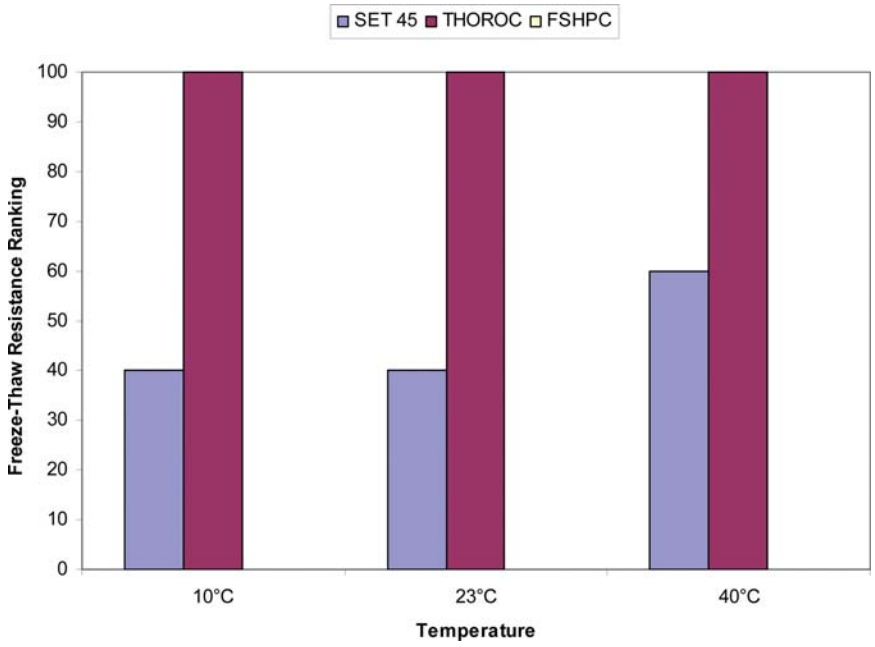

Figure 2.17 Freeze-thaw resistance ranking (*21*).

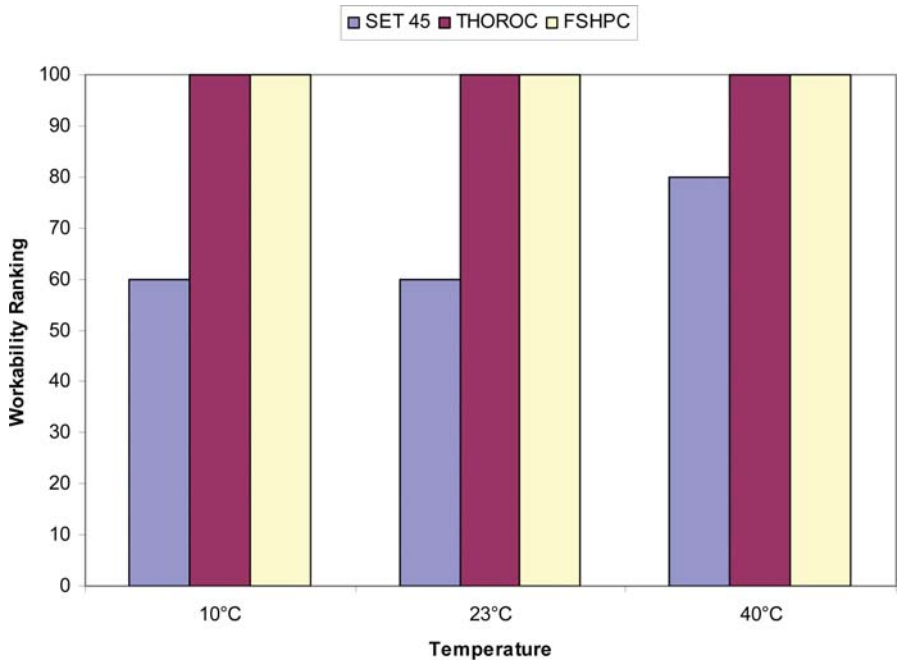

Figure 2.18 Workability ranking (*21*).

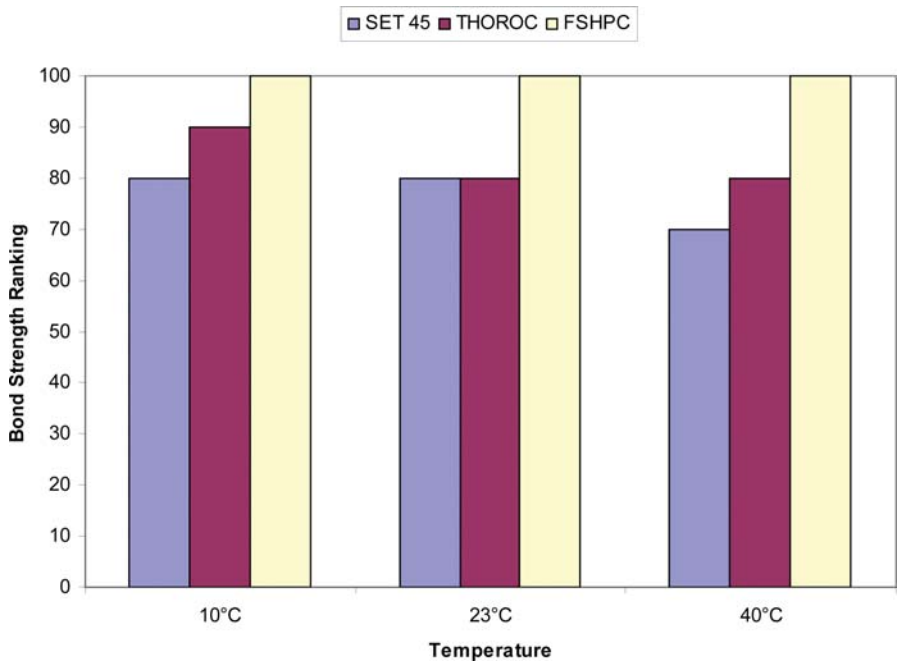

Figure 2.19 Slant-shear bond strength ranking (*21*).

TABLE 2.6
Selected Materials for Current Study

S.No	Material	Specimen Label*	Manufacturer	Type of Material
1.	SikaQuick 2500	SQ	Sika	Cementitious
2.	FX 928	FX	Fox Industries	Cementitious
3.	DOT Patch HD[2]	HD	Symons	Cementitious
4.	SET 45 Regular and SET 45 Hot Weather[3]	Set 45 R and SET 45 HW	Chemrex	Magnesium phosphate
5.	Thoroc 10-603	TR	Chemrex	Alumina cement
6.	Duracal Regular and Duracal Air Entrained	Dur-R and Dur-AE	US Gypsum	Gypsum cement

*Specimen labels used in Chapters 4, 5 and 6.
[1]SikaQuick 2500 has been chosen in place of SSRP since it is being discontinued.
[2]DOT Patch HD has been chosen in place of DOT Patch since it is being discontinued.
[3]On INDOT's list of approved materials.

represent different manufacturers and also the popularity among the DOTs. The rationale for selecting the materials is discussed below:

1. SSRP, FX and DOTP were selected primarily because of their excellent rate of strength gain and good dimensional stability characteristics.
2. SET 45 and SET 45 HW were chosen primarily because of their popularity among the DOTs.
3. THOROC was chosen primarily because of its superior freeze-thaw durability characteristics when compared to the other materials studied in SPR-2789 (*6*).
4. Duracal Regular and the Air-Entrained versions (Duracal-R and Duracal-AE) were chosen primarily because of excellent field performance based upon the input from the Indiana Department of Transportation (INDOT).
5. QRRR, SP and EMACO were not selected because of their low rate of strength gain when compared to the other materials studied in SPR-2648.
6. HPC, PPF and EMACO were not selected because of their low ranking in the dimensional stability category.
7. FSHPC was not selected because of its poor freeze-thaw resistance.

2.7 Summary

In summary, this chapter has presented a review of literature to discuss the critical properties of the repair materials which affect the long-term performance of the repaired systems. Specifically, the bond strength between the repair material and the substrate concrete, dimensional compatibility between the repair material and the substrate concrete, freeze-thaw durability characteristics of the repair material, workability, setting time and rate of strength gain have been discussed. The bond between the repair material and the substrate concrete has been identified as one of the most important properties governing the performance of repair patches. The repair materials need to have a higher modulus of elasticity than the substrate concrete and must show volume stability when exposed to various temperature and moisture conditions. It was also elucidated that the freeze-thaw durability properties are a key issue in the selection of repair materials and that a material may have poor durability characteristics even though it has good mechanical properties. Finally, the data analysis performed on the test results of two recently completed research projects dealing with rapid-setting repair materials has been presented to aid in the selection of the matrix of repair materials for the current study.

3. LABORATORY PROCEDURES

3.1 Introduction

This chapter presents the details of the selected rapid-setting repair materials and their mixture proportions that have been used in this research project. In addition, the adopted test methods to evaluate the fresh and hardened properties of the materials for the laboratory portion of this study are also presented.

3.2 Materials

As discussed in Chapter 2, six commercial rapid-setting repair materials (RMs) were chosen for this study based upon the extensive laboratory investigation carried out earlier at Purdue University and on the review of other literature on the topic (*5,6*). The list of these materials is presented in Table 3.1. Although initially selected for this study (see Table 2.6), SET 45 R and SET 45 HW were removed from the test matrix as the pea-gravel extension available locally was declared by the manufacturer as not suitable for these materials (due to high calcareous content). Figure 3.1 shows the infrared (IR) spectroscopy of the locally available pea gravel tested by BASF. Evidence of high amounts of calcium carbonate in the pea gravel can be observed.

The first four RMs (FX-928, SQ-2500, HD-50 and ThoRoc 10-60) were pre-packaged mortars. The fifth repair material was supplied in two formulations—regular (Duracal-R) and air-entrained (Duracal-AE). Each of these two formulations was supplied in the form of bulk cement, without any pre-mixed aggregate. Repair materials 1 through 3 were Portland cement based materials and ThoRoc 10-60 was an alumina-cement based repair material. Duracal R and AE were

TABLE 3.1
Mixture Proportions of the Repair Materials

Repair Material	Specimen Label[1]	Aggregate Extension (%)[2]		Mix Water (l per 50 lbs of RM)		
		PG[3]	Sand	Actual	Recommended[4]	% Extra
FX-928[5]	FX	60	NA	3.22	3.22	0
SQ-2500[5]	SQ	60	NA	2.70	2.60	3.8
HD-50[5]	HD	60	NA	3.00	3.00	0
ThoRoc 10-60[5]	TR	60	NA	3.07	2.60	18.1
Duracal R[6]	Dur-R	100	100	6.62	5.58	16.5
Duracal AE[6]	Dur-AE	100	100	6.62	5.58	16.5

[1]The specimen labels will be used in Chapters 4, 5, and 6.
[2]% by weight of material.
[3]PG: Pea gravel extension.
[4]Recommended by the material manufacturer.
[5]For 'neat' mixes (material+water) of FX, SQ, HD and TR, the manufacturer recommended mix water was used.
[6]Duracal R and AE 'neat' mixes were prepared using a 100% sand extension by weight. The manufacturer recommended amount of mix water was adopted.

gypsum cement based binders. Table 3.1 also provides information on the mixture composition of all repair materials. The manufacturer data sheets for each of the materials used are included in *Appendix C*.

To study the effect of the locally available pea gravel on the rate of strength gain, the SET 45 R mixtures were prepared using neat as well as the material extended 60% by weight with pea gravel. It was observed that mixtures prepared with the pea gravel extension did not exhibit any strength gain after two hours (Figure 3.2). However the same was not observed in the case of the neat mixtures. Hence, the locally available pea gravel was deemed to be unsuitable for the SET 45 material.

The fine aggregate used to prepare the repair mixtures was natural sand with absorption of 1.85% and a specific gravity of 2.63 while the coarse aggregate used was locally available pea gravel with maximum diameter of 9.5 mm with absorption of 2.36% and a specific gravity of 2.64. Figure 3.3 shows the gradation curves for both the sand and pea gravel used.

3.3 Mixer and Mixing Sequence

A small capacity (1 ft^3) portable mortar mixer (Figure 3.4) was used to carry out the mixing operations in the laboratory. These types of mixers are typically used on small repair jobs.

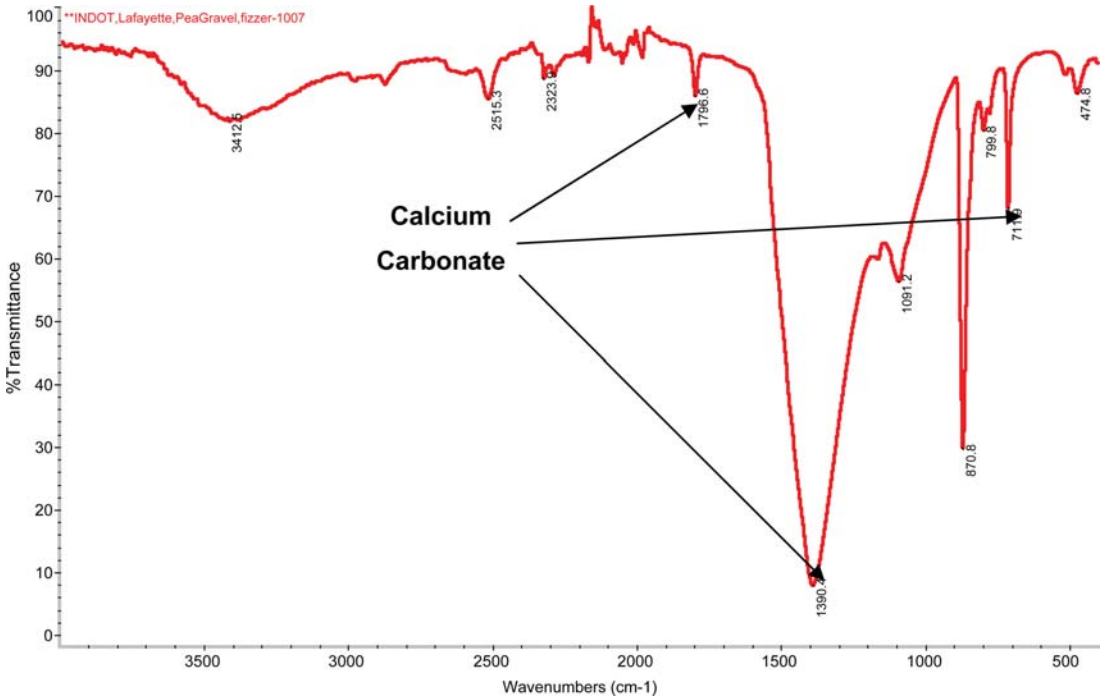

Figure 3.1 IR Spectroscopy of locally available pea gravel. (Courtesy: BASF.)

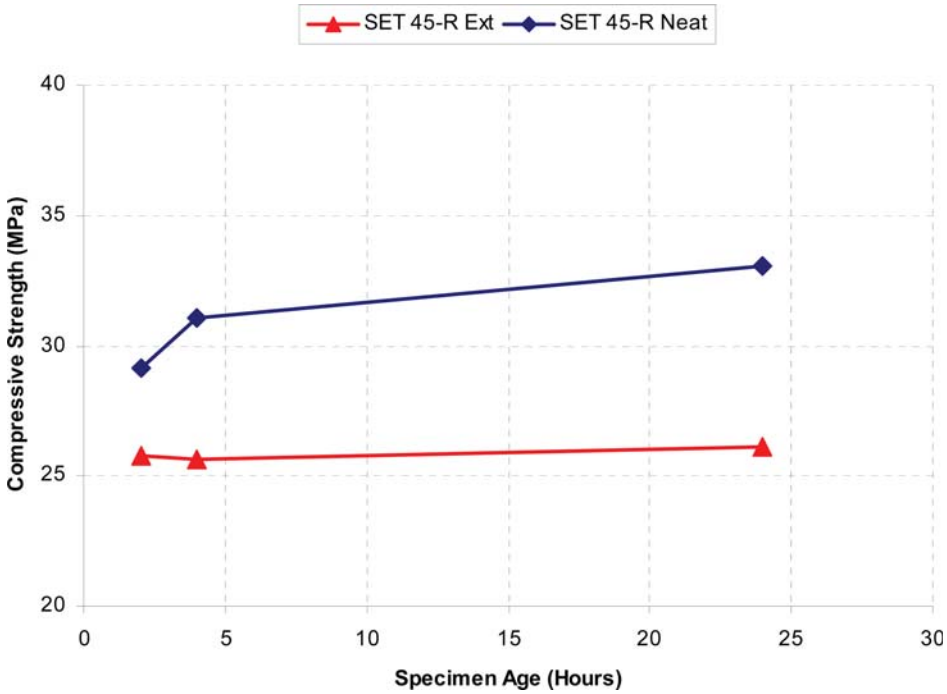

Figure 3.2 SET 45 R : Compressive strength—neat vs. extended mixtures.

The mixing sequence adopted is shown in Figure 3.5.

3.4 Test Procedures

All laboratory concretes were prepared, cured and tested at constant temperature of $23 \pm 2^{\circ}C$. Based upon the review of literature, the following properties were identified as being critical to ensure adequate performance in the field and are presented in Table 3.2. The properties listed in Table 3.2 are discussed in the following sections (3.4.1 through 3.4.10).

3.4.1 Setting Time

The setting time was measured using the Gillmore Needles apparatus in accordance with ASTM C 266 (*22*). The experiment was performed using neat (mortar) specimens. Even though this test method is

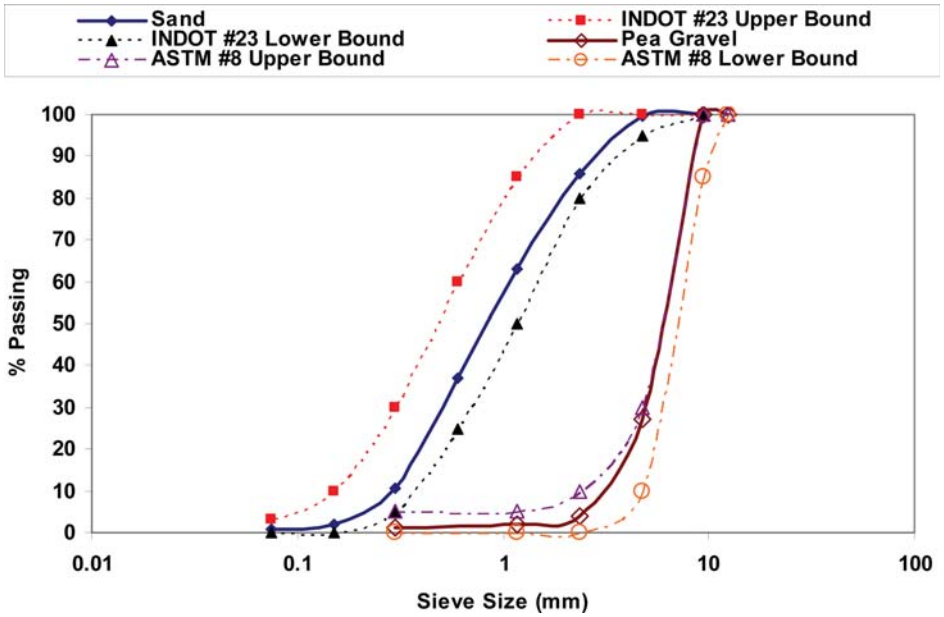

Figure 3.3 Gradation curve of aggregates.

Figure 3.4 Mortar mixer.

generally used for paste specimens, this method was adopted as it is the most widely used test method to determine the setting time of rapid-setting materials.

3.4.2 Temperature Development

The temperature signature data were collected using Type-T (Copper-Constantan) thermocouples placed in 3×6 inch cylinders. The specimens were placed in a controlled laboratory environment of $23 \pm 2^{\circ}C$ in sealed plastic cylinders. The data was collected every 15 seconds using a CR10-X data-logger system. The measurements were continued until the specimens attained equilibrium with the laboratory temperature.

3.4.3 Workability

The workability of the repair concrete was measured in terms of slump or spread depending upon the "wetness" and the consistency of the mixtures. The test was performed according to a modified ASTM C 143 test method (*23*) where the material was not rodded.

3.4.4 Compressive Strength

The compressive strength of the neat (mortar) and the extended mixtures (with pea gravel) was tested using 3x6 inch cylinders at the ages of 2, 4, 24 hours and 28 days. The specimens were cast in three layers and consolidated using the vibration table. The specimens tested at the age of 2 hours were de-molded right before testing. The other specimens were de-molded 2 hours after addition of water and were moist-cured at 23°C and 100% relative humidity (RH) until tested. The test was performed according to ASTM C 39 (*24*). The compressive strength specimens cast in the field were de-molded and tested after 12 hours (this was the only strength data collected).

3.4.5 Bond Strength

The bond strength was evaluated at the age of 1 and 7 days. The bond strength specimens were moist-cured up to the time of testing. In addition to the slant-shear test (ASTM C 882 method) (*25*), the bond strength was also evaluated using a non-standard Iowa shear test (Iowa DOT Test Method 406-C-2000) (*20*) which is typically used to test the shear bond strength between asphalt and Portland cement concrete.

For the slant-shear test, the repair material (extended) was installed on a saturated surface-dry substrate mortar which was prepared according to the modified ASTM C 109 (*26*) (natural sand was used instead of standard Ottawa sand). The substrate specimens were moist cured for 28 days before the repair material was bonded to it. For the Iowa shear test, the substrate specimens (4 x 4 inch cylinders) were saw cut from 4×8 inch cylinders which were prepared using INDOT QC/QA specification concrete used in the construction of bridge decks in Indiana. The specimens were moist cured for 28 days before the repair material was bonded to it. Further details on the test method and the specimens used are available in section 4.3.2.

In addition, the effect of the environmental exposure on the bond-strength was also evaluated. These specimens were moist cured for 7 days and then exposed to the natural environment for 60 days (Dec. 6, 2007–Feb. 5, 2008). The variation of the exposure temperature is shown in Figure 3.6.

3.4.6 Free Shrinkage

The free shrinkage test (Figure 3.7) was performed according to ASTM C 157 (*27*) on both neat and extended mixtures. The dimensions of the specimens used were $3 \times 3 \times 11$ inch prisms. The specimens were cast

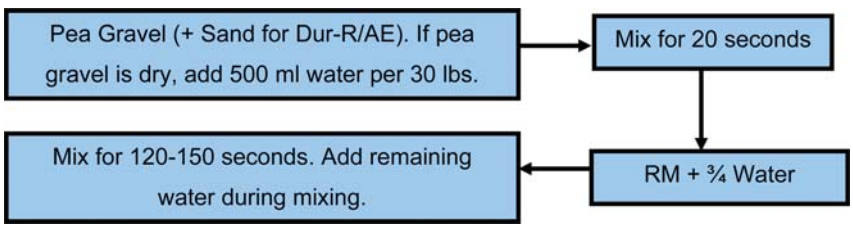

Figure 3.5 Mixing sequence.

TABLE 3.2
Laboratory Testing Procedures

Test	Specification	Neat Material	Extended Material
Setting time	ASTM C 266	X	
Slump test	ASTM C 143		X
Free shrinkage	ASTM C 157	X	X
Restrained shrinkage	ASTM C 1531		X
Compressive strength of cylindrical concrete specimens	ASTM C 39	X	X
Bond strength by slant shear	ASTM C 882		X
Iowa shear test	Iowa DOT, Section 4.7		X
Freeze-thaw durability	ASTM C 666		X
Scaling resistance to deicing chemicals after 25 cycles of freezing and thawing	ASTM C 672		X
Rapid chloride permeability	ASTM C 1202		X

in two layers and consolidation was carried out using the vibration table. The specimens were de-molded 1¾ hours after the addition of mix water and the initial length measurement was performed at the age of 2 hours. After the initial measurement was performed, the specimens were immediately placed in a controlled environment of 23 ± 2°C and 50% RH. The subsequent length measurements were carried out at the ages of 1, 2, 4, 7 and 28 days.

3.4.7 Restrained Shrinkage

The restrained shrinkage test was performed in accordance with AASHTO PP 34 (*28*). The strain measurements were commenced within 15 minutes after addition of mix water. The specimens were de-molded 2 hours after the addition of mix water and the top surface was sealed using aluminum foil. The data was collected at intervals of 30 minutes using a data-logger. The measurements were continued for up to 35 days. The test setup for the restrained shrinkage test is shown in Figure 3.8.

3.4.8 Freeze-Thaw Resistance

The resistance to freeze-thaw cycles was evaluated according to ASTM C 666—Procedure A (freezing and thawing in water) (*27*). The dimensions of the specimens were 3 × 4 × 16 inch prisms. The specimens cast in the laboratory were de-molded 2 hours after addition of mix water and were moist-cured at 23 ± 2°C and 100% RH for 14 days before the commencement of the test.

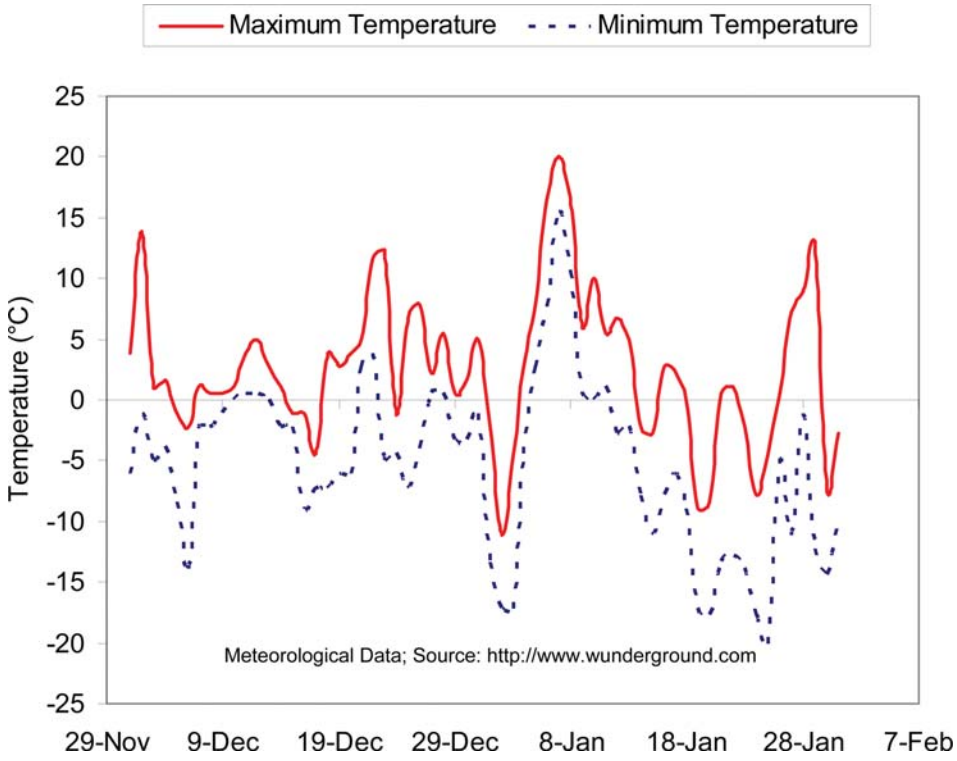

Figure 3.6 Ambient Temperature History for Bond Durability Test.

Figure 3.7 Free shrinkage measurements.

The freeze-thaw specimens cast in the field were de-molded 12 hours after addition of water and were exposed to the natural environment (stored in conditions similar to the repair site) for 12 days. The specimens were then brought to the laboratory environment and immersed in lime water at room temperature 48 hours before the test. The test for the field specimens was also commenced 14 days after they were cast. A view of the freeze-thaw chamber used for the test is shown in Figure 3.9.

Figure 3.8 Restrained shrinkage test.

Figure 3.9 Free-thaw chamber.

3.4.9 Scaling Resistance

The surface scaling resistance test was performed according to ASTM C 672 (*30*) by exposing the test specimens to 25 cycles of freezing and thawing in the presence of de-icing salts. The depth of the specimens was 3 inches and their top finished area (72 sq. inches) was exposed to the deicer solution. The deicer used was a calcium chloride solution with a concentration of 4 grams of anhydrous calcium chloride per 100 ml of solution. The specimens were moist-cured for 14 days and then dried at $23 \pm 2^{\circ}C$ and 50% RH for 14 days before the commencement of the test.

3.4.10 Resistance to Chloride-Ion Penetration

The resistance to chloride ion penetration was evaluated according to ASTM C 1202 (*30*). The specimens were 2 in. thick slices of 4 in. diameter cylinders. The slices were collected from the top and bottom halves of the cylinder. Figure 3.10 shows a cross section of the 4×8 inch cylinder from where the slices were collected for testing. The specimens were moist-cured for 28 days before the test was performed. Figure 3.11 shows a setup for the rapid chloride permeability (RCP) test.

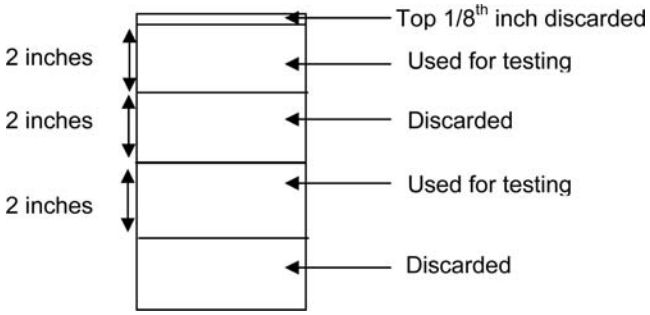

Figure 3.10 RCP specimen detail.

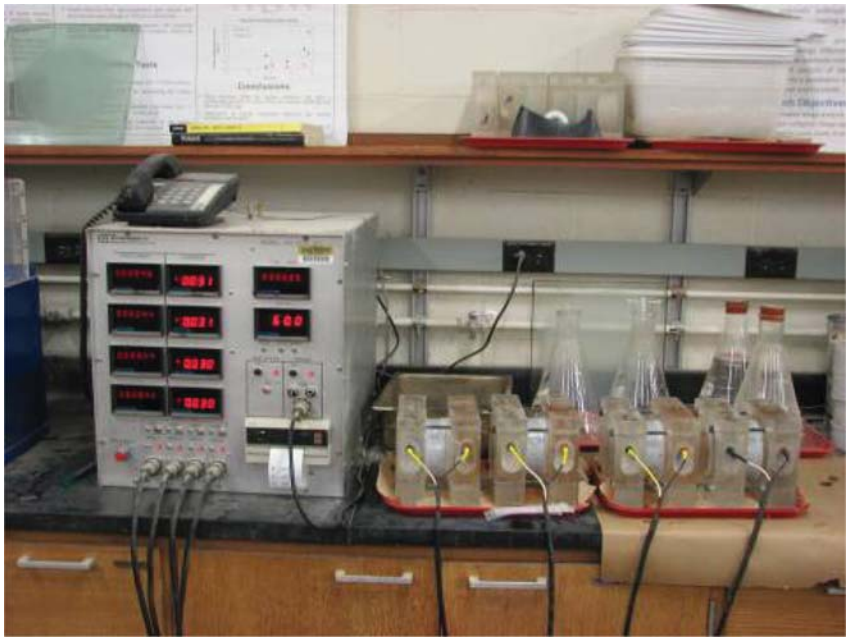

Figure 3.11 RCP test setup.

3.4.11 Monitoring of Performance of Mock-up Repair Patches

To get an insight on the effects of environmental conditions on the performance of repair concrete, mock-up pavement slabs with repair patches were cast in the laboratory. Ready-mix (INDOT QC/QA specification) concrete was used to prepare the slabs. The dimensions of the slabs were 48×24 inches with a depth of 12 inches. The dimension of the repair patches were 24×12 inches with a depth of 5 inches. The repair patches were instrumented with embedment strain gages (EGP-series strain gages from Vishay Micro-Measurements) to capture the strain-time response of the repair material. The strain gages were located at the geometric center of the patches. Thermocouples located close to the top surface of the slabs were used to monitor the ambient temperature around the slabs. Figure 3.12 shows the top view of the instrumented slab. A data-logger was hooked up to measure the strain and temperature continuously at half hour intervals.

Figure 3.13 shows a view of the setup of the mock-ups. A close-up view of the data-acquisition system installed is shown in Figure 3.14.

3.5 Target Values for Performance Requirements of Repair Materials

Table 3.3 provides information on the target performance criteria adopted for this project. These performance criteria were chosen based upon the information gathered from the manufacturer data-sheet, ASTM C

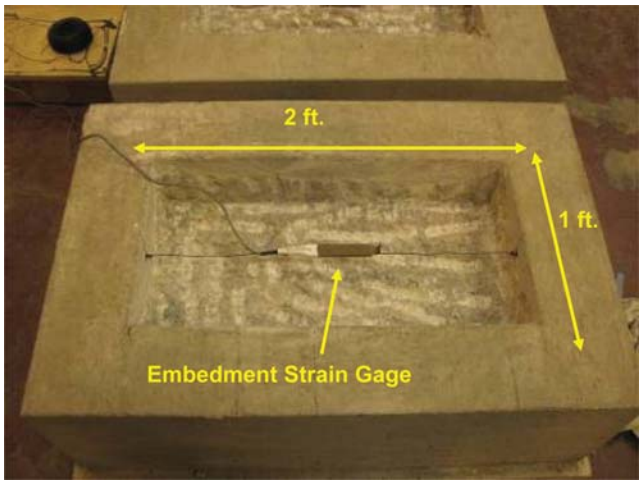

Figure 3.12 Instrumented mock-up slab.

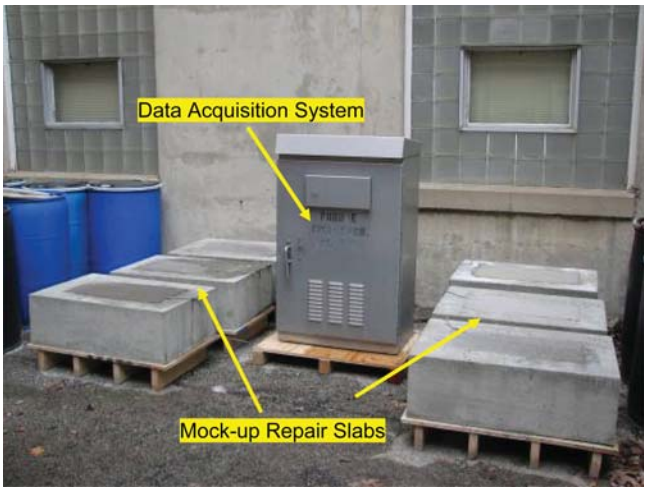

Figure 3.13 Mock-up repairs.

Figure 3.14 Data-acquisition system.

928 guidelines (*32*) as well the analysis performed in the earlier study (SPR-2789) (*6*) in which the performance specifications for rapid-setting materials adopted by various DOTs were reviewed in detail.

3.6 Summary

The first three sections of this chapter discussed the materials, mixture proportioning and the mixing procedure adopted for use during the laboratory part of the project. The laboratory test procedures were discussed in section 3.4. Finally, the performance requirements for the fresh and hardened concrete properties were outlined in section 3.5.

4. LABORATORY TEST RESULTS

4.1 Introduction

This chapter presents a comparison of the mechanical and durability properties of the rapid-setting repair materials (RMs) evaluated in the laboratory. Section 4.2 deals with the fresh properties and is followed by the discussion of the mechanical properties (strength gain, bond strength) in section 4.3. The dimensional stability properties are presented in section 4.4 and are followed by section 4.5 which describes the durability properties (freeze-thaw resistance, scaling resistance and rapid chloride permeability) and section 4.6 which discusses the performance of the mock-up repairs. The summary and analysis of all properties evaluated are presented in section 4.7.

4.2 Fresh Properties

The setting time, temperature development and workability (slump/flow) properties are discussed in this section.

TABLE 3.3
Target Performance Requirements

Property	Test Method	Requirement
Workability (mm)		
Slump	ASTM C 143 (no rodding)	200–250
Spread	ASTM C 143 (no rodding)	400–700
Set Time (min.)		
Initial	ASTM C 266	10–20
Final	ASTM C 266	20–40
Compressive Strength (MPa)		
2 h	ASTM C 39	14
4 h	ASTM C 39	21
24 h	ASTM C 39	28
28 days	ASTM C 39	35
Slant Shear Bond Strength (MPa)		
1 day	ASTM C 882 modified by ASTM C	7
7 days	928	10
28-day free shrinkage	ASTM C 157	$<750\ \mu\varepsilon$
Restrained shrinkage	AASHTO PP 34	No cracking up to 28 days
Freeze-thaw resistance	ASTM C 666 Procedure A	Min 60% RDM after 300 cycles
Scaling resistance	ASTM C 672 (25 Cycles)	Rating—0
28-day rapid chloride permeability	ASTM C 1202	Moderate to low

4.2.1 Setting Time and Temperature Development

Figure 4.1 shows a comparison of the initial and final setting times for all materials used in this study.

The initial setting time for all the materials was between 10 and 20 minutes, except TR which had an initial setting time of 34 minutes. TR and Dur-AE are the only materials with the final setting site of over 45 minutes; the rest of the materials had a final setting time of at most 35 minutes.

The temperature development curves for the RMs are shown in Figure 4.2.

There is a steep surge in the temperature curves for FX, HD and SQ products which occurs within 20 minutes after addition of mix water. TR shows a slightly delayed response. The rate of temperature evolution in Dur-R/AE was considerably slower than that in other materials. When compared to Dur-R, the curve for Dur-AE is slightly shifted to the right which may be explained by the fact that Du-AE has admixed air-entraining agent which may retard the rate of hydration. High dosages of air entraining agent may reduce rate of cement hydration (*33*). After 6 hours, the temperature of all materials returned to the level of ambient laboratory temperature.

4.2.2 Workability

Depending upon the "wetness" of the mixtures, their workability was measured either in terms of slump or slump flow. The basis for assessment of the workability was maximum allowable mix water (according to material manufacturer) for all the materials except SQ, for which 0.1 liter of mix water (per 50 lbs of material) was added in addition to maximum recommended dosage to achieve adequate workability for the SQ mixtures.

The workability was measured in terms of slump for SQ and HD materials and in terms of flow (spread) for the other materials. The results are shown in Figure 4.3. SQ and HD had a slump of about 9 inches (about 230 mm). FX and TR had a flow of 550 and 400 mm (or about 21.6 and 15.7 inches), respectively, while Dur-R and Dur-AE had flow values of over 700 mm (27.5 inches).

Figure 4.4 shows the appearance of the RMs after the slump (flow) test. It is evident that FX, TR, Dur-R and Dur-AE displayed good flow characteristics and may be considered self-leveling products. SQ and HD experienced rapid slump loss and they should be placed within 4–8 minutes of mixing to avoid consolidation problems. It is to be noted that around 16-18% (above that recommended in manufacturer's literature) extra-water was added for TR, Dur-R and Dur-AE to achieve the reported flow characteristics.

4.3 Mechanical Properties

The compressive strength and bond properties are discussed in this section.

4.3.1 Compressive Strength

Figure 4.5 and Figure 4.6 show the rates of compressive strength gain for the neat and extended mixtures, respectively.

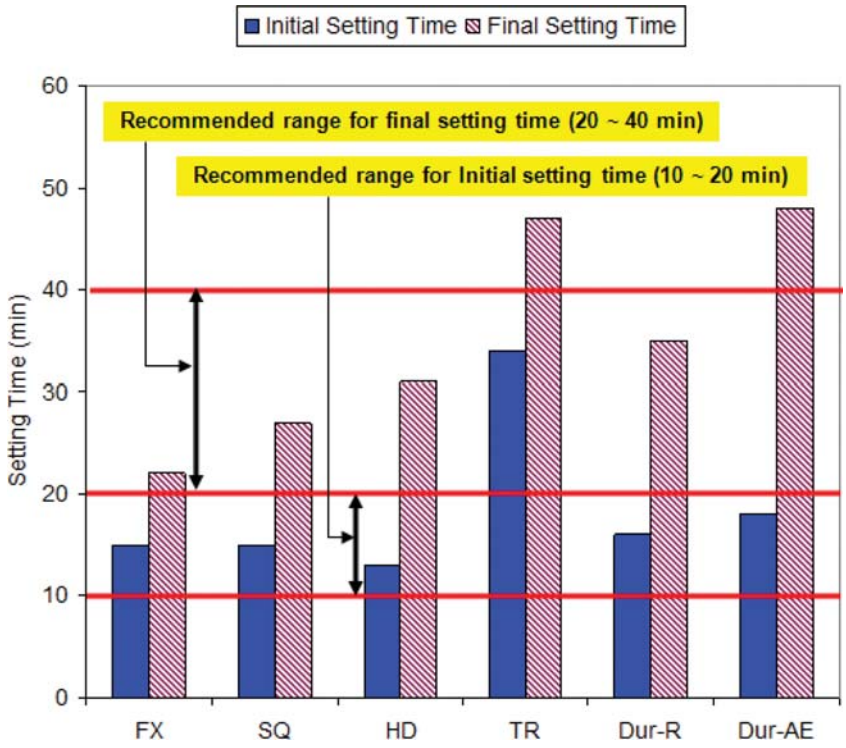

Figure 4.1 Setting time.

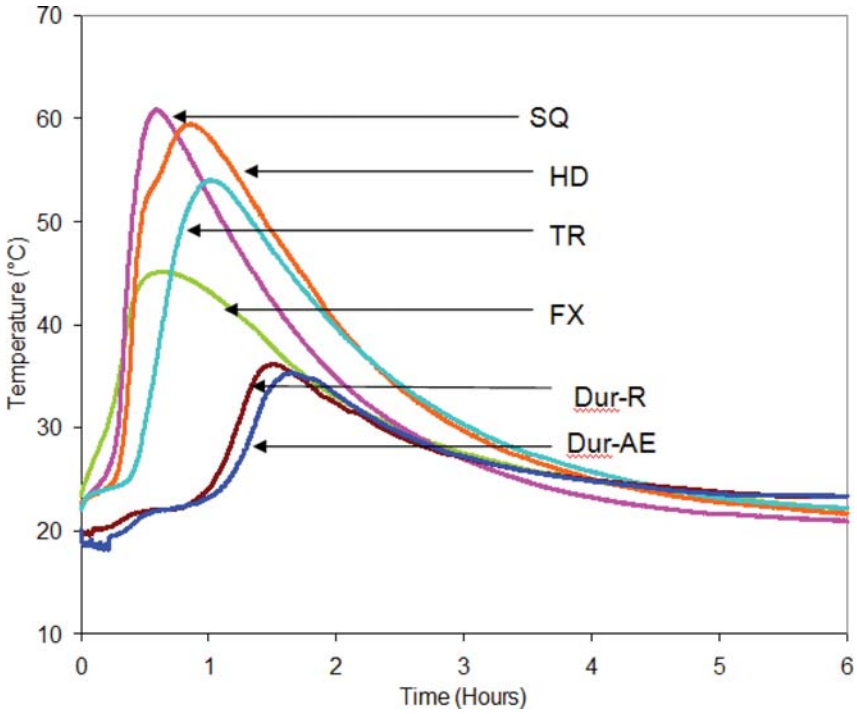

Figure 4.2 Temperature development curves.

For neat mixtures (Figure 4.5), the Dur-R and Dur-AE are the only materials which do not meet the project specified strength at the age 2 and 4 hours. All materials achieved the project-required compressive strength values after 1 and 2 days.

For extended mixtures (Figure 4.6), at the ages of 2, 4 and 24 hours, Dur-R and Dur-AE were the only two materials with strengths well below the project specified requirements. At the age of 28 days, only Dur-AE had strength lower than the required value of 35 MPa. The

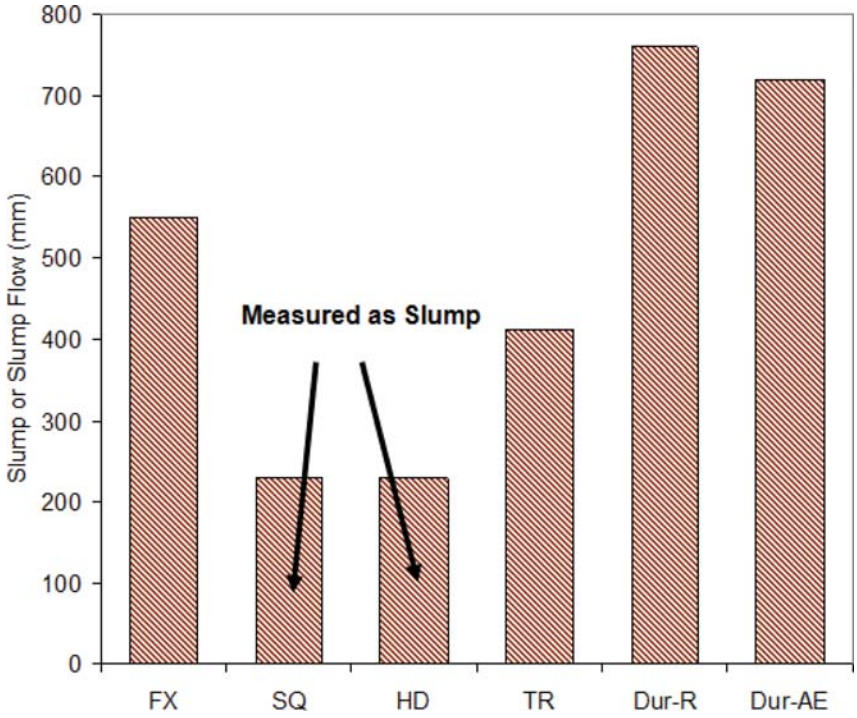

Figure 4.3 Slump/flow.

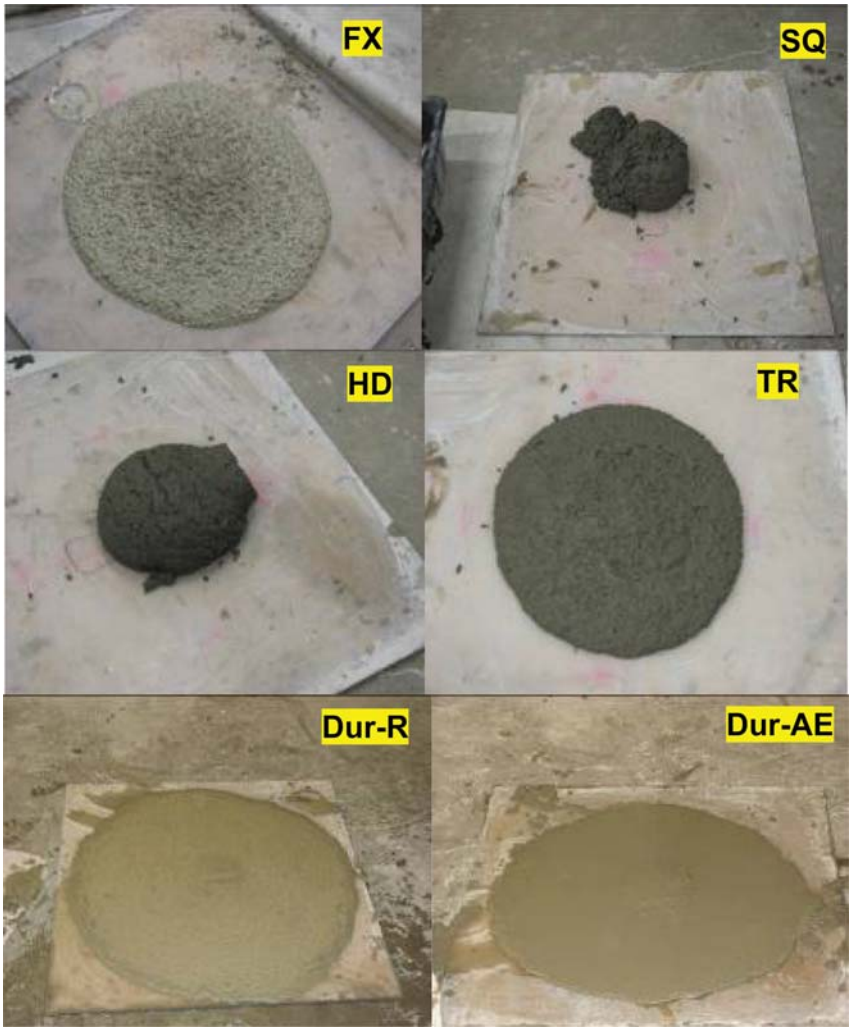

Figure 4.4 Appearance of RMs after the slump/flow test.

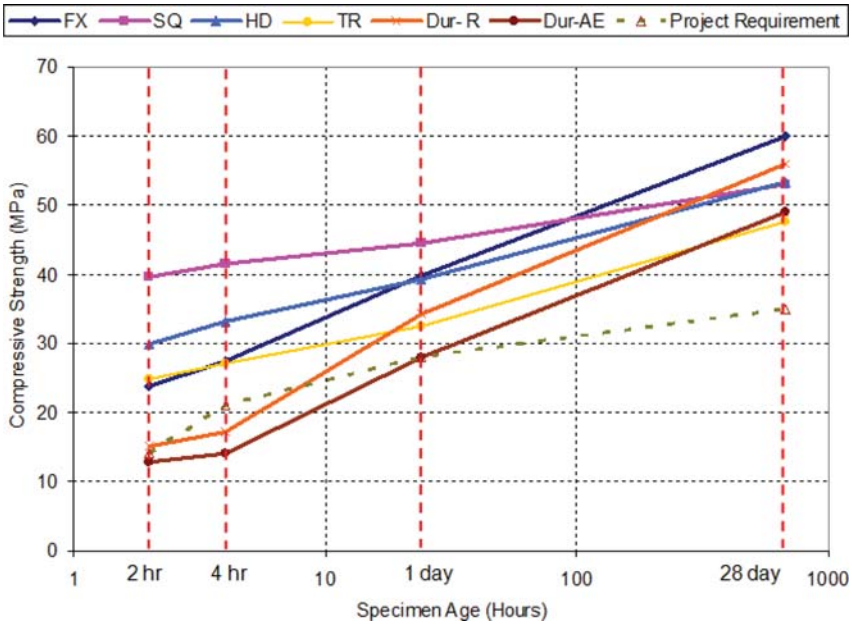

Figure 4.5 Rate of compressive strength gain (neat materials).

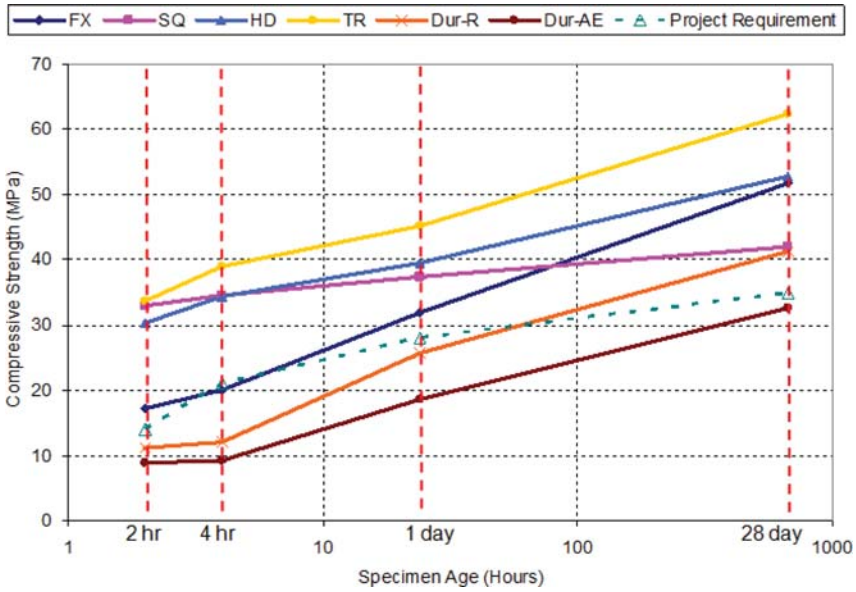

Figure 4.6 Rate of compressive strength gain (extended material).

other repair materials have excellent rates of strength gain under laboratory conditions of $23 \pm 2^{\circ}C$. The lower rate of strength gains (at least at early ages) observed for Dur-R and Dur-AE materials can be attributed to the slower rate of hydration which is evident from the temperature development curves (Figure 4.2) which show a significantly delayed response (compared to other materials).

Table 4.1 shows the linear regression models developed to predict the rates of strength gain for the neat and extended mixtures under laboratory conditions. It is seen that all the materials show very strong correlations, with the R^2 values being consistently over 0.99. It is to be noted that these models can be applied only when the mixture proportioning and curing conditions are similar to those adopted in this project.

4.3.2 Bond Strength

The bond-strength between the repair material and substrate mortar (concrete) was evaluated using two test methods: the slant-shear test (ASTM C 882 Method) (*25*) and the IOWA shear test (IOWA DOT Test Method 406-C-2000) (*20*).

The results of the slant-shear test are shown in Figure 4.7. All materials tested achieved the project-required bond-strength. The increase in bond strength from 1-day to 7-days is negligible for FX and SQ but is about 15% for HD and TR; and about 35% for Dur-R and Dur-AE. In order to study the effect on this property of the natural freeze-thaw exposure, another set of specimens was moist-cured for 7 days and then exposed to the natural environment during the time period from Dec. 6, 2007, to Feb. 5, 2008. The ambient temperature history for the environmental exposure was discussed in section 3.4.5. Although the temperature during the exposure period varied from -20°C to over +20°C, these variations did not seem to have any negative effect on the slant-shear bond strength values. In fact, there was an increase in bond strength for all the repair materials which may be due to later-age hydration. The failure mode in all the cases was along the bonding plane.

The Iowa-shear bond strength results are presented in Figure 4.8. The same curing/exposure regime was

TABLE 4.1
Regression Models for Rate of Compressive Strength Gain*

	Neat Material		Extended Material	
RM	**Model****	**R^2**	**Model****	**R^2**
FX	y = 6.2681Ln(x) + 19.284	0.9992	y = 6.0302Ln(x) + 12.466	0.9985
SQ	y = 2.2852Ln(x) + 37.932	0.994	y = 1.5075Ln(x) + 32.324	0.9947
HD	y = 4.0081Ln(x) + 27.07	0.9979	y = 3.7609Ln(x) + 28.194	0.9941
TR	y = 3.9339Ln(x) + 21.444	0.9906	y = 4.7697Ln(x) + 31.002	0.9927
Dur-R	y = 7.2549Ln(x) + 9.26	0.9919	y = 5.3899Ln(x) + 6.7123	0.9857
Dur-AE	y = 6.4543Ln(x) + 6.9946	0.9929	y = 4.2596Ln(x) + 4.7789	0.9909

*Laboratory mixes.
**y = compressive strength (MPa); x = specimen age (days) and $1 \leq x \leq 28$.

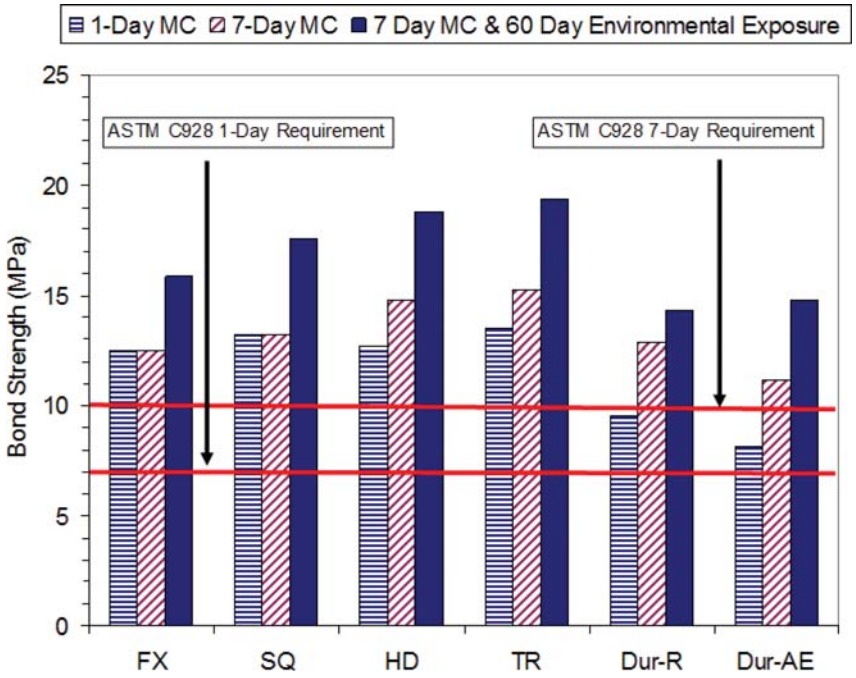

Figure 4.7 Slant-shear bond strength.

adopted as in the case of the slant-shear test. For FX, SQ, HD and TR, the increase in the Iowa shear bond strength from 1-day to 7-days is not very significant. However, for Dur-R and Dur-AE there is an evident increase in the 1-day and 7-days bond strengths (around 75%). Another interesting observation was that, the 60-days environmental exposure resulted in a very conspicuous decrease in the Iowa-shear bond strength for Dur-R and Dur-AE. However, the same was not observed in the case of the slant-shear test. As in the case of the slant-shear test, the failure mode in all cases was along the bonding plane. Additional field investigations must be carried out to verify these results.

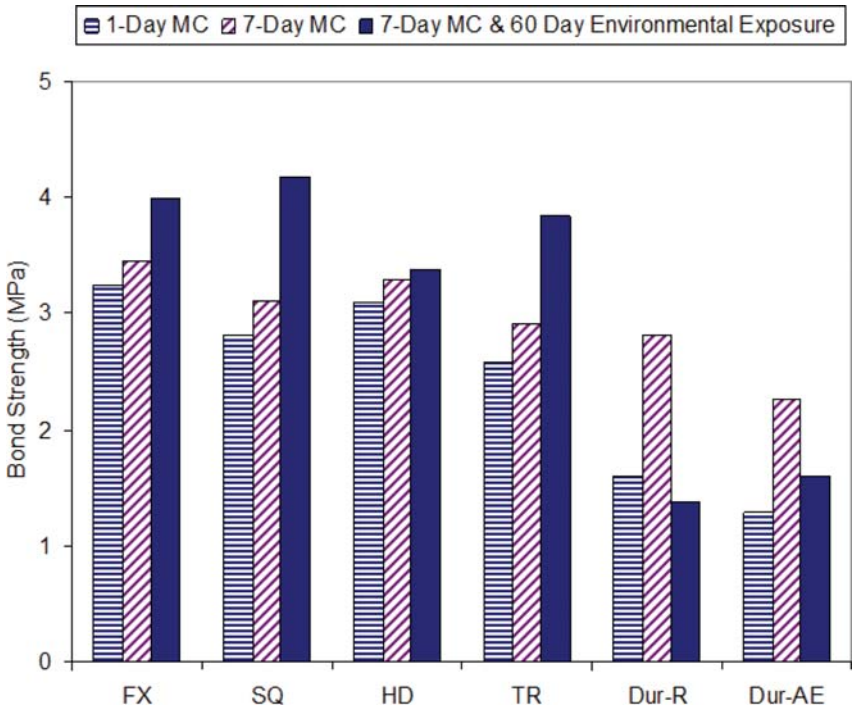

Figure 4.8 Iowa-shear bond strength.

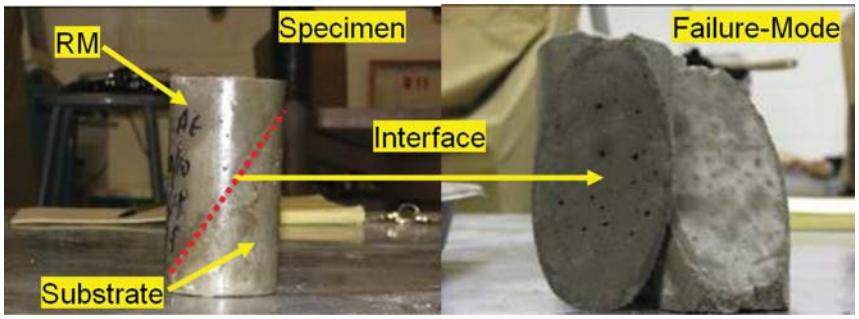

Figure 4.9 Slant-shear bond test—specimen and failure mode.

It must be noted that, in the slant-shear test, the repair concrete is installed on substrate mortar, where there is no coarse aggregate exposure along the bonding plane (Figure 4.9).

However, in the Iowa shear test a significant number of coarse aggregate grains are present along the bonding plane (smooth saw-cut surface). Also, in the slant-shear test, the stress configuration at the interface is a state of combined shear and compression, whereas, in the Iowa-shear test, the interface is in a state of pure shear. Hence, one would expect significantly lower bond-strengths in the case of the Iowa-shear test. The test specimen and the failure mode in the Iowa shear test are shown in Figure 4.10.

4.4 Dimensional Stability

This section presents the results of the free and restrained shrinkage tests performed on the repair materials.

4.4.1 Free Shrinkage

The free shrinkage responses of the neat and extended materials are shown in Figure 4.11 and Figure 4.12, respectively.

From Figure 4.11 and Figure 4.12 it is observed that the majority of the shrinkage occurred within the first two days. After the initial reading, subsequent measurements were performed at the ages of 1, 2, 4, 7, 14 and 28 days. SQ and HD displayed the maximum shrinkage after 28 days, with the values for the neat mixtures being around 1000 $\mu\varepsilon$ for HD and 1100 $\mu\varepsilon$ for SQ. The values for the extended mixtures were around 600 $\mu\varepsilon$ for SQ mixes and about 700 $\mu\varepsilon$ for HD mixtures. The FX mixtures had the lowest shrinkage after 28 days; the values being around 300 micro-strains for both neat and extended mixtures. It must be noted that the initial measurement of the shrinkage beams was performed 1 hour 45 minutes after the addition of mix-water. Hence, the dimensional changes of the material from time zero until 1 hour 45 minutes have not been captured. Since these materials undergo a significant increase in temperature at very early ages, they will undergo considerable expansion which in-turn may result in lower values of net shrinkage. Alternate test methods for evaluating dimensional changes at very early ages, like the corrugated tube method (*34*), must be considered when evaluating these materials.

The mass losses on drying for the neat and extended mixtures are shown in Figure 4.13 and Figure 4.14, respectively. Dur-R and Dur-AE experienced the maximum mass loss (around 3-3.5%) on drying—due to greater amount of mix-water required when compared to the other materials. SQ and HD exhibited lowest mass loss on drying (around 1%).

Table 4.2 shows the linear regression models developed to predict the rates of strength gain for the neat and extended mixtures at laboratory conditions. It is seen that all materials show very strong correlations, with the R^2 values being consistently over 0.90. It is to be noted that these models can be applied only when the mixture proportioning, curing conditions and initial measurements are performed as described in Chapter 3.

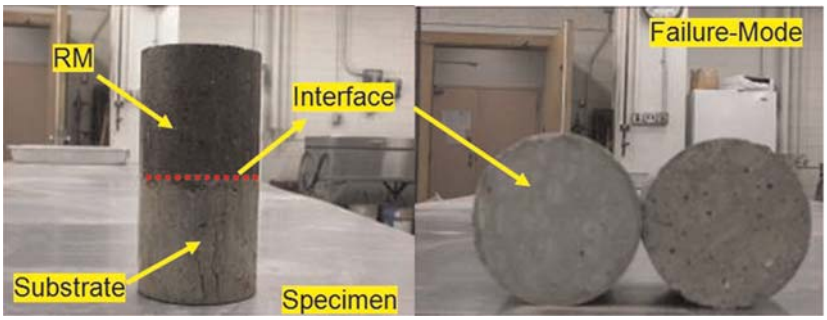

Figure 4.10 Iowa-shear bond test—specimen and failure mode.

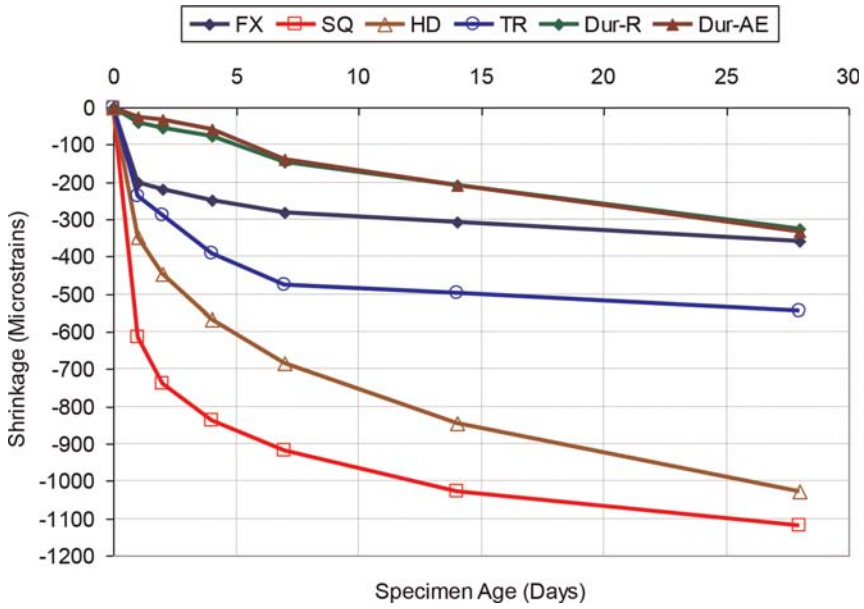

Figure 4.11 Free shrinkage—neat material.

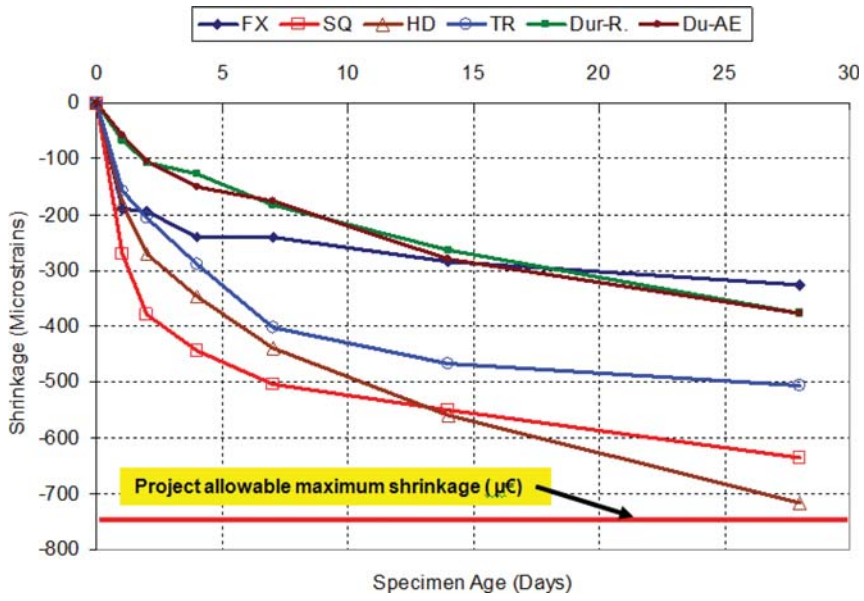

Figure 4.12 Free shrinkage—extended material.

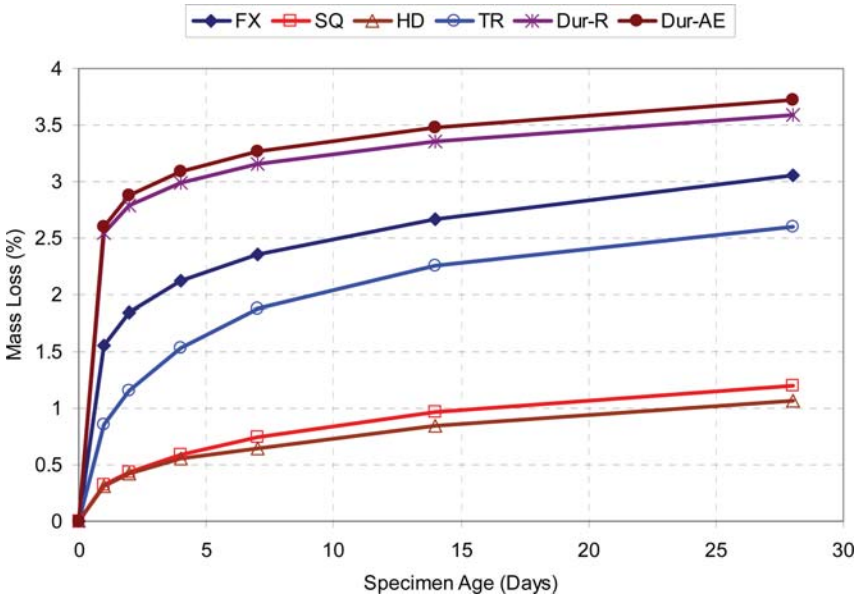

Figure 4.13 Mass loss on drying—neat material.

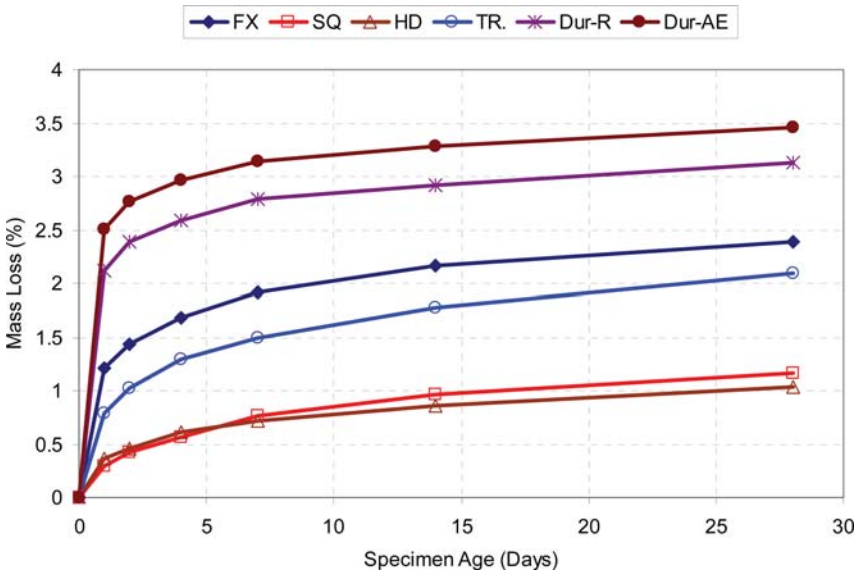

Figure 4.14 Mass loss on drying—extended material.

TABLE 4.2
Regression Models for Free Shrinkage Response

	Neat Material		Extended Material	
RM	**Model**	**R^2**	**Model**	**R^2**
FX	y = 47.388Ln(x) + 191.05	0.9798	y = 41.108Ln(x) + 177.34	0.9466
SQ	y = 150.81Ln(x) + 624.85	0.9981	y = 104.33Ln(x) + 290.06	0.9865
HD	y = 204.53Ln(x) + 312.01	0.9878	y = 158.18Ln(x) + 155.35	0.983
TR	y = 97.587Ln(x) + 243.52	0.9603	y = 114.16Ln(x) + 148.13	0.9741
Dur-R	y = 85.46Ln(x) - 0.1624	0.9059	y = 90.081Ln(x) + 37.138	0.9292
Dur-AE	y = 92.77Ln(x) - 20.675	0.9002	y = 93.73Ln(x) + 34.392	0.9539

y = free shrinkage ($\mu\varepsilon$); x = specimen age (days) and $1 \leq x \leq 28$.

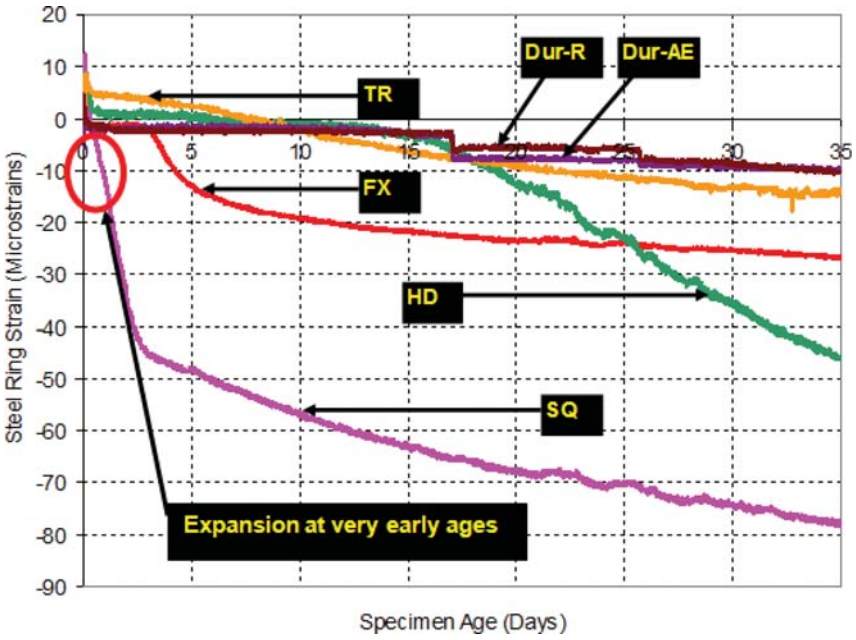

Figure 4.15 Restrained shrinkage test results.

4.4.2 Restrained Shrinkage

To study the cracking tendency of the repair materials, the restrained shrinkage test was performed. The strains were monitored for a period of 35 days in a controlled environment of 23°C and 50% RH using the AASHTO PP 34 test method (*28*), as previously described in section 3.4.7. The results are shown in Figure 4.15.

SQ developed the highest strains (around 80 $\mu\varepsilon$) after 35 days. None of the repair materials cracked. All the materials underwent an initial expansion (within the first 2 hours) which is probably due to the heat generated by the hydration process and the inherent expansive nature of some of these materials which may have caused the steel ring to expand. Most of the rapid-setting materials are designed to expand at early ages in order to provide a 'locking' effect into the patch in which they are installed. To quantify this expansion accurately, the dual-ring test (*35,36*) should be adopted. None of the materials cracked after 35 days and hence, all the materials can be considered to be dimensionally stable with respect to restrained shrinkage cracking.

4.5 Durability

This section presents the durability properties of the repair materials—freeze-thaw resistance, scaling resistance and resistance to chloride ion penetration.

4.5.1 Freeze-Thaw Resistance

Figure 4.16 provides results on the change in relative dynamic modulus (RDM) of elasticity of the specimens subjected to accelerated freeze-thaw (F-T) conditions in the laboratory.

The laboratory mixes of FX, SQ and HD showed excellent freeze-thaw resistance (RDM>80% after 300 F-T cycles). The laboratory specimens of TR and Dur-R mixes failed after 30 cycles of freezing and thawing (The Dur-R specimens failed before the first RDM measurement could be recorded). The specimens of Dur-AE reached a RDM of 60% after 220 cycles of freezing and thawing. These specimens also underwent severe scaling. This could be attributed to the excess water added (~17%) above the manufacturer's recommendation. Also, all test specimens were consolidated by vibration, which might have altered the air-void system resulting in poor F-T resistance for TR and Dur-R and reduced F-T resistance for Dur-AE.

The appearance of FX after 300 cycles of freezing and thawing is shown in Figure 4.17. The specimens showed moderate scaling but were structurally sound. Figure 4.18 shows the appearance of SQ after 300 F-T cycles. The specimens showed minor scaling—minor pop-outs being the nature of distress observed.

The appearance of the HD specimens after 300 cycles of freezing and thawing is shown in Figure 4.19. The specimens exhibited minor surface scaling.

Figure 4.20 and Figure 4.21 show the appearances of TR and Dur-R specimens, respectively, after 35 F-T cycles. The specimens were completely deteriorated.

The appearance of Dur-AE specimens after 300 F-T cycles is shown in Figure 4.22. The specimens showed severe surface scaling, exposing the pea-gravel completely.

Figure 4.23 shows the mass loss of the specimens after 300 F-T cycles. The FX, SQ and HD specimens had an overall mass loss of less than 2%. Dur-AE had the maximum mass loss (of around 12.5%).

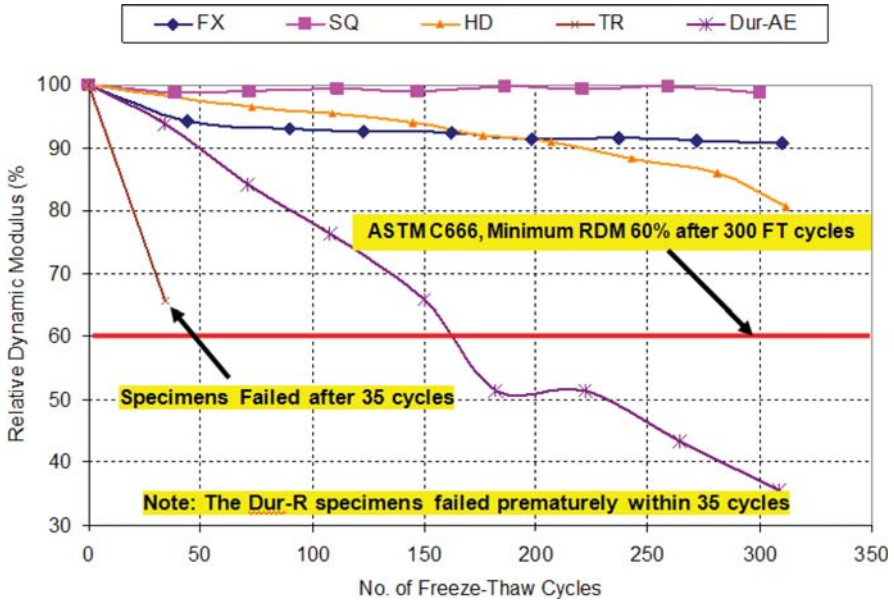

Figure 4.16 Freeze-thaw resistance.

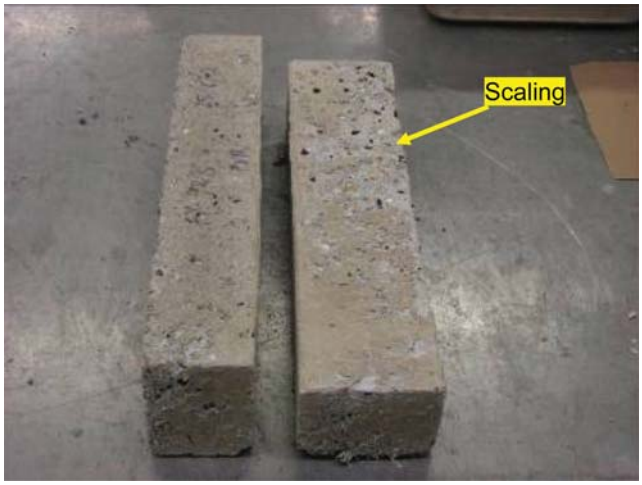

Figure 4.17 Appearance of FX after 300 F-T cycles.

Figure 4.19 Appearance of HD after 300 F-T cycles.

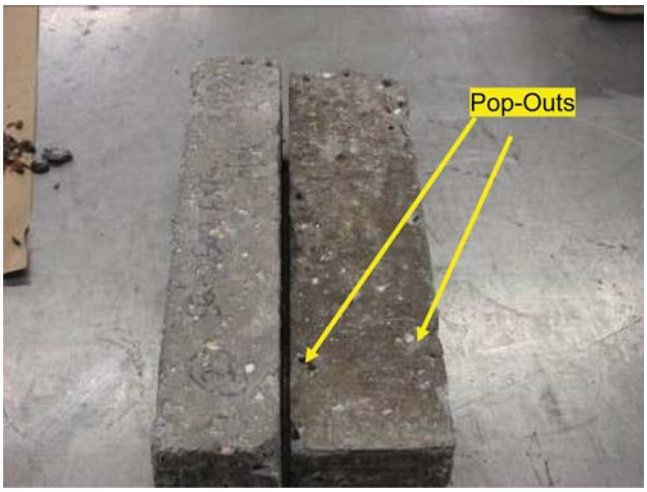

Figure 4.18 Appearance of SQ after 300 F-T cycles.

Figure 4.20 Appearance of TR after 35 F-T cycles.

Figure 4.21 Appearance of Dur-R after 35 F-T cycles.

Figure 4.22 Appearance of Dur-AE after 35 F-T cycles.

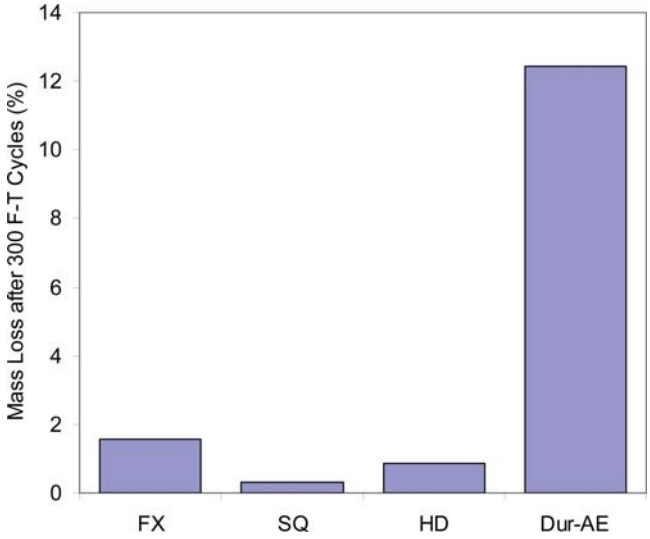

Figure 4.23 Total mass loss after 35 F-T cycles.

4.5.2 Scaling Resistance

Figure 4.24 shows the amount of material scaled after exposure to 25 cycles of freezing and thawing in the presence of de-icing salts. The scaling resistance of Dur-R and Dur-AE could not be evaluated because of technical problems with the freeze-thaw chamber. The reference specimens used were plain-cement-concrete (PCC) specimens prepared and evaluated by Rudy et al. (*37*).

The FX specimens displayed the highest amount of scaling (approximately 80 g/m^2 of material scaled from surface area exposed). The other materials (SQ, HD and TR) had less than 40 g of scaled material per m^2 of surface area exposed. In general, all materials exhibited good scaling resistance.

The appearance of the FX and SQ scaling specimens after 25 F-T cycles in the presence of de-icing salts is shown in Figure 4.25 and Figure 4.26, respectively. These specimens underwent slight scaling and minor pop-outs can be observed on the surface of both of these materials.

The appearance of HD and TR scaling specimens after 25 F-T cycles in the presence of de-icing salts is shown in Figure 4.27 and Figure 4.28 respectively. Minor pop-outs can be seen on the surface and these specimens underwent negligible scaling.

4.5.3 Resistance to Chloride-Ion Penetration

Figure 4.29 provides information on the relative resistance of tested mixtures to chloride-ion penetration.

The HD material had the lowest value of the total charge passed after 6 hours (336 coulombs) which corresponds to very low chloride-ion permeability according to AASHTO T 277 (*38*). The SQ material had low chloride-ion permeability and FX, TR and Dur-R materials had moderate chloride-ion permeability. Dur-AE had the highest value (8159 coulombs) for the total charge passed after 6 hours, indicating that it could potentially be unsafe to be used in direct contact with rebars under condition of salt exposure.

4.6 Performance of Mock-up Repairs

Mock-up pavement slabs with repair patches were cast in the laboratory to mimic the field repairs. The slabs were instrumented with embedment strain gages and the strains were recorded continuously every 30 minutes for a period of 3 months. The ambient temperature was also monitored alongside using thermocouples.

Figure 4.30 through Figure 4.35 show the strains developed within the repair patches for all repair materials. A negative value strain indicates tension and a positive value indicates compression. The FX and HD gages malfunctioned occasionally; however, there was no serious loss of data.

A combined plot of the strains developed for all the repair materials is shown in Figure 4.36.

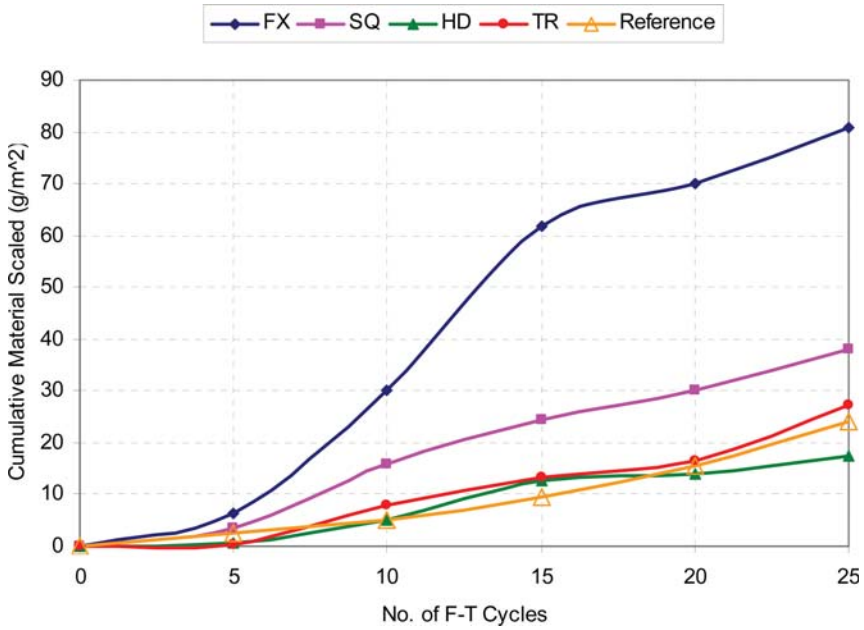

Figure 4.24 Scaling resistance of the repair materials.

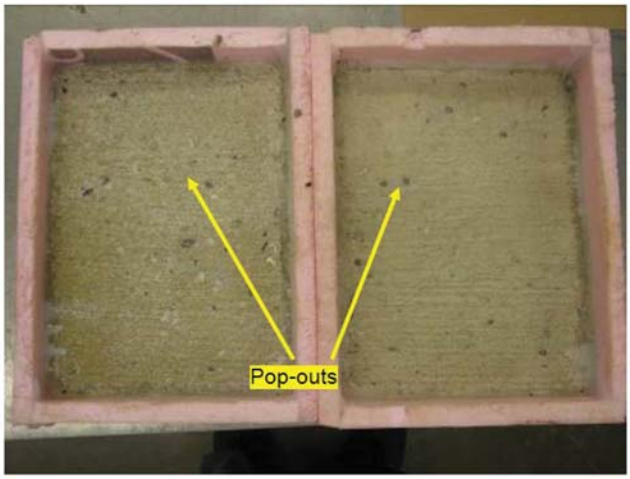

Figure 4.25 FX specimens after 25 cycles of the scaling test.

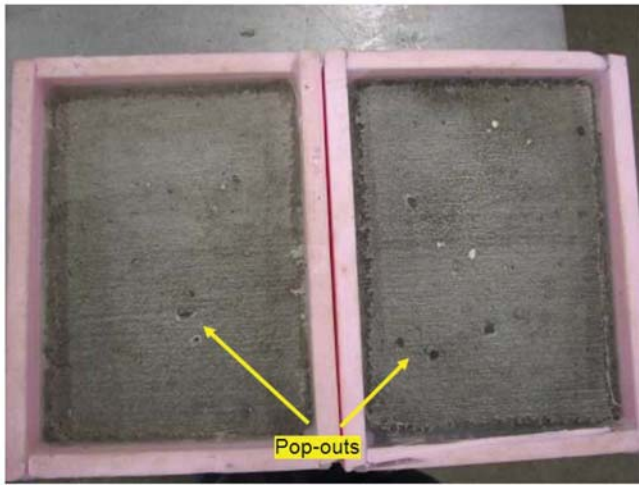

Figure 4.27 HD Specimens after 25 cycles of scaling test.

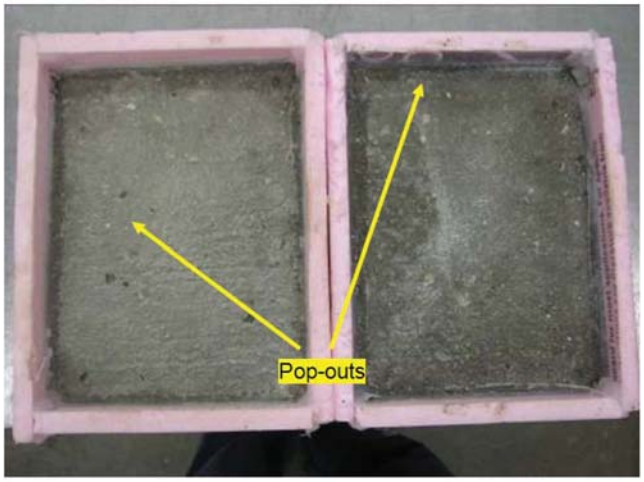

Figure 4.26 SQ Specimens after 25 cycles of scaling test.

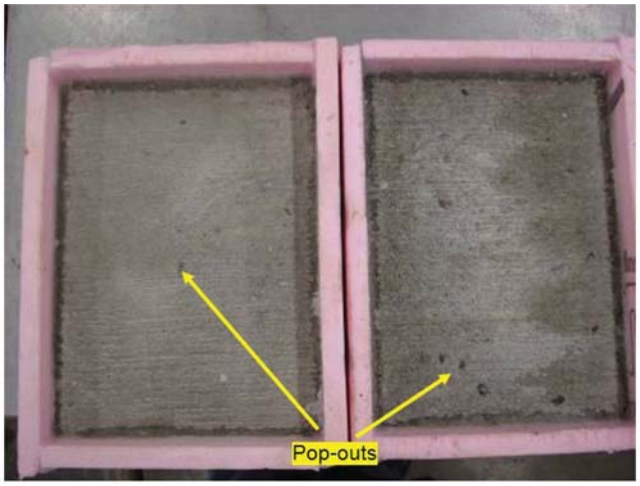

Figure 4.28 TR Specimens after 25 cycles of the scaling test.

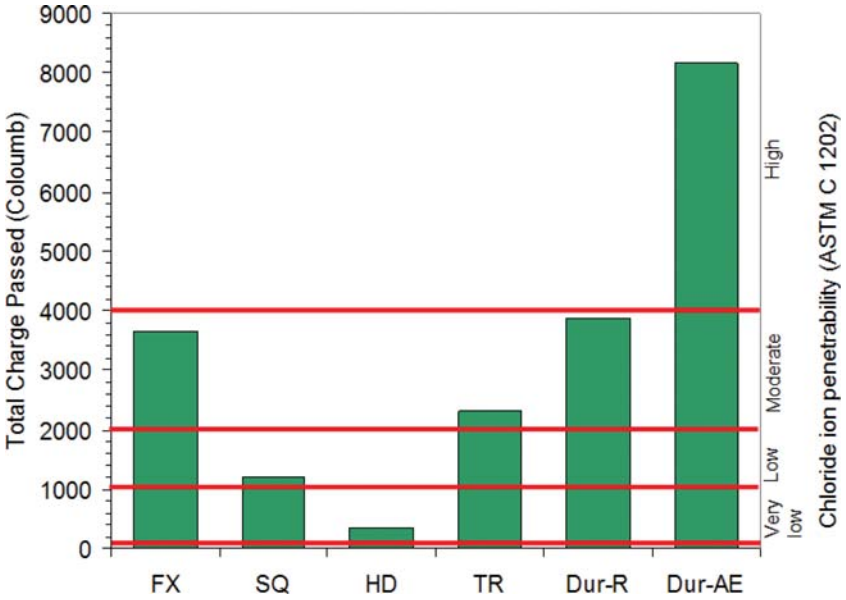

Figure 4.29 Resistance to chloride-ion penetration.

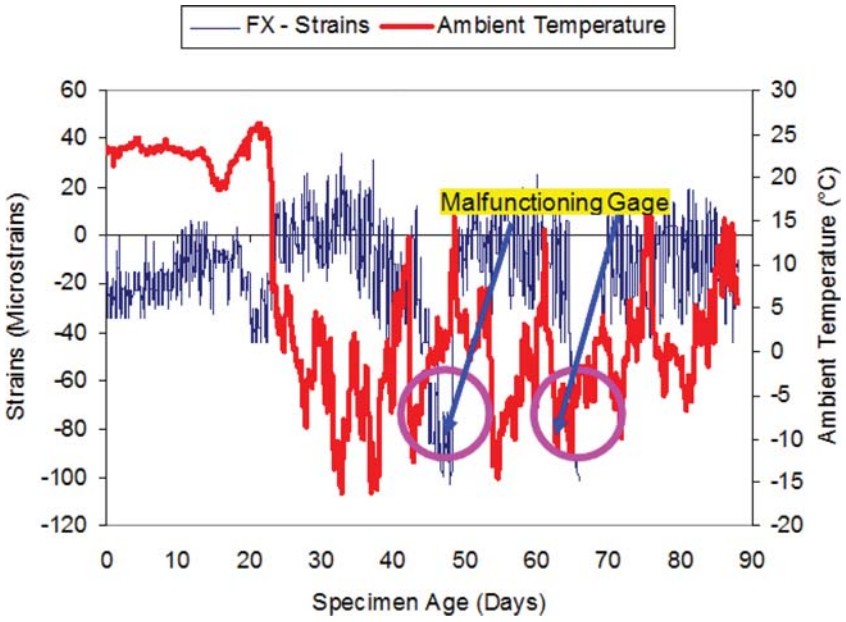

Figure 4.30 FX strains developed within repair patches.

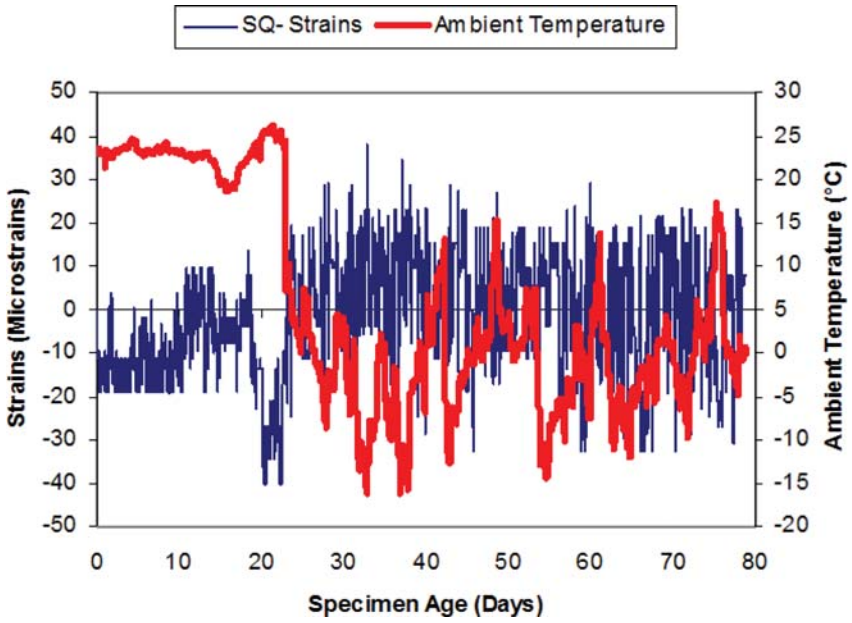

Figure 4.31 SQ strains developed within repair patches.

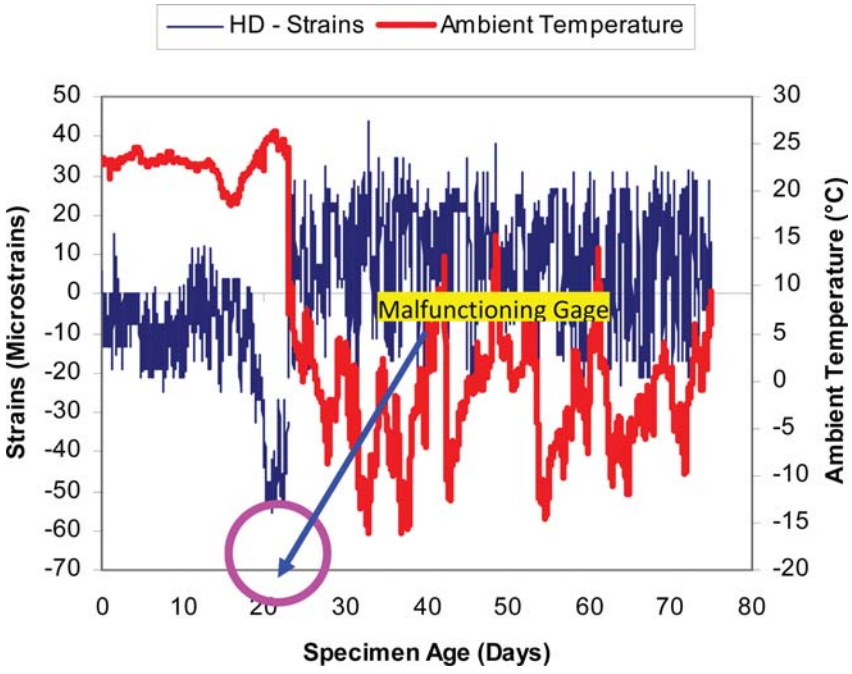

Figure 4.32 HD strains developed within repair patches.

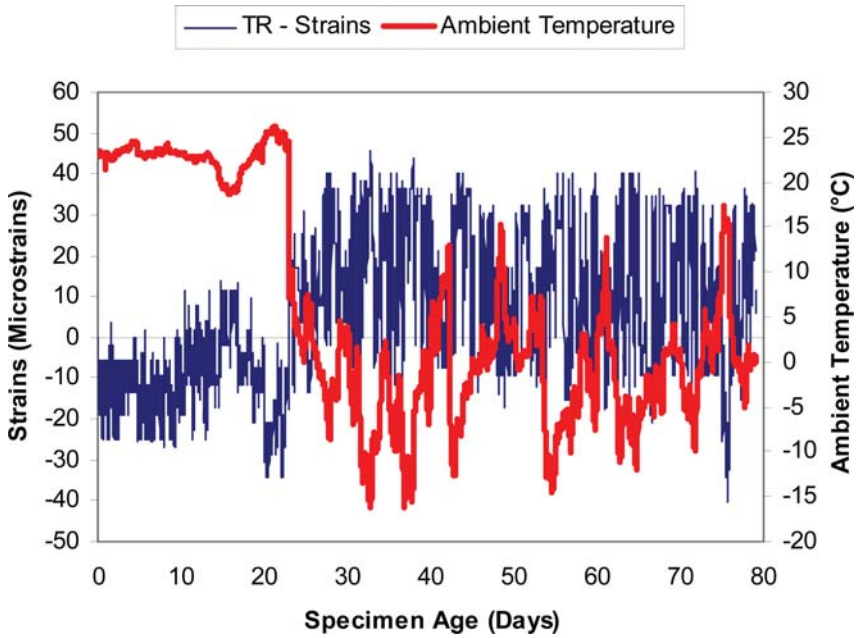

Figure 4.33 TR strains developed within repair patches.

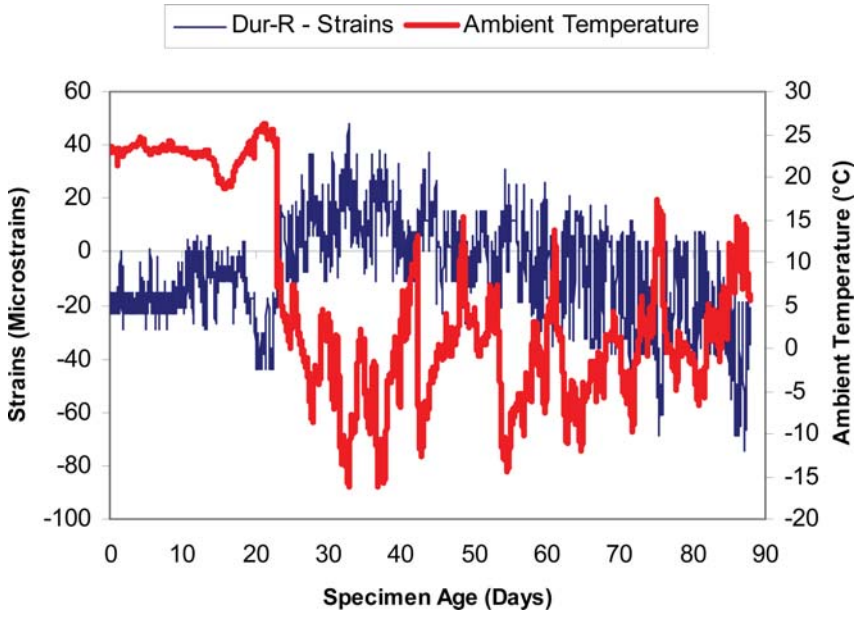

Figure 4.34 Dur-R strains developed within repair patches.

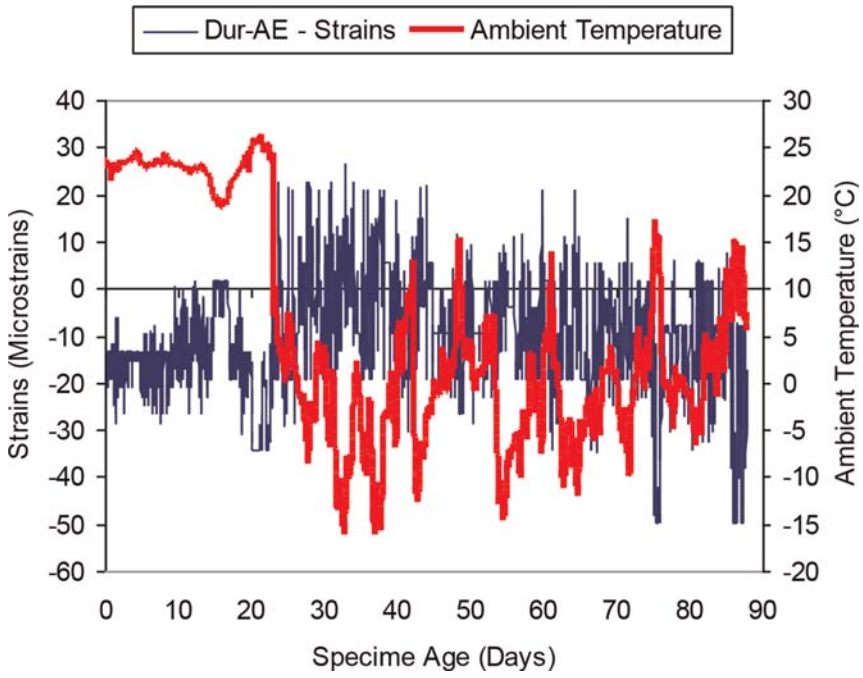

Figure 4.35 Dur-AE strains developed within repair patches.

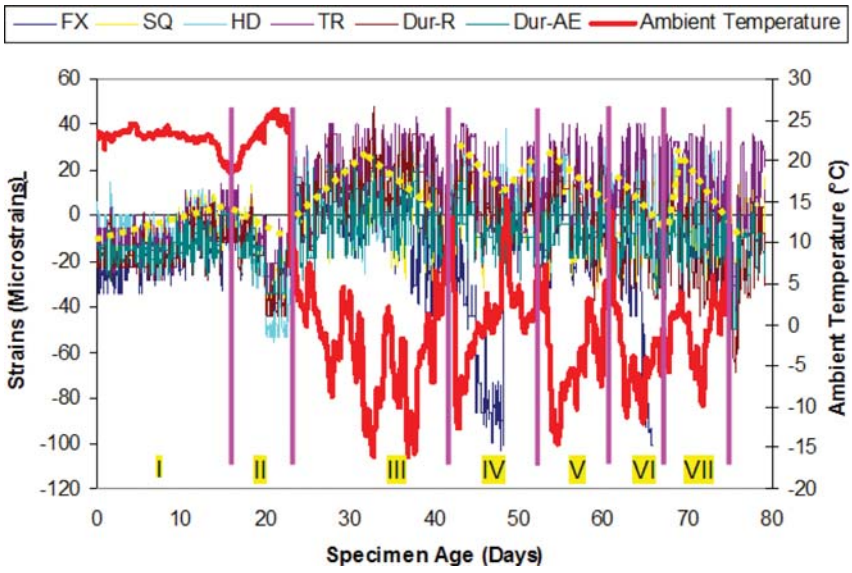

Figure 4.36 Mock-up repair slabs strains developed within repair patches.

Certain trends (shown by the dashed line in Figure 4.36) were observed from the strain-time plots. For the first 20 days, the slabs were placed in a semi-controlled environment with an ambient temperature of around $23 \pm 2^{\circ}C$. The relative humidity, however, was varying. The trends observed in the seven stages indicated in Figure 4.36 are discussed below:

- **Stage I:** There is an initial expansion in all the cases—probably due to the heat generated during the hydration of the materials which resulted in the expansion of the strain gages. After the materials set, the gages would have remained in the expanded state. Then, all the materials begin to shrink.
- **Stage II:** There is a sudden increase in the ambient temperature in the semi-controlled environment due to unknown reasons. Consequently, all the materials expand due to the increase in the ambient temperature.
- **Stages III–VII:** The temperature effects seem to be the dominant factor in these stages. As the ambient temperature decreases, the slabs show a compressive response and as the temperature increases, the slabs show a tensile response, which is expected.

No clear conclusions can be drawn from the behavior/condition of the repair materials from the strain-time-temperature response. On visual inspection of the patches after 3 months of environmental exposure, all the patches except Dur-R) showed no visible signs of distress. The Dur-R patches showed a map cracking pattern on the surface. A close-up view of the Dur-R patches is shown in Figure 4.37.

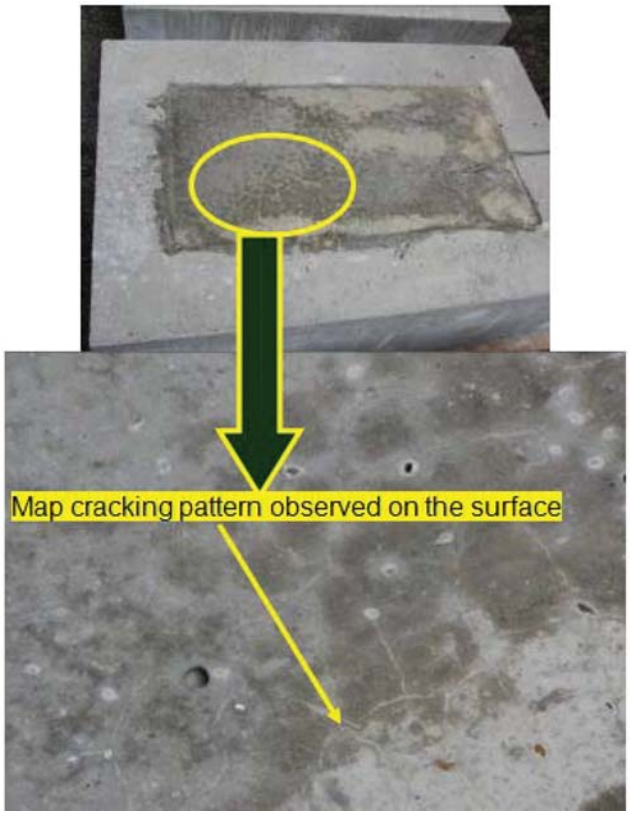

Figure 4.37 Dur-R mock-up repair—close-up view.

4.7 Summary

Based on the test results of the selected rapid-setting materials the following observations have been made:

- The repair materials studied in this project had varying chemical compositions which influenced performance in terms of mechanical and durability parameters.
- FX, TR, Dur-R and Dur-AE materials displayed good flow characteristics and can be considered as having self-leveling characteristics. SQ and HD experienced rapid slump loss.
- All the materials (except Dur-AE) showed acceptable rate of strength gain.
- In general, all materials developed good bond with substrate concrete.
- The cracking tendency of all materials was low.
- Relatively poor freeze-thaw durability was observed for TR, Dur-R and Dur-AE materials; possibly the result of additional water that needed to be added to maintain adequate workability of extended mixtures.
- All materials displayed good scaling resistance. The visual rating according to ASTM C 672 can be estimated to be 0 to 1 for all the materials.
- Dur-AE displayed poor resistance to chloride-ion penetration relative to the other materials tested.
- All the mock-up repairs seemed to perform well after 4 months of exposure except for Dur-R which showed a map-cracking pattern on the surface.

5. FIELD INSTALLATIONS

5.1 Introduction

In order to verify the performance of the rapid-setting repair materials in the field, they were used to repair deteriorated sections on a bridge deck over Wabash River in the Tippecanoe County in Indiana. Representatives from each (except FX) manufacturer of the materials used were present on site to ensure proper mixing and placement of their products. Due to traffic control and scheduling problems, the field installation of Duracal-R could not be carried out. The installations were carried in the third and fourth weeks of October, 2007. Table 5.1 shows the list of the materials used for field installations.

5.2 Location of Repair Site

FX, HD, SQ-2500, SQ-1000 and TR were installed in the driving lane on a bridge deck near the mile marker 176 on Interstate 65 southbound (I-65 SB) over Wabash River in Lafayette, Indiana. Dur-AE and Dur-AE-F were installed on the passing lane of the same highway in the northbound direction (I-65 NB). The geographical location of the repair site is shown in Figure 5.1.

A view of the northbound lane of the bridge deck on which the repairs were carried out is shown in Figure 5.2.

TABLE 5.1
Materials Used for the Field Installations

Material	Specimen Label	Manufacturer
FX-928	FX	Fox Industries
SikaQuick-2500	SQ-2500	Sika Corporation
SickQuick-1000	SQ-1000	Sika Corporation
HD-50	HD	Dayton Superior
ThoRoc 10-60	TR	BASF
SET 45 Regular	SET 45-R	BASF
SET 45 Hot Weather	SET 45-HW	BASF
SET 45 50/50 Blend	SET 45-50/50	BASF
Duracal Air Entrained	Dur-AE	US Gypsum
Duracal Air Entrained with Fibers	Dur-AE-F	US Gypsum

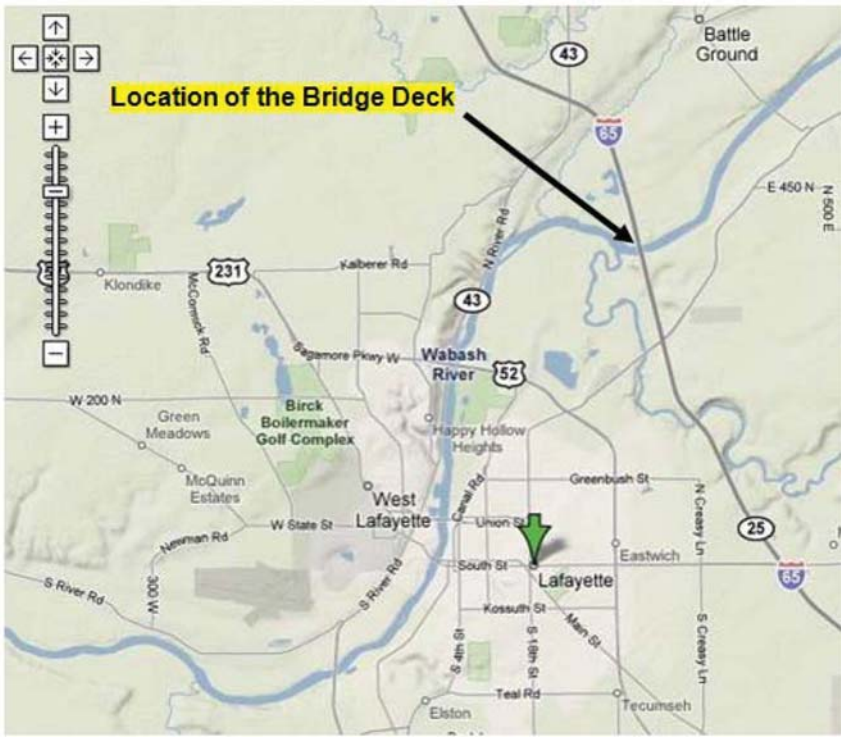

Figure 5.1 Geographical location of the repair site. (Maps: Courtesy Google Maps.)

Figure 5.2 View of the bridge deck on I-65 NB. (Courtesy: Google Maps.)

5.3 Observed Distresses

The following distresses were predominantly observed on the bridge deck (both northbound and southbound directions) prior to the installation of the rapid-setting material repair patches:

- Failure of existing patch: heavy cracking/de-bonding from existing concrete (Figure 5.3).
- Failure of existing concrete: potholes(spalls) and heavy cracking (Figure 5.4 and Figure 5.5).

Figure 5.3 shows a sample distress where an existing concrete has deteriorated along the periphery of a previously repaired patch (previous repair was performed with asphalt concrete). Severe cracking of the deck was another commonly observed distress (Figure 5.4). Figure 5.5 shows a pothole (spall) in the existing concrete.

5.4 General Installation Procedures

This section describes the traffic control measures implemented during the field repair process as well as the details on the general procedures involved in the preparation of the repair areas and installation of the patches.

5.4.1 Traffic Control and Safety Measures

The arrangements for traffic control and safety measures were provided by Indiana Department of Transportation (INDOT), Crawfordsville district. The driving lane in the southbound direction and the passing lane in the northbound direction were closed to the general traffic from 12:00 AM until 8:00 AM on the day of the installation.

5.4.2 Repair Patch Preparation

In preparation for the repairs, the surface of the bridge deck was sounded with a hammer to identify the boundaries of deteriorated areas. The removal of concrete from these areas was accomplished using concrete saws (Figure 5.6) and pneumatic jackhammers (Figure 5.7). If rebars were present, the concrete was removed to the depth of 1 inch below the rebars.

Figure 5.3 Distress I: cracking along boundaries of an existing patch (southbound direction).

Figure 5.4 Distress II: severe cracking of existing concrete (northbound direction).

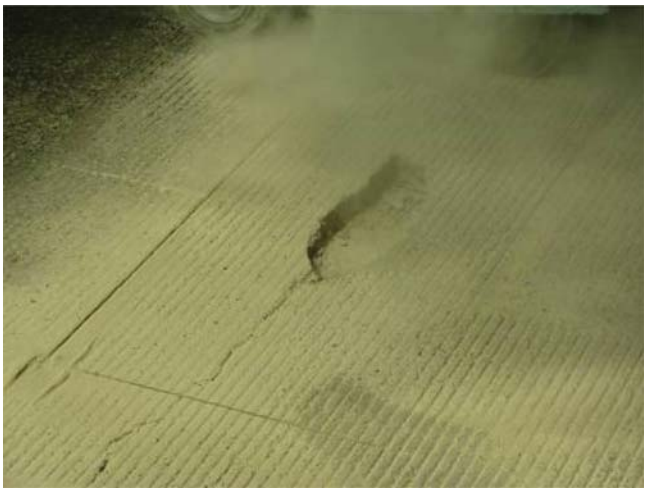

Figure 5.5 Distress III: pothole (spall) in the existing concrete (northbound direction).

The repair area was then cleared using a blast of high pressure air (Figure 5.8). The cleared surface was then wetted to avoid removal of mixture water from the repair material by the existing/dry concrete. An example of repair area prepared for patching is shown in Figure 5.9.

5.4.3 General Procedures for Installation of Repair Patches

After the preparation of the patch area was completed, the repair material was mixed on-site, typically in a drum mixer (for all the materials except SET 45), shown in Figure 5.10 in one or more batches depending upon the size of the patch. For SET 45, a

Figure 5.6 Saw-cutting operation.

Figure 5.8 Cleaning operation.

mortar mixer was used (Figure 5.11). A three bag mix was typically used for small patches and a six bag mix was used for larger patches.

First, the water and the aggregates were introduced into the mixer and the mixer was switched on. The material was then added into the mixer as the mixing was being carried out. The material was added directly from the bags. The aggregates were not weighed. A judgmental approximation to the mass was performed before they were introduced into the mixer. The water was added using 1 gallon containers. The mix water and the mixing time varied from batch to batch. Based upon the visual observation of the material in the mixer, extra water was added by the manufacturer to achieve better workability.

After mixing, the material was discharged to the wheel barrows and delivered to the place of installation. After discharging from the wheel barrow, the repair material was consolidated in the patch area by tamping with the shovels. The surface of the newly placed patches was finished with concrete trowels (Figure 5.12)

Figure 5.9 Repair area prepared for patching.

Figure 5.7 Jackhammering operation.

Figure 5.10 Drum mixer used on-site.

Figure 5.11 Mortar mixer used on-site for SET 45.

Figure 5.13 Finished patch (HD).

and textured using a broom. Except for TR, no specific curing regime was recommended by the representatives of all other material manufacturers present on site. As a result, those patches were not cured after placement. For TR, the placed material was covered with a plastic sheet. Figure 5.13 shows a sample patch after finishing. More details on the location and installation of the patches using the individual materials are given in section 5.5.

5.5 Detailed Installation Procedures for each Repair Material

This section presents the repair patch details and the installation procedures for each of the repair materials. The following sections have been organized in the chronological order in which the patches were installed. All the repair patches had an average depth of 5 inches. The average ambient temperature during the placement for all the materials was about 10°C.

5.5.1 HD-50

Three patches were installed using the HD-50 material. The first patch installed with HD-50 is shown in Figure 5.14. The patch was located in the wheel path of the traffic (southbound direction).

The second patch installed with HD-50 is shown in Figure 5.15. This patch was not located along the wheel path of the traffic. A coffee cup can be seen in the image. This was used to block the through-hole (to hold the freshly placed material within the patch) that was created in the bridge deck during the jack-hammering operation. The concrete beneath this repair area was heavily deteriorated which led to the formation of the through-hole while the concrete was being chipped out in preparation for the placement of the patch.

The third patch installed with HD-50 is shown in Figure 5.16. This patch was located along the dividing line. All HD-50 mixes produced were very consistent with respect to the appearance and the workability aspects.

Figure 5.12 Finishing operation.

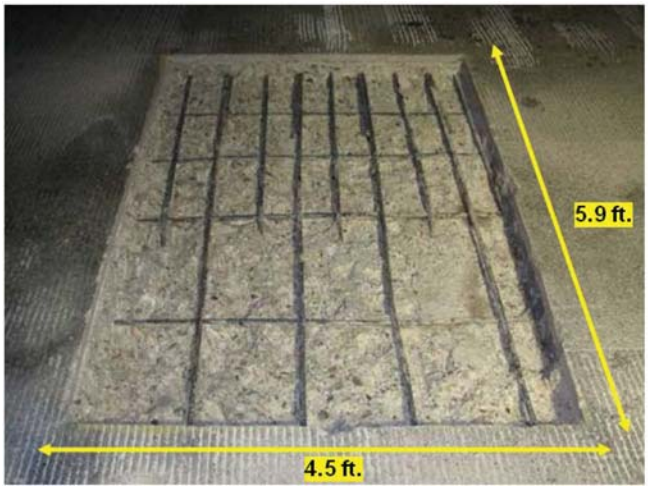

Figure 5.14 HD-50: patch area-I.

Figure 5.15 HD-50: patch area-II.

Figure 5.16 HD-50 patch area-III.

Figure 5.17 HD-50: finished patch-I.

Figure 5.18 HD-50: finished patch-II.

The finished patches are shown in Figures 5.17 through 5.19. The edges were not sealed properly in patch-I.

5.5.2 SikaQuick-1000

SikaQuick-1000, though not a part of the original test matrix, was used for the field trials due to the insistence from the material manufacturer. One patch was installed using this material (Figure 5.20). Moderate corrosion was observed in one of the rebars before the installation of the patch. No attempt was made to remove the rust from the rebars before the installation of the material. Ideally, when corroded rebars are present, the rust must be cleared by sand blasting before the repair material can be installed. This patch was not located on the wheel path.

The finished SQ-1000 patch is shown in Figure 5.21. As can be seen from the figure, the material exhibited excessive bleeding. The mix was slightly over-watered which was the cause for the bleeding. Also, due to the slope of the surface, the material in its fresh state flowed out of the patch, which resulted in uneven edges of the hardened patch.

Figure 5.19 HD-50: finished patch-III.

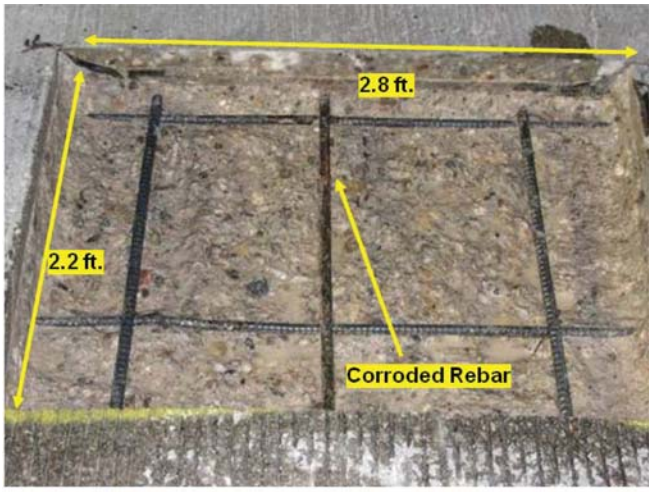

Figure 5.20 SQ-1000: patch area.

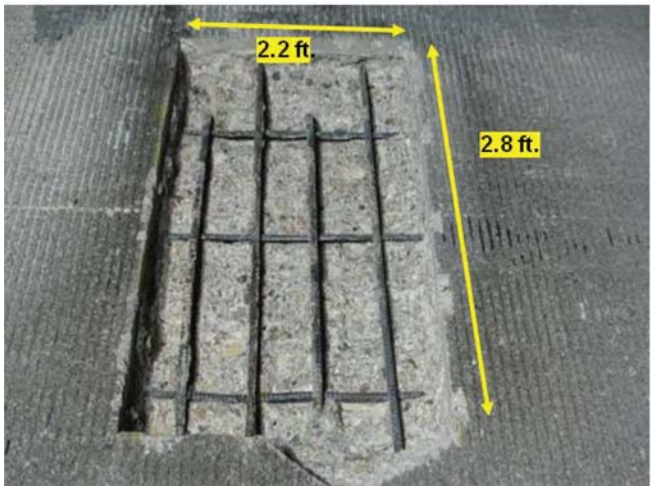

Figure 5.22 SQ-2500: patch area-I.

5.5.3 SikaQuick-2500

Three patches were installed using SikaQuick-2500. The first and second patch areas are shown in Figure 5.22 and Figure 5.23 respectively. The patches were located along the wheel path.

The finished patches are shown in Figures 5.24 and 5.25. The mix in patch-I had excessive water which led to heavy bleeding and poor finishing (Figure 5.24). The mix in patch-II had better consistency and, as a result, did not show signs of excessive bleeding upon finishing.

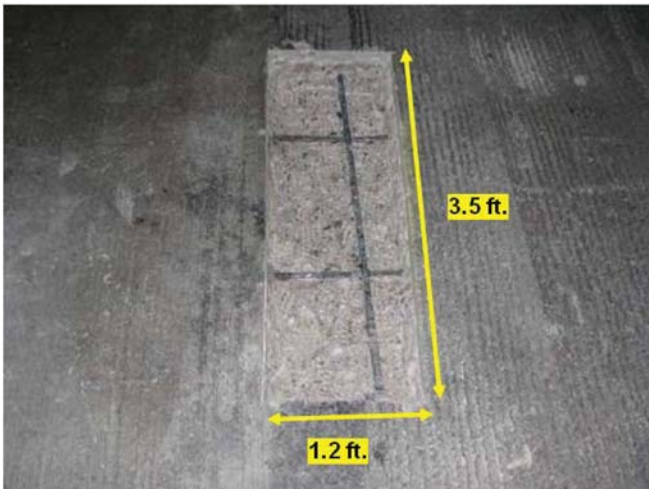

Figure 5.23 SQ-2500: patch area-II.

5.5.4 FX-928

Two patches were installed using FX-928 material. Since the material manufacturer representative was not present on-site, the mixing operation was carried out by the INDOT crew.

Figure 5.26 shows the first patch prepared for patching.

The second patch area is shown in Figure 5.27. Both of these patches were located along the wheel path.

Figure 5.21 SQ-1000: finished patch.

Figure 5.24 SQ-2500: finished patch-I.

Figure 5.25 SQ-2500: finished patch-II.

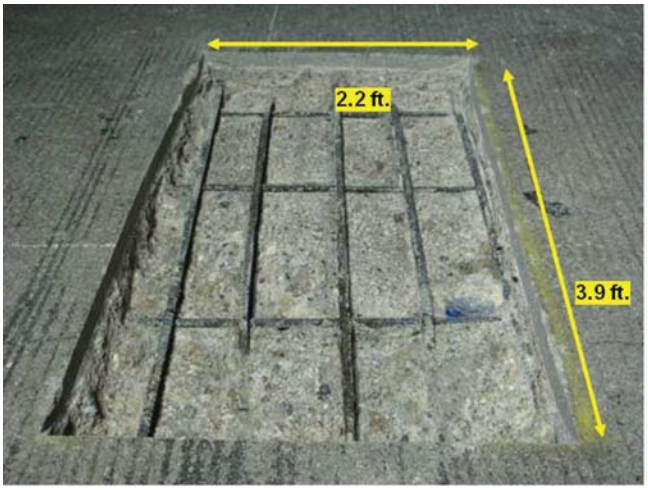

Figure 5.26 FX-928: patch area-I.

All mixes produced with FX-928 were very consistent with respect to the workability and the appearance. The finished patches are shown in Figures 5.28 and 5.29.

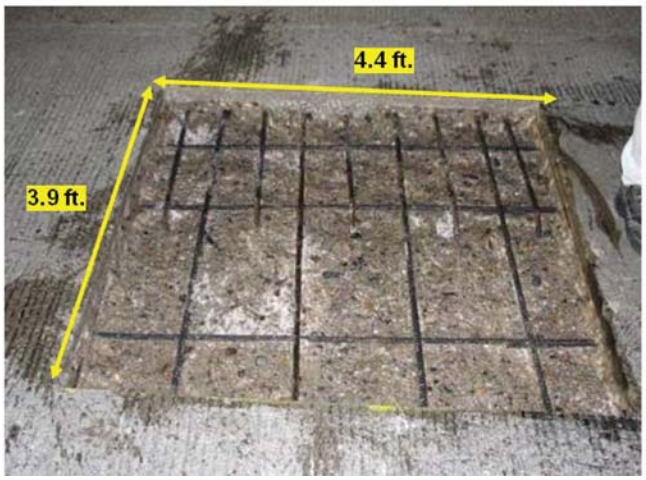

Figure 5.27 FX-928: patch area-II.

Figure 5.28 FX-928: finished patch-I.

The edges of the patches were not properly sealed and small gaps were visible between the new and the old concrete.

5.5.5 ThoRoc 10-60

One patch was installed using ThoRoc 10-60. The patch area prepared for installation is shown in Figure 5.30. The patch was located along the wheel path.

The patching mixture had a good workability. Once placed, the patch was covered with a plastic sheet for curing purposes. The finished patch is shown in Figure 5.31.

5.5.6 SET 45

Three versions of SET 45 were installed in the field:

- SET 45 Regular
- SET 45 Hot Weather
- SET 45 50/50 Blend : 50% SET 45 Regular + 50% SET 45 Hot Weather

Figure 5.29 FX-928: finished patch-II.

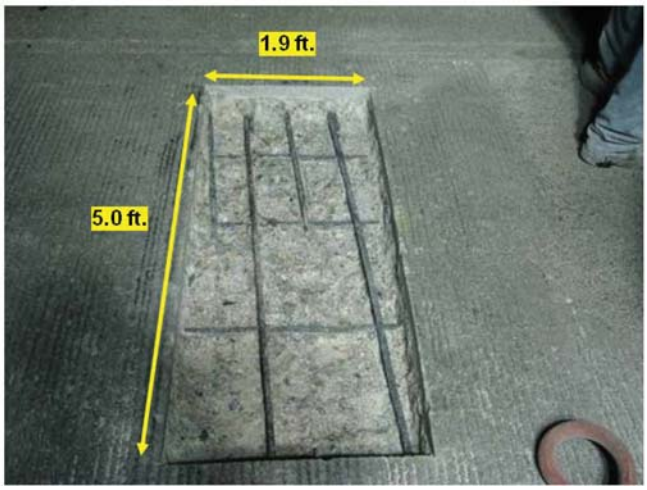

Figure 5.30 ThoRoc 10-60: patch area.

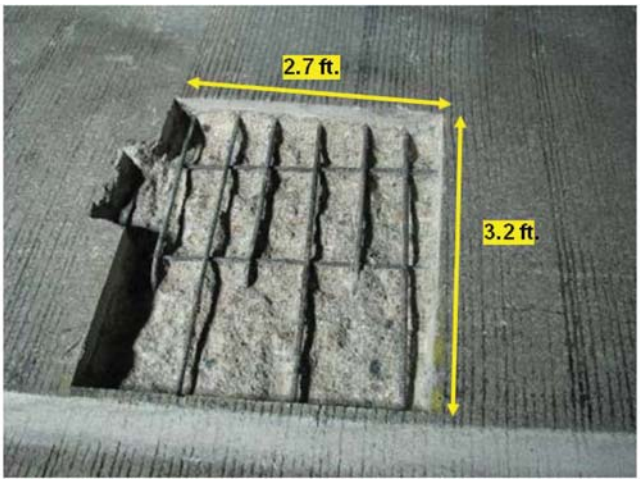

Figure 5.32 SET 45 Regular: patch area.

The regular and the 50/50 Blend versions of SET 45 were installed using pea-gravel extension while the Hot Weather version was installed without any pea-gravel extension. The patch area for SET 45 Regular material is shown in Figure 5.32 whereas the patch area for SET 45 Hot Weather material is shown in Figure 5.33. The 50/50 Blend version of the material was installed in two patch areas (see Figure 5.34 and Figure 5.35). All patches were located on the wheel path.

The SET 45 Regular finished patch is shown in Figure 5.36. The material developed air-bubbles on the surface after placement which was possibly due to the adverse interaction between the calcareous pea-gravel and the Magnesium Phosphate in the SET 45 binder (see section 3.2). Since SET 45 is not compatible with calcareous minerals, the manufacturers do not recommend the use of this material with aggregate containing such minerals.

The SET 45 Hot Weather finished patch is shown in Figure 5.37. Since this material was intended for use in Hot Weather conditions, the set-time was considerably increased due to the low ambient temperature

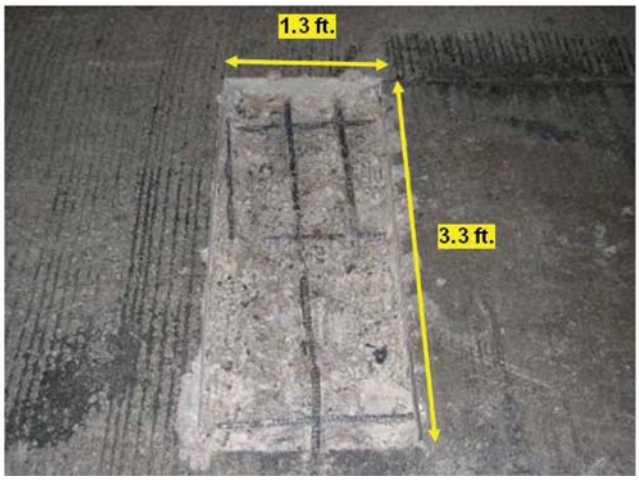

Figure 5.33 SET 45 Hot Weather: patch area.

Figure 5.31 ThoRoc 10-60 finished patch.

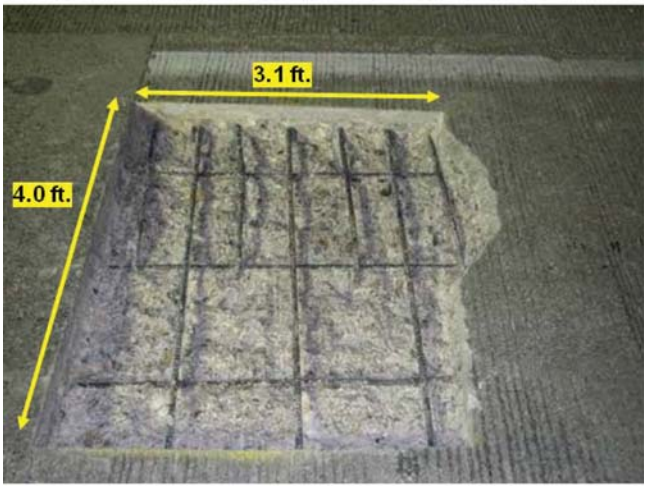

Figure 5.34 SET 45 50/50 Blend: patch area-I.

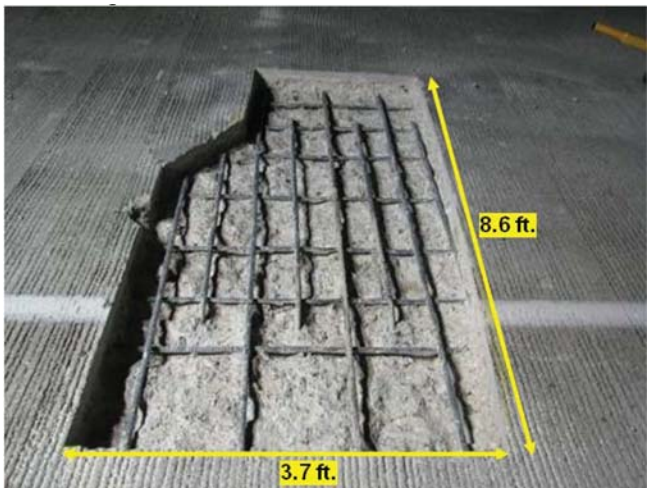

Figure 5.35 SET 45 50/50 Blend: patch area-II.

Figure 5.36 SET 45 Regular: finished patch.

conditions. This patch was installed in the un-extended form—primarily to study whether the pea-gravel used had any adverse effects on the performance. Due to the delayed setting time, the material flowed out of the patch due the grade of the surface, leading to uneven surfaces near the edges.

The SET 45 50/50 Blend finished patches are shown in Figure 5.38 and Figure 5.39. The surface air-bubbles previously observed for SET 45 Regular material were not observed for these mixes—possibly because of the retarding ingredient in the formulation of SET 45 Hot Weather material.

5.5.7 Duracal

Duracal material was available in three formulations:

- Duracal-Regular (Dur-R)
- Duracal-Air Entrained (Dur-AE)
- Duracal-Air Entrained with Fibers (Dur-AE-F) (At the time of this field placement the product was in the development stage and not yet available on the market.)

Based on the input from INDOT, Duracal-Air Entrained is the most commonly used material for rapid repairs in the state of Indiana. Also, INDOT has had good experiences with this material with respect to the long term durability when compared to the other materials they used in the past. Duracal-Regular could not be installed due to traffic control and scheduling related issues. As a result, only Dur-AE and Dur-AE-F were actually used.

As mentioned earlier, each of these two materials was installed in a single patch beside each other—due to the large size of the patch. This was approved by the material manufacturer representative present on site, who confirmed that placing the two materials side-by-side will not result in any compatibility issues as the constituent ingredients in both binders are the same—the only difference being the added fibers. The patch prepared for repair is shown in Figure 5.40. The patch was located along the wheel path (northbound direction).

The finished patches of Duracal-AE and Duracal-AE-F are shown in Figure 5.41. Extra water was added to the surface of the patch to get a proper finish—this

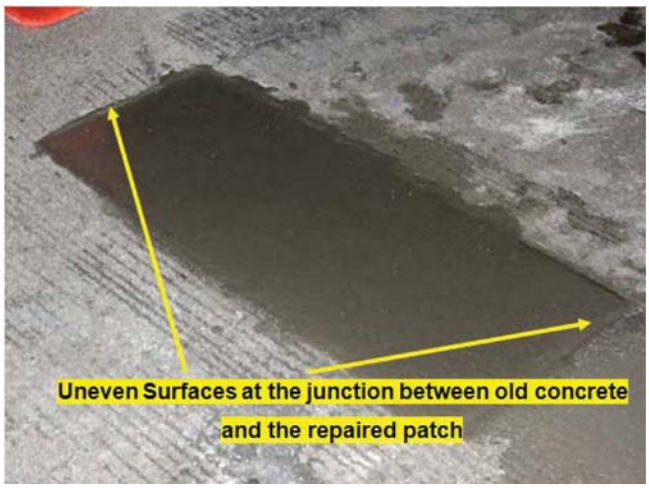

Figure 5.37 SET 45 Hot Weather: finished patch.

Figure 5.38 SET 45 50/50 Blend: finished patch-I.

Figure 5.39 SET 45 50/50 Blend: finished patch-II.

Figure 5.40 Duracal-AE and Duracal-AE-F: patch area.

is an incorrect practice as it will make the surface of the repair more susceptible to scaling.

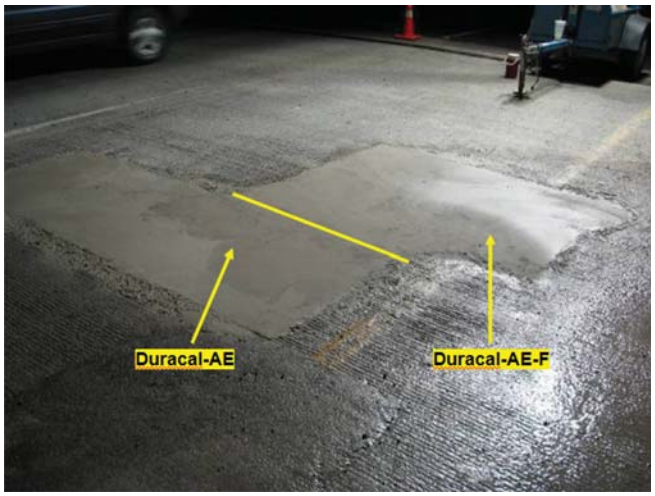

Figure 5.41 Duracal-AE and Duracal-AE-F: finished patch.

6. LABORATORY STUDY FOR GRANCRETE MATERIALS

6.1 Introduction

Near to the end of the project, one additional new rapid-setting material (Grancrete PCW) was recommended by INDOT for inclusion in the study. In order to establish the base-line characteristics of this material before its potential inclusion in the summer 2010 field trials, it was first tested in the laboratory. The laboratory tests included determination of compressive strength, setting time, freeze thaw durability and several other properties as indicated in Table 6.1. Since the performance of the Grancrete PCW material during the freeze-thaw testing was not satisfactory, its manufacturer replaced it with another formulation named Grancrete B.

Both of the products (i.e. Grancrete PCW and Grancrete B) were incorporated as binders in extended mixtures prepared using 60% of pea gravel, 15% of sand and 25% Grancrete material. The mixtures prepared during the initial phase of the laboratory trials utilized only the originally supplied binder (i.e. the Grancrete PCW material) and were produced using portable mortar mixer (see Figures 3.4 and 6.1 (a)).

Although the manufacturer recommended that the optimal water content in the mixture should not exceed 22% by the volume of the binder, that amount of water resulted in mixtures that were too stiff and thus difficult to prepare in the mortar mixer. As a result, the amount of water in the mixture had to be increased (to 31% by weight of the binder). Since, as indicated earlier, the freeze-thaw performance of these initial mixtures was not satisfactory, the increase in the water–binder ratio was not desirable. Therefore, in addition to changing the binder formulation (from Grancrete PCW to Grancrete B) the manufacturer also suggested replacing the previously described portable mortar mixer with the drill mixer (see Figure 6.1 (b)). Since this new type of the mixer provided for higher mixing efficiency, it was possible to reduce the water content of the mixture back to the originally recommended value of 22% (for the Grancrete PCW binder) and to 18% (for the Grancrete B binder). It should be pointed out, however, that the overall size of the mixture prepared with the drill mixer was only about 1/3 of that which could be prepared in the mortar mixer.

The preparation of the mixture in the drill mixer involved the following steps:

- Sand and pea gravel were placed in the bucket and mixed for about 30 seconds;
- Grancrete material and mixing water were added to the bucket;
- The initial temperature of the materials was measured using the temperature gun positioned at the constant height over the bucket (this temperature was generally in the range between 65°F and 70°F);
- The speed of the mixing was set to high, the mixing paddle was switched on and moved manually in clockwise direction along the periphery of the bucket to ensure

TABLE 6.1
Testing Matrix for Grancrete Materials

Test	Grancrete PCW	Grancrete B
Setting time (ASTM C 266)	Yes	No
Compressive strength after 2,4, 24 hours (ASTM C 39)	Yes	Yes
Compressive strength after 28 days (ASTM C 39)	Yes	No
Scaling Resistance (ASTM C672)	Yes	Yes
Free Shrinkage (ASTM C157)	Yes	No
Chloride ion penetration resistance (ASTM C1202)	Yes	Yes
Temperature profile	Yes	No
Freezing and thawing resistance (ASTM C 666, Procedure A)	Yes	Yes
Freezing and thawing resistance (ASTM C 666, Procedure B)	Yes	Yes

uniform mixing action. The mixing process continued until the temperature of the mix increased by 10°F.

- Once the mixing process was completed, the resulting extended mixture was used to prepare the test specimens. All casting was completed within 10 minutes of finishing of the mixing operation.

The experimental results obtained from specimens prepared using these and both types of Grancrete materials are discussed in the subsequent sections.

6.2 Compressive Strength

6.2.1 Comparison of the Effects of Drill and Mortar Type Mixers

The compressive strengths were measured on 3 x 6 in. cylindrical specimens after 2, 4 and, 24 hours of curing in moist room at 100% RH and 23°C. Table 6.2 summarizes the compressive strength achieved by extended Grancrete PCW mixtures batched with water content of 31% using two different types of mixers. As can be seen, at all ages, mixtures prepared using the mortar mixer had lower compressive strength than those prepared using the drill mixer. As an example, the average compressive strength at 2 hours of mixtures prepared using the drill mixer was 3042 psi as compared to the strength of mixtures prepared using the mortar mixer (2631 psi). The compressive strengths measured after 4 hours and 24 hours also followed similar trend.

The values of the average reduction in compressive strength for the extended mixtures at different times when mortar mixer was used instead of drill mixer are given in Table 6.3. It can be seen that these values were all about 14%, irrespective of the age of the specimen at the time of testing.

6.2.2 Comparison of Extended Mixtures with Grancrete PCW and Grancrete B

As previously mentioned, the manufacturer recommended to use 22% water for the extended mixtures with Grancrete PCW instead of 31% which was used initially in the laboratory. It was also suggested to reduce the batch size to avoid the problem of the stiffer mix in drill mixer. The third recommendation was to use Grancrete B mixture instead of Grancrete PCW, which was formulated have lower water demand and to achieve higher compressive strength. Table 6.4 shows the compressive strengths
of the extended mixtures prepared with both Grancrete PCW and Grancrete B for a period up to 28 days.

The water content of 22% was used for the Grancrete PCW while 18% water was used for Grancrete B. The average compressive strength for PCW mixture was 4587 psi at 2 hours and increased up to 5568 psi at 24 hours which indicated good performance in terms of strength gain. The 28-day compressive strength was 6325 psi for these mixtures.

The compressive strength of the extended mixture of Grancrete B at 2 hours was 5833 psi which was much higher compared to the strength of mixture with Grancrete PCW. The compressive strengths at 4 and 24 hours were also higher for the extended mixture with Grancrete B as compared to those with Grancrete PCW. However, the 28 days compressive strength for

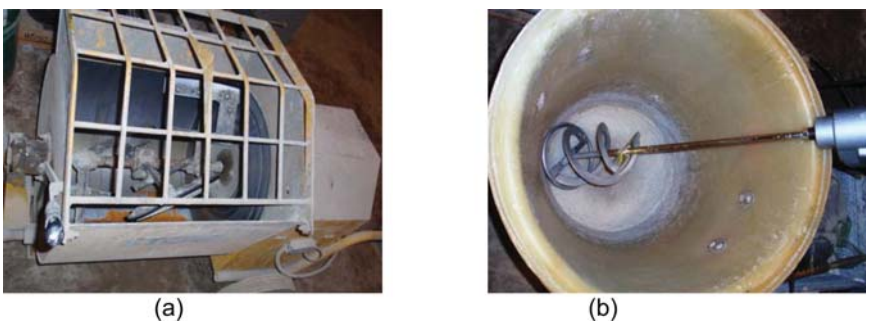

Figure 6.1 (a) Mortar mixer and (b) drill mixer.

TABLE 6.2
Compressive Strengths of the Extended Grancrete PCW Mixtures (31% Water Content) Prepared Using Drill and Mortar Mixers

Grancrete PCW (31% Water)	Drill Mixer			Mortar Mixer		
Age	2 hrs	4 hrs	24 hrs	2 hrs	4 hrs	24 hrs
Specimen 1 (psi)	3128	3302	3375	2793	2798	2924
Specimen 2 (psi)	3023	3313	3503	2641	2801	2992
Specimen 3 (psi)	2975	3046	3535	2459	2835	3094
Average (psi)	3042	3220	3471	2631	2812	3003

TABLE 6.3
Percentage of Compressive Strength Reduction Resulting From the Use of Mortar Mixer

Strength Reduction	After 2 hrs	After 4 hrs	After 24 hrs
Specimen 1 (%)	11	15	13
Specimen 2 (%)	13	15	15
Specimen 3 (%)	17	7	12
Average (%)	14	13	13

Grancrete B extended mixtures was lower than that achieved at 24 hours and lower than that of the Grancrete PCW mixtures at 28 days. The origin of this apparent strength regression is not clear.

In addition to the compressive strengths, the hardened concrete air contents of specimens from both of these two materials were measured using the flatbed scanner method (*39*). The following procedure was implemented for this purpose.

1. The 3×4 in. specimens were polished (as per ASTM C457 procedure) and their surface was colored black using thick tip marker. The coloring was performed using even, long and slightly overlapping strokes. The coloring proceeded in one direction after which the specimen was rotated 90 degrees and colored in other direction. At least 3 layers of ink were applied in each direction—more if the specimen was not uniformly black.
2. The barium sulfate ($BaSO_4$) powder was pressed in the holes present on the surface of the specimen using flexible spatula to spread it uniformly over the entire surface (the zinc oxide (ZnO) can also be used for this purposes). The powder was reapplied (as needed) until all voids completely filled. Note: the dust mask should be used during this operation.
3. The surface was cleared of excess deposits of $BaSO_4$ (by wiping it off with the palm of an open hand until the protruding powder was removed) and any powder-filled voids present in aggregates ware colored black with a fine-tip marker.
4. A small (~0.25 x 0.25 in.) self-sticking paper squares were applied to each corner of the black-colored surface to elevate it slightly and thus to prevent direct contact with the glass plate of the scanner (to prevent scratching of the surface of the glass).
5. Surface was then wiped off gently one more time with slightly oiled palm of the open hand and placed on the glass plate of the scanner.
6. The cover of the scanner was then closed and the image of the surface of the specimen was acquired for further analysis of the air-void system parameters.

The results of this analysis for the extended mixtures with Grancrete B and Grancrete PCW specimens are depicted in Figure 6.2. The air contents for these two specimens are, respectively 4.8 and 3.9%, which is less that the amount typically required for proper freeze/thaw (F/T) protection of the plain concrete ($6.5 \pm 1.5\%$) respectively which is less than required for good FT resistance. Similarly, the values of the spacing factors were also above those recommended for the plain concrete (0.2 mm) as being indicative of the adequate frost resistance. It should be pointed out, however, that it is possible that Grancrete concrete may require different F/T resistance criteria than those developed

TABLE 6.4
Compressive Strength (psi) for Mixtures with Grancrete PCW and Grancrete B

	Grancrete PCW (Water Content 22%)				Grancrete B (Water Content 18%)			
Specimen	2 hrs	4 hrs	24 hrs	28 days	2 hrs	4 hrs	24 hrs	28 days
1	4885	4670	5470	6245	5500	6105	6320	6015
2	4520	4630	5705	6240	6215	5905	6300	5790
3	4355	4605	5530	6490	5785	6110	6455	6015
Average	4587	4635	5568	6325	5833	6040	6358	5940

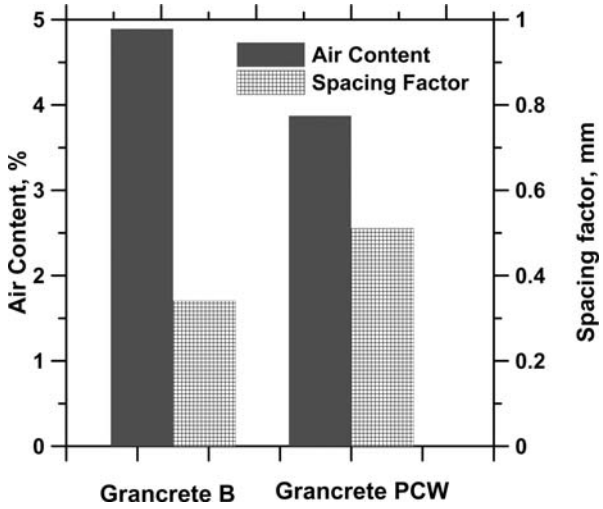

Figure 6.2 Air void parameters in hardened Grancrete concrete using the flatbed scanner method.

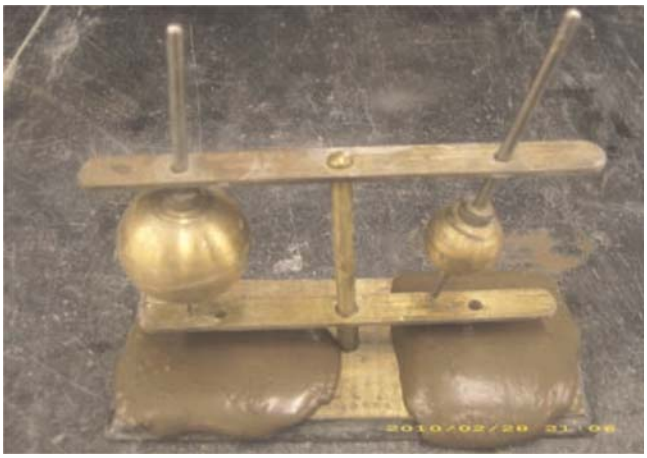

Figure 6.3 Gillmore apparatus and test specimen used for measuring the setting time.

for plain concrete. In addition, the presented results can't be generalized as only one of each specimen was tested and these specimens might have not represented the typical properties of the material.

6.3 Setting Time

Figure 6.3 shows the Gillmore apparatus (ASTM C266) (*22*) used for measuring the initial and final setting time of the Grancrete PCW. The normal consistency was measured to be 18%. The initial and final setting times obtained using this method, were, respectively 21 and 37 minutes.

6.4 Free Shrinkage

The set-up used for free shrinkage measurement is shown in Figure 6.4(a). Figure 6.4(b) shows the values of free shrinkage for Grancrete PCW extended mixture with 31% water which indicate that the free shrinkage develops rapidly (within the first day or two after casting) but it stabilizes after about seven days. The observed ultimate level of shrinkage was within about 800 to 1,000 micro-strains and it was comparable with (although slightly higher) the level of shrinkage observed in other rapid-setting materials discussed earlier in this report.

6.5 Temperature Evolution

The temperature evolution profile for extended mixture prepared with the PCW material is shown in Figure 6.5. The mixture reached the maximum temperature of about 57°C (135°F) about 45 minutes after mixing. The specimen cooled down to room temperature within about 3.5 hours after mixing.

6.6 Rapid Chloride Permeability Test (RCPT) Results

The rapid chloride permeability test was performed on specimens prepared from extended Grancrete materials

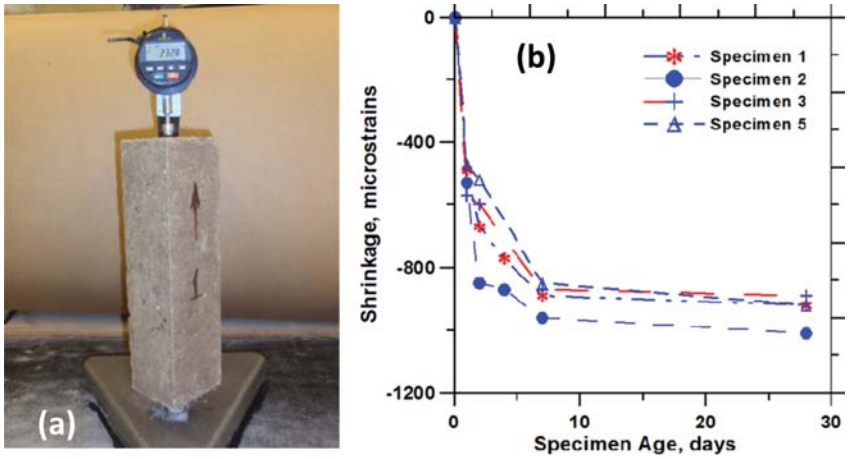

Figure 6.4 Free shrinkage measurement setup (a) and shrinkage results (b) for PCW mixtures with 31% of water.

cured in a moist room (100% RH and 23°C) for 28 days. The test procedure followed the requirements of the ASTM C 1202 test method (*31*). The results of these tests are presented in Table 6.5.

It can be observed that charges recorded for the Grancrete B mixtures were very high compared to those obtained for the Grancrete PCW material. Using the ASTM C1202 criteria (*31*), the Grancrete B specimens will be classified as having low resistance to chloride ion penetration. This conclusion was further confirmed by significant (more than 30°C) increase in the temperature of the anolyte (NaCl solution) observed during the test.

6.7 Freeze Thaw Resistance of the Extended Mixtures

The freeze thaw resistance of the extended mixtures was initially evaluated using ASTM C666 procedure A (rapid freezing and thawing in water) (*29*). The test was latter repeated (on different set of specimens) using the ASTM C666 procedure B (rapid freezing in air and thawing in water) to evaluate the role of test method and FT resistance of these mixtures.

6.7.1 Test Results for Grancrete PCW Concrete Using ASTM C 666 Procedure A

The results of the F/T testing performed on the Grancrete PCW concrete prepared with 31% water content and tested according to the ASTM C66, procedure A method are shown in Table 6.6.

The Set I specimens showed a very drastic (about 50%) reduction in the value of the relative dynamic modulus of elasticity (RDME) after only about 36 F/T cycles and failed (disintegrated) after less than about 72 cycles. The test was repeated for the same mixture with new set of specimens (Set II) and the results showed very little improvement compared to Set I specimens.

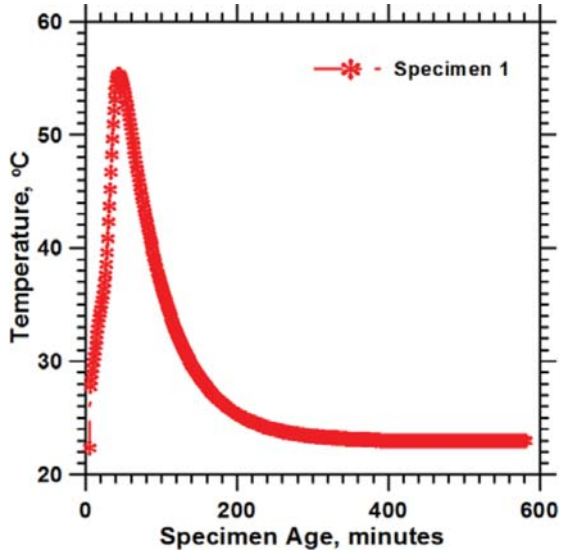

Figure 6.5 Temperature profile for the extended mixture of Grancrete PCW.

The Set II specimens also failed (disintegrated) at about 72 F/T cycles. Using the commonly accepted criteria for adequate F/T resistance of concrete, the RDME values should be a minimum of 60% and should not be reached before the concrete experiences at least 300 F/T cycles. Considering these criteria, the Grancrete PCW mixtures will be classified as having inadequate F/T resistance.

6.7.2 Test Results for Grancrete PCW and Grancrete B Concretes Using ASTM C 666 Procedure A

This section compares the F/T results for mixtures prepared with two different materials: Grancrete PCW and Grancrete B. Unlike the Grancrete PCW mixtures presented in the previous section, which contained 31% of water, the PCW mixtures presented in this section were prepared with lower water content (22%). The specimens made from Grancrete B extended mixture contained even lower (18%) amount of water. Both types of specimens were exposed to the same F/T test method—the ASTM C666 procedure A (rapid freezing and thawing in water).

Similarly to what was reported in the previous section, both types of specimens showed poor F/T performance and experienced significant (about 50%) reduction in the RDME values after only about 36 cycles. In addition, their surfaces showed significant amount of scaling as illustrated in in Figure 6.6.

In summary, despite the reduced content of water both the original (Grancrete PCW) and reformulated (Grancrete B) materials exhibited very poor F/T resistance when tested according to ASTM C 666 Procedure A.

6.7.3 Test Results for Grancrete PCW and Grancrete B Concretes Using ASTM C 666 Procedure B

This section compares the F/T resistance of the same Grancrete materials (PCW and B) as those described in the previous section but using the ASTM C666 procedure B test method (rapid freezing was in air and thawing in water) which is considered less harsh than procedure A (rapid freezing and thawing in water). Specifically, the specimens were thawed in water for 8 ± 1 hours at 23°C and were subjected to freezing in air for 10 hours at -18°. The total length of the complete freeze-thaw cycle was 24 hours and included the ramp-up time to reach the target temperatures. The ASTM procedure B test method was performed at the insistence of the manufacturer who indicated that Grancrete

TABLE 6.5
The RCPT Charge Passed for Grancrete PCW-A and Grancrete B Mixtures

	RCPT Charge (Coulombs)	
Extended Mix with	**Specimen 1**	**Specimen 2**
Grancrete PCW	3553	2371
Grancrete B	9131	7243

TABLE 6.6
Relative Dynamic Modulus of Elasticity (RDME) for Grancrete PCW Concrete (Sets I and II) with 31% Water Content (ASTM C666, procedure A)

	Set I (Grancrete PCW, 31% Water Content)		
Number of Cycles	Specimen 1	Specimen 2	Average
0	100	100	100
36	51.06	54.85	52.96
72	Failed	Failed	Failed
	Set II (Grancrete PCW, 31% Water Content)		
0	100	100	100
36.0	57.6	62.0	59.8
72	Failed	Failed	Failed

materials are hydrophobic and thus their F/T performance may be negatively affected by the exposure to water.

The results of F/T tests for these materials are shown in Figure 6.7.

The Grancrete B mixture again exhibited poor F/T resistance as indicated by excessive (to below 40%) loss of RDME values after only 14 F/T cycles. Due this high loss of the RDME the testing of mixture with Grancrete B was discontinued at 14 days. On the other hand the F/T performance of the Grancrete PCW mixture (with 22% water content) improved significantly when compared with the results obtained when testing using the ASTM C666 procedure. Specifically, the value of the RDME after 76 F/t cycles was 83%, still well above the minimum recommended value of 60%. Unfortunately, the test had to be discontinued at this time due to failure of the environmental chamber used for testing.

The changes in mass of the F/T specimen paralleled the trends observed for the RDME values. Initially, specimens from both types of materials experienced small (about 1%) mass gain. As already mentioned, the test for Grancrete B was discontinued after 14 days. However, the mass of the Grancrete PCW remained more-or-less constant until the termination of that test (after 76 days).

6.8 Scaling Resistance

The visual ratings (as per ASTM C 672) (*30*) of the surface for the extended mixtures with Grancrete materials are shown in Table 6.7.

The condition of the surface of both types of mixtures after 25 F/T cycles was ranked as 1, which indicates only slight scaling and overall good scaling performance. Unfortunately the problem with the environmental chamber prevented the researchers form continuing this test up to the recommended length of 50 cycles. It should be also mentioned that relatively high stiffness and rapid hardening rate of these materials made the task of preparation of the scaling specimens more challenging that that experienced when preparing specimens form plain concrete mixtures.

6.9 Summary

This section summarizes the performance of the two new materials added to the original test matrix. These materials were: Grancrete PCW and Grancrete. The tests completed on these materials resulted in the following observations:

1. The type of mixer used to prepare the materials had significant influence on their strength characteristics. Specifically, the compressive strength of the mixtures prepared in a drill mixer (which is recommended by the manufacturer of the Grancrete material) was 10-20 % higher than the compressive strength of the same material prepared in the mortar mixer. The limitation of a drill mixer is a small batch size which will create problems during field patching of larger areas.
2. The compressive strengths of Grancrete PCW extended mixture with 22% water and Grancrete B extended mixture with 18% water were satisfactory at all ages tested with Grancrete B showing better strengths at early ages.

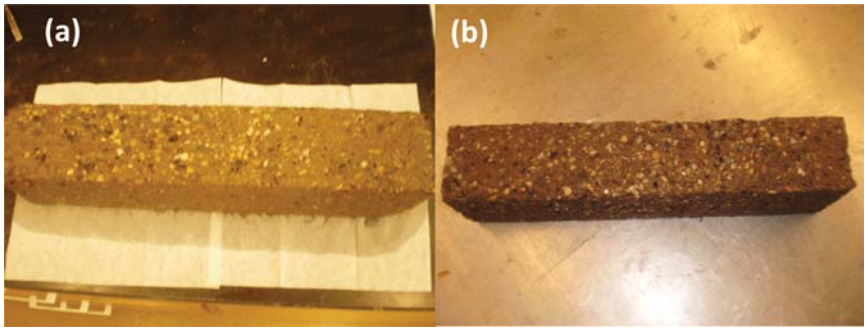

Figure 6.6 Scaled surfaces of FT of specimens made with (a) Grancrete PCW extended mixture and (b) Grancrete B extended mixture after 36 FT cycles.

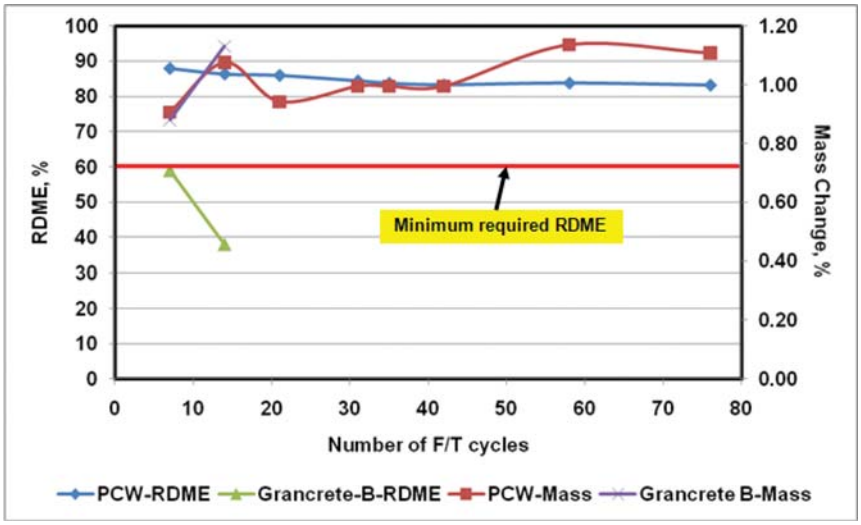

Figure 6.7 Values of relative dynamic modulus of elasticity (RDME) and mass changes for Grancrete materials exposed to FT cycles as per ASTM C666 Procedure B.

TABLE 6.7
Visual Ratings of Slabs Exposed to 4% $CaCl_2$ Solution

	5 cycles	10 cycles	15 cycles	20 cycles	25 cycles
Grancrete PCW	0	0	0	1	1
Grancrete B	0	0	1	1	1

3. The first set of freeze thaw specimens utilizing extended mixture with Grancrete PCW material containing 31% of water failed before reaching 72 cycles in procedure A of ASTM C 666. The Grancrete B materials with 18% water exhibited poor performance in FT test under both procedures A and B of ASTM C 666.
4. The Grancrete PCW with 22% water showed relatively high (about 83%) value of the RDME after 76 FT cycles when tested using procedure B of ASTM C666. That material has potential to last 300 FT cycles when tested using this procedure but this possibility will have to be by additional testing.
5. The chloride ion penetration resistance (as per ASTM C1202 RCPT) (*31*) indicated high chloride ion permeability (charge >4000 Coulombs) for both of the extended mixtures.
6. The development of the temperature, free shrinkage, and setting time tests were not carried out for the extended mixture with Grancrete B due to limited time available during the project and limited quantities of material supplied by the manufacturer.
7. The observations reported above are applicable only to particular mixtures used in the study and will likely change if different extension level or w/c ratio were used.

7. LABORATORY INVESTIGATIONS OF SPECIMENS FROM SUMMER 2010 FIELD INSTALLATIONS

7.1 Introduction

This chapter focuses on 4 commercial rapid-setting patching materials which were added to the collection of 10 other rapid-setting materials previously installed in patches on the deck of the I-65 bridge near West Lafayette, Indiana (see section 5.1 of this report). The installation of the original 10 materials took place in October 2007. The new (added) materials were also installed at the same location as the original ones. That installation was performed on July 7–8, 2010.

Due to the time limitations the detailed laboratory study of the new materials was not conducted prior to their filed installation. However, both cylindrical (3 x 6 in.) and prismatic (3 x 4 x 16 in.) specimens were cast on site at the time of field installation and used for a limited study of basic properties. These properties included: compressive strength, freeze-thaw (F/T) durability, mixture temperature (after 25 minutes of placement) and characteristics of the air void system in the hardened concrete. In addition, qualitative evaluation of such properties as ease of placement, physical appearance and workability was also performed based on the field observations of the installation process. The results from these tests and observations are discussed in the following sections.

7.2 Materials Used and Fresh Mixtures Properties

The four new rapid-setting materials used for the field installation of patches included the following: MG-Krete (IMCO Inc.), Zero-C (BASF), Pro-Poxy 2500 (Unitex) and Fastrak (L&M). The MG-Krete material was installed during the night of July 7, 2010, whereas the remaining three materials were installed during the night of July 8, 2010.

Each of the freshly-batched rapid-setting patch material was used to prepare two freeze-thaw beams ($3 \times 4 \times 16$ in.) and 9 cylinders (3×6 in.). These specimens were placed in a curing room for 12 hours before demolding. A set of three cylinders was used to evaluate the value of the compressive strength (as per ASTM C39) at each of the two testing periods (12 hours and 28 days). In addition, cylindrical specimens from each material were cut into half and each half was prepared for air void analysis using scanner method (*39*).

Two weeks after its original installation, the patch using the Zero-C material had to be replaced as apparently the mixture was not batched correctly the first time around. While on the bridge to re-sample the new batch of Zero-C material, the research team had the opportunity to observe the condition of the surface of the patches from the three other materials. These observations are documented in Figure 7.1. It can be seen that while the surfaces of the Fastrack and Pro-Poxy patches appear to be crack-free, the surface of the MG-Krete patch displays the network of extensive cracking. Since this cracking occurred during the summer time, it is likely that it will get worse when the patch is subjected to the cycles of freezing and thawing during the winter months and thus necessitate the replacement of the patch.

Table 7.1 provides a general summary of the fresh mixture properties collected at the time of batching and placing. While all but one (temperature) pieces of information provided in Table 7.1 are quantitative in nature, that summary offers useful insight into the potential issues that need to be addressed by the installers of these materials.

7.3 Compressive Strengths

The compressive strength was determined on 3 x 6 in. cylinders 12 hours and 28 days of curing in 50% relative humidity room at 23°C.

7.3.1 Compressive Strength at 12 Hours

Table 7.2 and Figure 7.2 show the values of the compressive strength for each material after 12 hours. Depending on the material, the values of the average compressive strength spanned a wide range (from about 1,300 psi to about 5,700 psi). Two of the materials (MG-Krete and Pro-Poxy 2500) achieved similar strengths (about 3,200 psi). At about 5,700 psi the Fastrak material was the strongest whereas the strength of the Zero-C material was the lowest (only about 1,300 psi).

The Zero-C values shown in Figure 7.2 are for the first mix that had to be replaced two weeks after the original installation due to batching problems.

7.3.2 Compressive Strength after 28 Days of Air Curing

Table 7.3 and Figure 7.3 show the values of the compressive strength for each material after 28 days. The average compressive strength for MG-Krete specimens was 5050 psi while it was 5810 psi for Pro-Poxy 2500 and 9810 psi (the highest among materials tested) for Fastrak. The 28-day compressive strength of Zero-C material was only 1765 psi. As mentioned earlier, this mixture started crumbling and coming came out of the patch the very next day after original placement and had to be replaced after only 2 weeks of service. The replacement patch used the same material as the original patch but this time the material was mixed by hand in the bucket (rather than by mortar mixer as was the case for the mixture used in first installation). The 28-day compressive strength results shown in Table 7.3 and in Figure 7.2 are for the second batch of this material and indicate that it was still the lowest performer with respect to strength.

7.4 Air Contents of the Hardened Concretes by Scanner Method

In addition to strength, the F/T resistance is the most important property of the patching materials which is intended for use in locations with cold winters. The freeze thaw resistance of any concrete material depends on the quality of the air void systems of the matrix. To analyze the existing air voids systems of patching materials presented in this chapter, the cylinders cast from these materials were cut along the long axis, polished and used for determination of the percent of air voids as well as associated spacing factor values. Two specimens of each material were used to obtain air void system parameters using flatbed scanner method (*39*). The results of this test are presented in Table 7.4.

The results summarized in Table 7.4 show much higher air contents for Zero-C and Pro-Proxy materials that that observed for Fastrak and MG-Krete. This is likely the results of the presence of excessive amounts of entrapped air present in the former materials which were either stiff or sticky and thus difficult to compact (see Table 7.1). The Fastrak material was very much workable and thus it did not experience the problem of

Figure 7.1 Appearance of the surfaces of the 2-weeks-old patches for (a) MG-Krete, (b) Fastrak, and (c) Pro-Poxy 2500 materials.

TABLE 7.1
Summary of Field Observations Collected during Batching and Patching Operations

Brand (# of Patches)	Temp. after 25 Min.	Mixing Method	Workability/Appearance	Special Mixing Requirements
MG-Krete (3)	95°F	Hand mixed & drum mixer	Good / good	Do not use water
Zero-C (2)	110°F	Mortar mixer, Hand mixed in bucket	(1) Poor / extremely dry, difficult to work, (2) fair / fairly good, watery	Requires curing compound
Pro-Poxy 2500 (1)	86°F	Hand mixed in bucket	Appearance was good but it was a very sticky material, difficult to work with	Parts A and B are mixed for 3 min. and poured in drum and Part C was added during mixing
Fastrak (2)	80°F	Drum mixer	Good / excellent, cohesive mix	None

TABLE 7.2
Compressive Strength of Rapid-Setting Materials after 12 Hours

	MG-Krete	Zero-C	Pro-Poxy 2500	Fastrak
Specimen 1	3065	1060	3090	6170
Specimen 2	3525	1635	3430	4735
Specimen 3	3135	1240	3665	6380
Average (psi)	3155	1312	3395	5762

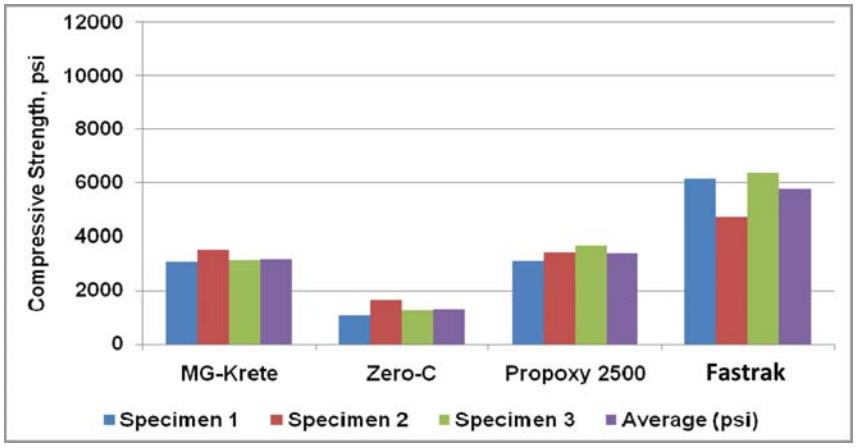

Figure 7.2 Compressive strength of rapid-setting materials after 12 hours.

TABLE 7.3
Compressive Strength after 28 Days

	MG-Krete	Zero-C	Pro-Poxy 2500	Fastrak
Specimen 1	5155	1770	5485	9700
Specimen 2	5110	NA	5690	9920
Specimen 3	4890	1755	6255	9960
Average (psi)	5052	1763	5810	9860

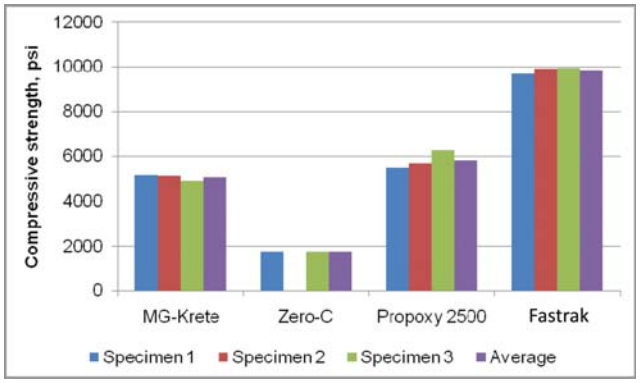

Figure 7.3 Compressive strength of rapid-setting materials after 28 days.

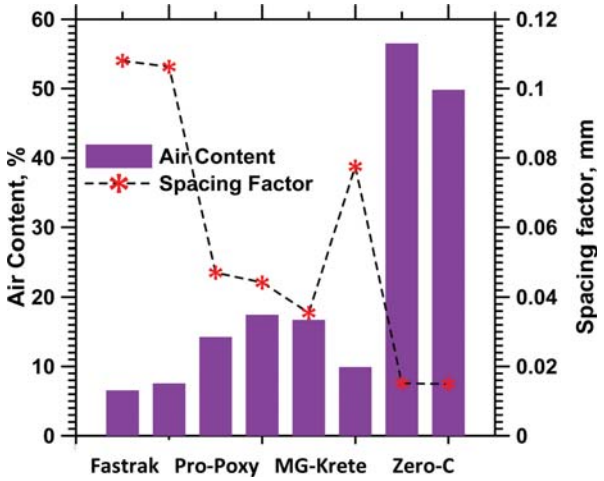

Figure 7.4 Graphical presentation of the air void system parameters for different patching materials.

entrapped air and exhibited parameters with respect to the air content and spacing factor. One of MG-Krete specimen also exhibited high air content due to entrapped air. These parameters need to be further investigated using laboratory mixtures as setting of these materials is fast and it is difficult to prepare a quality specimen during the night-time field placement. Figure 7.4 shows the graphical representation of the air void parameters given in Table 7.4.

7.5 Freeze Thaw Test Results

The FT test was performed by exposing the beams to F/T cycles in the freeze-thaw machine as per ASTM C 666 procedure A. The changes in mass, length, and resonant frequency due to the effects of rapid freezing and thawing cycles were reported after every 36 cycles. Figures 7.5(a) to 7.5(d) show the appearance of surfaces of the specimens after completion of 300 cycles of the F/T test. Significant amount of scaling was observed on surfaces of specimens from two of the tested materials (Zero-C specimens—Figure 7.5(a) and MG-Krete specimens—Figure 7.5(c)). In contrast, almost no scaling was visible on surfaces of specimens made from Pro-Proxy material (Figure 7.5(b). Figure 7.5 (d) indicates only a moderate scaling on surfaces specimens made from Fastrak material.

Figure 7.6 shows mass changes for specimens from all four materials. As expected, the specimens which experienced the most severe scaling (prepared with MG-Krete material) also show highest mass losses. Also the mass loss of these specimens was rather moderate (and on par with that observed form other specimens) up to about 140 cycles, the rate of mass changes increased rapidly upon further exposure and the total mass loss was about 25% after about 300 FT cycles. This significant mass indicates that unlike for three other materials (where the mass loss was due to peeling-off of the surface layers) the process of F/T deterioration in the MG-Krete specimens affected the entire cross-section of the samples.

Figure 7.7 shows changes in the relative dynamic modulus of elasticity (RDME) for all materials tested. The RDME values for Zero-C materials decreased slowly during the course of the test and reached the value of about 95% after 300 FT cycles indicating good performance for this material with respect to FT deterioration. It can also be seen from Figure 7.7 that

TABLE 7.4
Air Void Parameters for the Rapid-Setting Materials

Specimen	Air %	Specific Surface, mm^2/mm^3	Spacing Factor, mm
Fastrak 1	6.55	22.008	0.108
Fastrak 2	7.56	19.182	0.106
Pro-Poxy 1	14.24	21.323	0.047
Pro-Poxy 2	17.44	17.842	0.044
MG-Krete 1	16.71	23.437	0.035
MG-Krete 2	9.91	19.550	0.078
Zero-C 1	56.52	8.485	0.015
Zero-C 2	49.83	11.244	0.015

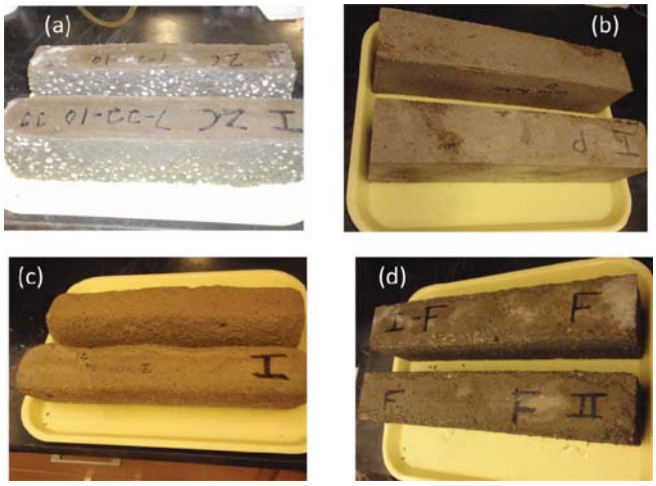

Figure 7.5 The appearance of surfaces of specimens at the completion of the F/T test: (a) Zero-C, (b) Pro-Poxy 2500, (c) MG-Krete, and (d) Fastrak.

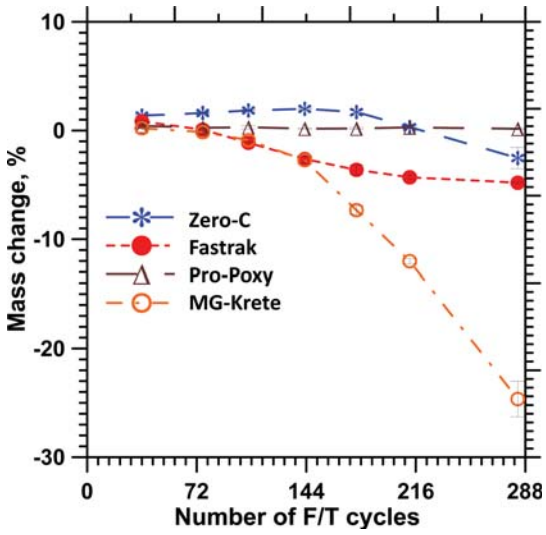

Figure 7.6 Mass changes during the FT testing.

the RDME values are almost constant for specimens from Fastrak throughout the 300 FT cycles, indicating excellent performance for this material during freezing and thawing. Similarly, the F/T performance of the Pro-Poxy 2500 material was also good. However, the performance of the MG-Krete material was not good, as indicated by the value of the RDME (durability factor) being lower than 60 %after about 288 F/T cycles.

7.6 Summary

The various categories of data presented in this chapter with respect to performance of the 4 rapid-setting materials installed in the patches of the bridge deck in the summer of 2010 lead to the following observations and conclusions:

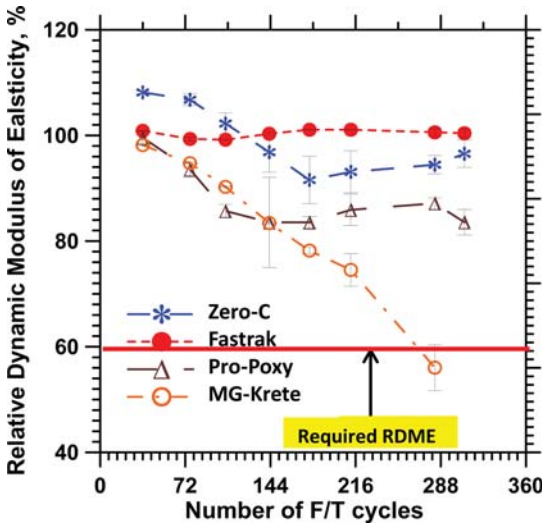

Figure 7.7 Changes in relative dynamic modulus of elasticity during FT test.

1. When tested 12 hours after mixing, the Fastrak material exhibited highest value of compressive strength (5762 psi) whereas the Zero-C material was the weakest (1312 psi). The other two materials (MG-Krete and Pro-Poxy 2500) developed adequate strengths of, respectively, 3155 psi and 3395 psi.
2. For the purposes of this project, the minimum 28-day compressive strength was set at 35 MPa (5076 psi). Three out of the four material tested (Fastrak, Pro-Poxy 2500 and MG-Krete) did satisfy this requirement. However, the 28-day compressive strength of the fourth material (Zero-C) was only 1763 psi, well below the target value.
3. The Freeze thaw durability of specimens made from Fastrak and Pro-Poxy 2500 materials was excellent as these specimens exhibited very little reduction in mass and the value of RDME. Although, MG-Krete exhibited good compressive strength at 12 hours, it scaled excessively during the FT testing and lost more than 25% of mass after 300 FT cycles. Also the % RDME value of the MG-Krete was found to be lower than the minimum acceptable value (60%).
4. The Fastrak material was the easiest to work with, as it could be mixed in regular drum mixer and exhibited great workability (resembling the self-compacting concrete in appearance). As a result the tasks of preparation of the mixture and its placing can be accomplished easily and very efficiently.
5. Based on the results of compressive strength and FT test Fastrak seemed to provide the best overall performance amongst the studied material while Zero-C was the least suitable material due to its much lower compressive strength and difficulty in mixing at the site in large quantities.

8. SUMMARY AND CONCLUSIONS

8.1 Introduction

The primary tasks of this research included laboratory evaluations of the mechanical and durability aspects of various repair materials followed by field installation of patches constructed using these materials and their in-service performance monitoring. During Phase-I of the study (laboratory study), it was observed that majority of the materials showed acceptable performance with respect to rate of strength gain, bond-strength, and shrinkage. However, some of the materials exhibited poor freeze-thaw resistance which is one of the primary factors that influences the long term performance of the repaired structures in a state like Indiana where the pavements/bridge-decks are exposed to severe freeze-thaw conditions during the winters. During Phase-II of the study (field installations), the construction related issues were also found to be playing a significant role in the durability of the repairs performed.

This chapter presents a summary of the laboratory test results and field installation related on the repair materials studied. Section 8.2 presents a compendium of the laboratory test results (using the laboratory mixes) followed by Section 8.3 which presents a summary of the field-performance of the materials. Section 8.4 presents a comparison between the

performance of the laboratory and field mixes (in terms of compressive strength and freeze-thaw resistance) of the repair materials. Possible modifications to INDOT's specification for rapid-setting repair materials and suggestions/recommendations for proper quality control of field mixes are presented in sections 8.5 and 8.6 respectively. Section 8.7 presents an analysis of the laboratory and the field performances of the materials in order to select the promising materials for further field testing. Section 8.8 highlights the future research directions while the concluding remarks are presented in section 8.9.

8.2 Summary of Laboratory Test Results

This section presents the summary of the laboratory test results. Table 8.1 presents a summary of the fresh properties of the repair materials.

8.2.1 Setting Time

- All except for two materials (TR and Dur-AE) had a final setting time shorter than (or equal to) 35 minutes. The final setting times of the TR and Dur-AE materials were longer than 45 minutes.

8.2.2 Ability to Flow

- The FX, TR, Dur-R and Dur-AE materials showed good flow characteristics and they may be considered to be self-leveling repair materials.
- The SQ and HD materials experienced rapid slump loss. These materials should be placed within 4-8 minutes of mixing to avoid consolidation/finishing problems.

8.2.3 Mechanical Properties

Table 8.2 presents an overview of the mechanical properties (compressive strength and bond strength) of the repair materials evaluated in the laboratory.

- In general, all materials (except Duracal-AE) showed acceptable rates of strength gain. Duracal-AE was the only material with compressive strength values of less than 25 MPa at the age of one day—possibly due to the excessive amount of water added during the mixing (above the levels recommended by the manufacturer).

TABLE 8.1
Fresh Properties

	Setting Time (Min)		Workability (mm)
Material	**Initial**	**Final**	**Slump (S)/Flow (F)**
FX	15	22	550 (F)
SQ	15	27	228.6 (S)
HD	13	31	228.6 (S)
TR	34	47	410 (F)
Dur-R	16	35	760 (F)
Dur-AE	18	48	720 (F)

- The SQ, HD and TR materials exhibited fastest early-age rates of strength gain and attained compressive strength of over 35 MPa (5076 psi) at the age of one day.
- All the materials exhibited good bond properties based upon the slant-shear test method.
- The ASTM C 928 requirements at the ages of 1 day (7 MPa) and 7 days (10 MPa) were met by all materials.
- For FX and SQ materials there was practically no difference between the 1-day and the 7-day slant-shear bond strengths.
- The Dur-R and Dur-AE materials were the only materials with bond strengths less than 10 MPa at the age of 1 day.

8.2.4 Dimensional Stability

Table 8.3 provides a summary of the dimensional stability (free and restrained shrinkage) data of the repair materials.

- The FX, Dur-R and Dur-AE exhibited the lowest shrinkage in the free-shrinkage test with values of less than 400 $\mu\varepsilon$.
- The SQ and HD materials exhibited the highest free shrinkage values of, respectively, over 600 and 700 $\mu\varepsilon$.
- In the restrained ring test, none of the materials cracked after 35-days which indicates that all materials have low cracking susceptibility.

8.2.5 Durability Properties

A summary of the durability properties (F-T resistance, scaling resistance and rapid chloride permeability) of the repair materials is presented in Table 8.4.

- The FX, SQ and HD materials showed excellent F-T resistance with RDM values of >80% after 300 F-T cycles.
- The Duracal-AE material performed relatively poorly in the F-T test (RDM of 35% after 300 F-T cycles).
- The TR and Dur-R specimens deteriorated completely after just 30 F-T cycles.
- The HD and TR specimens performed extremely well in the scaling test with a visual rating of zero.
- The FX and SQ specimens exhibited a slightly lower scaling resistance with visual rating values of 1.
- The overall performance of the all the materials in the scaling test was satisfactory.
- The Dur-AE was the only material with high chloride ion permeability values. All the other materials had moderate to low chloride ions permeability.

8.3 Summary of Field-Performance of the RMs

The field performances of the repair-patches were reviewed on April 19, 2008. After one winter season, the following were the observations:

- HD-50 was by far the best performing material.
- Duracal-AE and Duracal-AE-F came a close second to HD-50 barring the surface abrasions which are attributed to construction related issues (improper finishing practices).

TABLE 8.2
Mechanical Properties of Laboratory Mixes

Material	Compressive Strength (Extended) (MPa)				Slant Shear Bond Strength (MPa)		Iowa Shear Bond Strength (MPa)	
	2 Hr	4 Hr	1 Day	28 Day	1 Day	7 Day	1 Day	7 Day
FX	17.2	20.0	31.9	51.7	12.5	12.5	3.2	3.4
SQ	33.0	34.6	37.4	42.0	13.2	13.2	2.8	3.1
HD	30.3	34.4	39.5	52.8	12.6	14.8	3.1	3.3
TR	33.7	39.0	45.1	62.3	13.5	15.2	2.6	2.9
Dur-R	11.2	12.1	25.7	41.2	9.6	12.9	1.6	2.8
Dur-AE	8.8	9.2	18.6	32.6	8.1	11.2	1.3	2.3

TABLE 8.3
Dimensional Stability Properties

Material	28-Day Free Shrinkage (με)*	Cracking Susceptibility*
FX	-325	Low
SQ	-636.7	Low
HD	-716.7	Low
TR	-506.7	Low
Dur-R	-376.7	Low
Dur-AE	-376.7	Low

*Extended material.

- ThoRoc 10-60 SET 45-50/50 Blend and SET 45 Hot Weather versions performed reasonably well with minor surface cracks.
- FX-928 did not perform very well. It developed multiple surface cracks.
- SET 45 Regular is not suitable for use in the state of Indiana (with locally available pea-grave as an extender) as this aggregate may have high content of the calcareous material which has the potential to reduce durability of patches constructed with this binder.
- SikaQuick-1000 and SikaQuick-2500 did not perform well (developed cracking and surface abrasions) primarily due to improper mixing and construction related issues (poor consolidation).

8.4 Laboratory vs. Field Mixes: Compressive Strength and Freeze-Thaw Resistance

During the field installation of the repair materials, freeze-thaw and compressive strength specimens were cast on-site to compare the performance of the field mixes to the laboratory mixes and also to correlate the laboratory and field performances of the repair materials. The specimens cast on-site were de-molded after 12 hours and were exposed to the natural environment (same environment as the repair patches). Figure 8.1 shows the freeze-thaw resistance characteristics of specimens cast using the field mixes.

It can be noticed from Figure 8.1 that the SQ-2500 specimens failed after 160 F-T cycles and the SET 45 50/50 specimens failed after around 140 F-T cycles. The SET 45 R specimens failed within 30 F-T cycles (even before the first measurement could be performed).

The appearance of the SET 45-R specimens after 30 F-T cycles is shown in Figure 8.2. It is quite obvious that the specimens were severely damaged. The appearance of these F/T specimens was very similar to the appearance of the deteriorated patch constructed using the same the SET 45-R material (see Figure 8.3).

TABLE 8.4
Durability Properties

Material	FT Resistance: RDM after 300 F-T Cycles (%)	Scaling Resistance: Material Scaled after 25 F-T Cycles (Visual Rating)	Chloride Ion Penetrability
FX	90	1	Moderate
SQ	98	1	Low
HD	80	0	Very low
TR	*	0	Moderate
Dur-R	*	**	Moderate
Dur-AE	35	**	High

*Specimens failed within 30 F-T cycles.
**Test not performed due to technical problems with the F-T chamber.

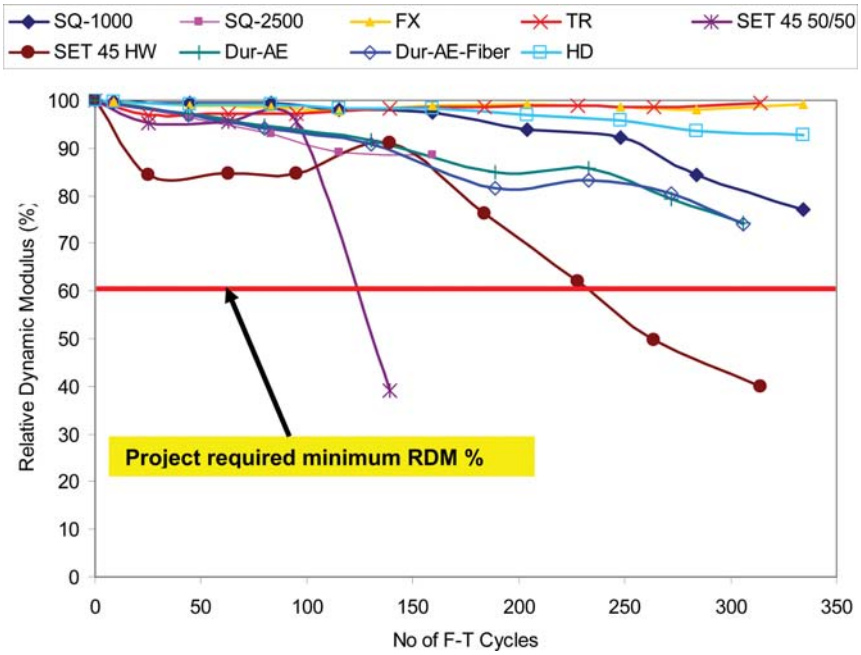

Figure 8.1 Freeze-thaw resistance of field mixes.

In general, none of the SET 45 brand products displayed adequate F-T resistance. The SET 45 50/50 failed prematurely after 140 F-T cycles and SET 45 HW specimens had a RDM of approximately 40% after 300 F-T cycles. It is evident that the aggregate compatibility issue mentioned by the manufacturer (incompatibility of SET 45 with calcareous aggregate, discussed in Chapter 5) is not the only reason for the poor performance of the SET 45 materials as the SET 45 HW mix did not have any pea gravel extension. The poor freeze-thaw resistance of the SET 45 mixtures in the laboratory was confirmed by the poor field performance of the same material.

The FX, HD and TR materials exhibited superior F-T resistance with RDM $>$ 90% after 300 F-T cycles. The SQ-1000, Dur-AE and Dur-R materials exhibited good F-T resistance (RDM $>$ 70% after 300 F-T cycles). A comparison between the F-T resistance of laboratory and field mixes is shown in Table 8.5.

The laboratory and field mixes of FX and HD had very comparable F-T performance. The SQ specimens cast in the field deteriorated after 160 cycles—possibly due to the inconsistent nature of the mixes discussed in Chapter 5 (field mixes were over-watered and exhibited severe bleeding). The laboratory specimens were consolidated by vibration whereas the field specimens were consolidated by rodding. The vibration of the laboratory specimens might have altered the air-void system resulting in poor F-T resistance for TR and Dur-R and reduced F-T resistance for Dur-AE when compared to the field specimens.

Figure 8.2 SET 45-R specimens after 30 F-T cycles.

Figure 8.3 Appearance of the SET 45-R material in the deteriorated patch.

TABLE 8.5
F-T Resistance: Lab vs. Field

Material	RDM after 100 Cycles (%)		RDM after 160 Cycles (%)		RDM after 300 Cycles (%)	
	Lab	Field	Lab	Field	Lab	Field
FX	93	98	91	99	90	99
SQ	99	90	99	*	98	*
HD	95	98	91	96	80	92
TR	*	97	*	98	*	99
Dur-R	*	NDA	*	NDA	*	NDA
Dur-AE	75	93	60	85	35	74

Figure 8.4 shows a comparison between the 12-hour compressive strength of the field specimens and, the 4-hour and predicted 12-hour compressive strength values of the laboratory mixes (12-hour strength values were predicted from the developed regression models discussed in Chapter 4).

The 12-hour compressive strength values of FX, SQ and Dur-AE materials were, respectively, around 80%, 240% and 45% higher than those of the field mixes. For HD and TR materials, the strengths from the laboratory and the field mixes are very comparable. For FX and SQ material the 12-hour compressive strength values of the field specimens were considerably lower than the 4-hour compressive strength values of the corresponding laboratory mixes. The ambient temperature during the field installations was around 10°C and, as a result, the setting time of the field mixes were extended in comparison to the laboratory mixes. The differences in the 12-hour compressive strengths of the laboratory and field mixes indicate that some of the repair materials (FX, SQ and Dur-AE) are more sensitive to temperature variations during early hydration than the others (HD and TR).

8.5 Recommended Performance Specifications

The summary of both, the current INDOT specifications and the recommended performance specifications is given in Table 8.6. The recommended specifications can be used as a basis for possible modifications of (or additions to) the current INDOT specifications.

The current INDOT specifications do not include any requirements for the workability of the rapid-setting patching materials. However, workability is a key factor which affects the placement and finishing of the patches and thus performance requirements for the consistency of fresh concrete in terms of slump or flow should be added to the specifications.

The current specifications suggest minimum compressive strength requirements only for neat material. In most practical cases, only extended material is used. So, the performance specifications should be modified to include compressive strength requirements for extended mixtures as well.

The freeze-thaw resistance requirement in the current specification is 95% minimum RDM after 300 F-T cycles according to ASTM C 666 Procedure B

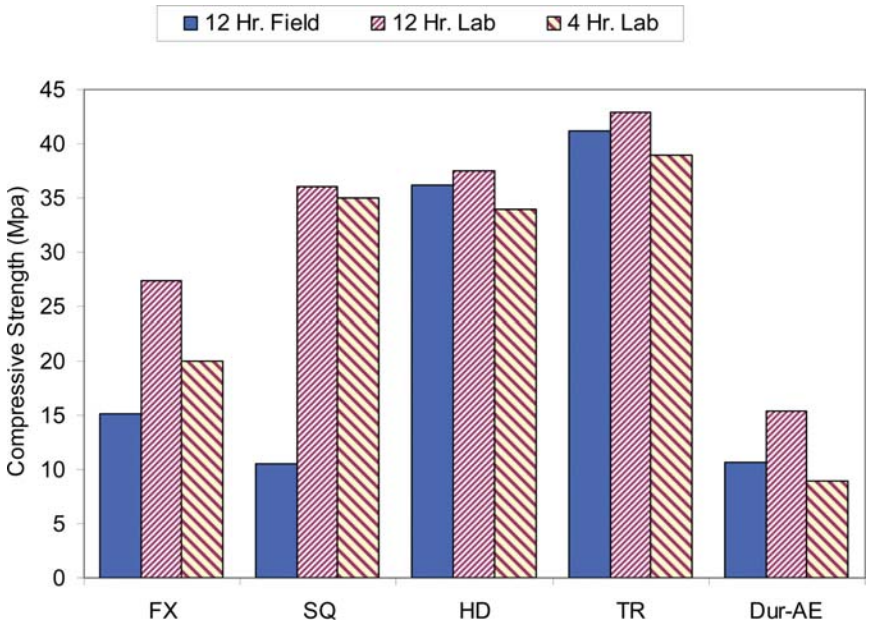

Figure 8.4 Compressive strength: lab vs. field specimens.

TABLE 8.6
Proposed Performance Requirements (Extended Material)

	Property	Recommended Specifications		INDOT Specifications		
		Test Method	Requirement	Test Method	Requirement	
			Workability (mm)			
i	Slump	ASTM C 143 (no	200–250	–	–	
ii	Spread	rodding)	400–700	–	–	
			Set Time (Min)			
i	Initial	ASTM C 266	10–20	ASTM C 266	10–20	
ii	Final	ASTM C 266	20–40	ASTM C 266	12–35	
			Compressive Strength (MPa)		**22°C (72°F)**	**35°C (95°F)**
i	1 h	ASTM C 39	14	ASTM T 109	14	–
ii	2 h	ASTM C 39	–	ASTM T 109	21	–
iii	3 h	ASTM C 39	–	ASTM T 109	–	21
iv	4 h	ASTM C 39	21	ASTM T 109	–	–
v	24 h	ASTM C 39	28	ASTM T 109	34.5	34.5
vi	28 days	ASTM C 39	35	ASTM T 109	55	55
			Slant Shear Bond Strength (MPa)			
i	1 day	ASTM C 882 modified	7	ASTM C 882	–	
ii	7 days	by ASTM C 928	10		–	
iii	28 days		–		17	
			Shrinkage			
i	28-day free shrinkage	ASTM C 157	$<750\ \mu\varepsilon$	ASTM C 157	$<300\ \mu\varepsilon$	
i	Restrained shrinkage	AASHTO PP 34	No cracking up to 28 days	–	–	
			Freeze-Thaw Resistance			
i	RDME after 300 cycles	ASTM C 666 procedure A	Minimum 60%	ASTM C 666 procedure B	Minimum 95%	
			Scaling Resistance			
i	5 cycles	ASTM C 672	–	ASTM C 672	0 rating	
ii	25 cycles	ASTM C 672	0 rating	ASTM C 672	0 rating	
iii	50+ cycles	ASTM C 672	–	ASTM C 672	1.5 rating	
			28-Day Rapid Chloride Permeability			
i	Charge pass	ASTM C 1202	Moderate to low	–	–	

(specimen surrounded by air during the freezing cycle and by water during the thawing cycle). Procedure A is a more realistic simulation of the field conditions (specimen completely surrounded by ice during the freezing cycle and water during the thawing cycle). Hence, it would be preferable to adopt the ASTM C666 procedure A for evaluation the freeze-thaw durability of the patching materials.

The slant-shear bond strength requirements for 1 and 7 days should be incorporated into the specification.

In the current INDOT specification, the maximum allowed shrinkage of the specimen is 300 $\mu\varepsilon$ after 28 days. However, none of the materials studied in this project (nor in the earlier projects (*5,6*) were able to meet these requirements. Hence, a more realistic value is necessary. Also, since the rapid-setting repair materials complete majority of the hydration process within the first few hours after mixing, the initial shrinkage measurement should be performed within 2 hours of addition of mix water. The specifications for cracking-susceptibility should also be included. Considering these issues, additional performance specifications resulting from this project are listed in Table 8.6.

It is important to note that, just because a material satisfied all the required performance criteria in the lab, it is not a guarantee that it will perform well in the field. Proper mixing, placement and finishing of the material must be ensured for adequate performance. A video-clip demonstrating good repair practices was developed as a part of the SPR-2648 study (*5*). The procedures demonstrated in that video for proper installation must be followed to ensure satisfactory field-performance. The general recommendations to ensure good field performance discussed in section 6.6 must also be considered.

8.6 General Recommendations—Field Installations

This section presents some general recommendations involving the improvements in the quality-control procedures for field mixes and also few suggestions regarding construction related issues to ensure adequate performance of the repair patches.

8.6.1 Improvements in Quality Control Procedures for Field Mixes

- Ambient temperature conditions played a vital role in controlling rate of strength gain. In Hot Weather conditions, cold water should be used to prevent flash-set of materials studied. In cold weather conditions, warm water should be used to accelerate hydration.
- The uniformity of the field installations can be improved by accounting for moisture content of the aggregate during the batching process.
- Calibrated buckets should be used to control the amount of water and aggregates added into each mix.
- Addition of extra water (beyond the quantities suggested by the manufacturer of the material) should be avoided.

8.6.2 Suggested Improvements to Patch-Installation Practices

- The level of the patch should be flush with the level of existing concrete in order to avoid uneven surfaces which results in the abrasion and corner breaks of the patch (especially along the edge closer to the approach of the traffic).
- The edges of the installed patches should be carefully finished (sealed if needed) to prevent ingress of water/salts into the repair patch area which will result in faster deterioration of the patch; especially during winter.
- The patching material must be consolidated properly during placement so that no voids are present underneath the rebars.
- After finding the repair a curing compound should be applied to the patch area to minimize the water loss.

8.7 Materials to Be Considered for Further Field Testing

The materials were ranked subjectively based on the relative laboratory and field performance. Section 8.7.1 discusses the laboratory performance ranking and section 8.7.2 discusses the field performance ranking.

8.7.1 Laboratory Performance Ranking

The laboratory performances of the materials were ranked in eight categories discussed below:

1. Workability
2. Setting time
3. Rate of compressive strength gain
4. Slant Shear Bond Strength
5. Free Shrinkage
6. Restrained Shrinkage
7. Freeze-thaw resistance and
8. Resistance to chloride ion penetration

One point was awarded to a material if it exceeded the performance criteria and 0.5 points was awarded if the material satisfied required criteria to an extent and no points were awarded if the material failed to satisfy the performance criteria. The performance criteria are those discussed in Table 8.6. Since the scaling resistance of Dur-R and Dur-AE could not be evaluated, this property was not included as a part of the ranking scheme.

From Table 8.7, it is seen that SQ and HD were the top performing materials with 7.5 points out of 8. FX came a close second with 7 points. TR received 5.5 points and Dur-R and Dur-AE received 4.5 and 4 points respectively.

8.7.2 Field Performance Ranking

The field performance of the repair patches was based on the inspection conducted about 6 months after they were installed on the bridge deck. It was a subjective rating that was based on a visual observation of the condition of individual patches on a scale ranging from o (the worst) to 5 (the best). The results of the field performance rankings are presented in Table 8.8. That table also includes rankings based on the results of two additional tests (freeze-thaw and 12-hour compressive strength). Although these tests were actually performed in the lab, they are included in this "field performance" table because the specimens used for testing were produced using field mixtures collected during installation of the patches. The freeze-thaw resistance and compressive strength ranking of field mixes were subjectively ranked on a scale of 1. The performance criteria for these two properties are same as those discussed in section 8.7.1.

From Table 8.8, it is seen that with respect to materials installed in 2007 HD received the highest points (7) with Dur-AE and Dur-AE-F coming a close second with 5.5 points each. SET 45-R was the worst performing material in the field with just 0.5 points.

Based on the rankings discussed in sections 8.7.1 and 8.7.2, and also considering the input from the INDOT's past experiences, the materials to be selected for further field testing are:

TABLE 8.7
Laboratory Performance: Relative Ranking

Specimen Label	Material	Set Time Ranking	Workability Ranking	Compressive Strength Ranking	Bond Strength Ranking	Free Shrinkage Ranking	Restrained Shrinkage Ranking	Freeze-Thaw Resistance Ranking	RCP Ranking	Total Points (out of 8)
FX	FX-928	1	1	0.5	1	1	1	1	0.5	7
SQ	SikaQuick 2500	1	1	1	1	0.5	1	1	1	7.5
HD	DOT Patch HD	1	1	1	1	0.5	1	1	1	7.5
TR	Thoroc 10-603	0.5	1	1	1	0.5	1	0	0.5	5.5
Dur-R	Duracal Regular	0.5	1	0.5	0.5	1	1	0	0	4.5
Dur-AE	Duracal Air Entrained	0.5	1	0	0.5	1	1	0	0	4

TABLE 8.8
Field Performance: Relative Ranking

Specimen Label	Material	Field Performance Ranking (Out of 5)	Freeze-Thaw Ranking*	Compressive Strength Ranking**	Total Points (Out of 7)
Patches installed October 2007, inspected April 2008					
FX	FX-928	2	1	0.5	3.5
SQ-1000	SickQuick-1000	2	1	1	4
SQ-2500	SikaQuick-2500	2	0	0	2
HD	HD-50	5	1	1	7
TR	ThoRoc 10-60	3	1	1	5
SET 45-R	SET 45 Regular	0	0	0.5	0.5
SET 45-HW	SET 45 Hot Weather	3	0	1	4
SET 45 50/50	SET 45 50/50 Blend	3	0	1	4
Dur-AE	Duracal Air Entrained	4	1	0.5	5.5
Dur-AE-F	Duracal Air Entrained with Fibers	4	1	0.5	5.5
Patches installed July 2010, inspected August 2011					
MG-Krete	MG-Krete	4	0	1	5
Zero-C	Zero-C	0	0	1	1
Pro-Poxy 2500	Pro-Poxy 2500	5	1	1	7
Fastrak	Fastrak	5	1	1	7

*Freeze-thaw resistance ranking for specimens cast using field mixes.
**12-hour compressive strength ranking of field mixes.

- **HD-50**—selected because of superior laboratory and field performance
- **Duracal-AE and Duracal-AE-Fibers**—selected primarily due to good field performance and INDOT's past experiences
- **SQ-2500**—selected primarily because of its superior laboratory performance

The analytical representation of both laboratory and field performance data of materials shown in Table 8.8 is also shown in Figure 8.5.

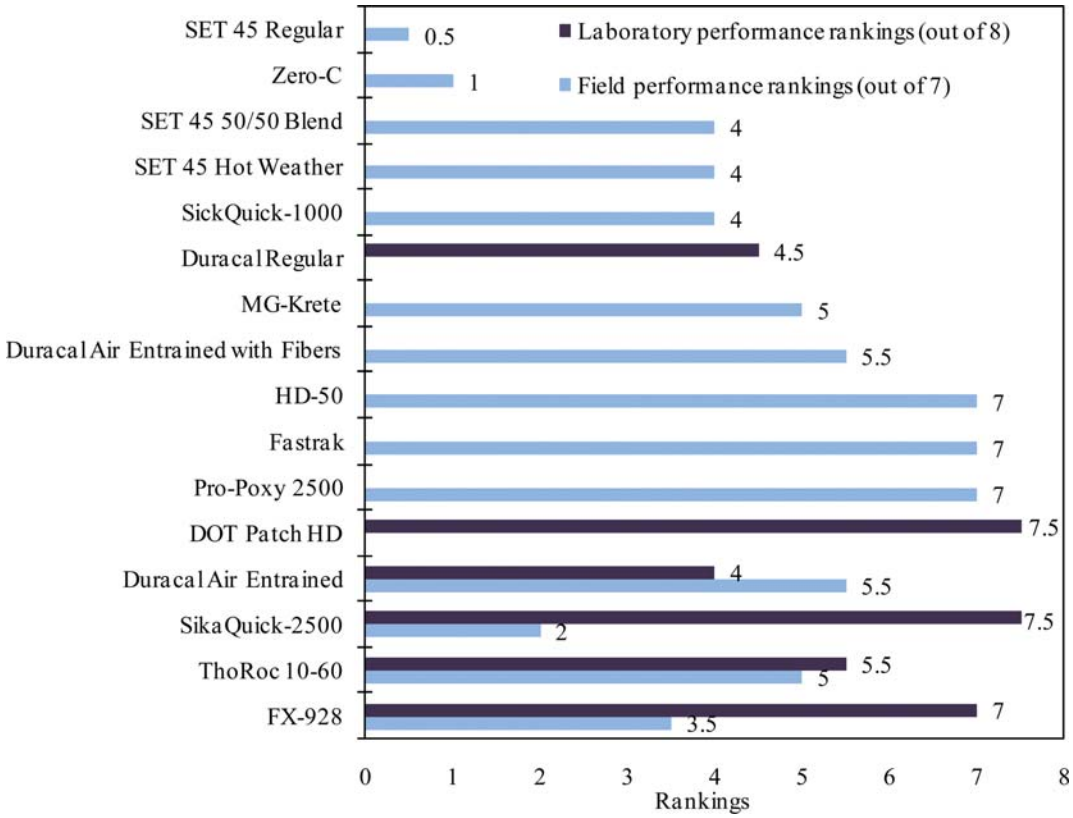

Figure 8.5 Laboratory and filed performance rankings of the repair materials.

8.8 Future Research Directions

The analysis of data of materials installed in July 2010 indicates the following as being top performers:

- Pro-Poxy 2500
- Fastrak

Both of these materials were easy to prepare, easy to place and developed good strength and durability characteristics.

When dealing with rapid-setting repair materials, there are quite a few uncertainties associated with the mixtures developed on site. These uncertainties primarily arise due to the following reasons: the amount of aggregate extension and amount of mix water added, deviations from recommended mix proportions (often in response to diminished performance, especially with respect to the workability of the repair material), rate of strength gain, and freeze-thaw resistance. Hence, it is very essential to study the sensitivity of rapid-setting materials to the various uncertainties present on site.

Figure 8.6 highlights the proposed study methodology to evaluate the robustness of the repair materials with respect to the uncertainties present in the field. The effect of variations in aggregate moisture content, excess in mix water content and the pea-gravel extension on the setting time, workability, rate of strength gain and the freeze-thaw resistance should be evaluated to identify the robustness of the materials.

8.9 Concluding Remarks

This research undertaking involved the performance evaluation of mechanical, dimensional stability and durability properties of six commercially available rapid-setting repair materials in the laboratory. In addition to the laboratory testing, the field performances of the repair materials were also evaluated. While some materials performed well in the lab, they did not necessarily perform well in the field and vice-versa.

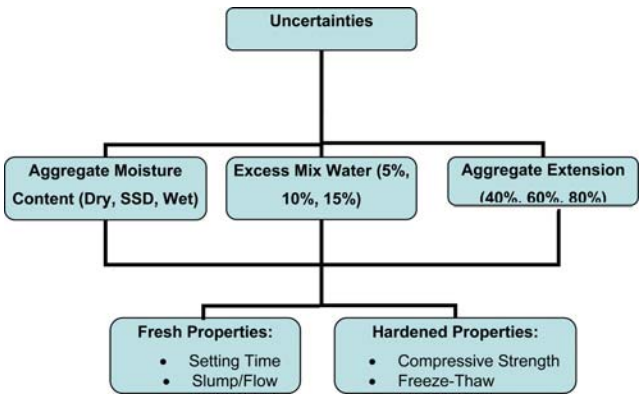

Figure 8.6 Proposed study methodology.

The following are some generalized conclusions from this study:

- Around 15% extra water was added to some materials (TR, Dur-R and Dur-AE) while preparing the laboratory mixes. Since these materials are very sensitive to excess water added, this resulted in a significant impact on the durability properties—especially the freeze-thaw resistance.
- In the field, for most of the materials, the consistency of the mixes varied from batch to batch—this can be attributed to the variations in the aggregate extension adopted, mix-water added and also the moisture content of the aggregates used.
- Construction related issues (consolidation and finishing) also played an important role in the performance of the repair patches.
- HD-50 and Dur-AE seemed to be the best performing materials based upon field studies.
- SET 45 cannot be used with calcareous pea-gravel. Calcareous aggregates cause premature failure of the patches.

Based upon laboratory and field results, modifications to the current INDOT performance specifications for rapid-setting repair materials have been suggested. Some recommendations for improvements in quality control measures of field-mixes and construction related issues have been suggested. Future research directions involving the evaluation of the robustness of the repair materials with respect to the uncertainties present on site have also been highlighted.

REFERENCES

1. Vaysburd, A. M. Holistic System Approach to Design and Implementation of Concrete Repair. *Cement and Concrete Composites*, Vol. 28, 2006, pp. 671–678.
2. Vaysburd, A. M., P. H. Emmons, N. P. Mailvaganam, J. E. McDonald, and B. Bissonnette. Concrete Repair Technology—A Revised Approach is Needed. *Concrete International*, Vol. 26, 2004, pp. 59–64.
3. McDonald, J. E., A. M. Vaysburd., P. H. Emmons, R. W. Poston, and K. Kesner. Selecting Durable Repair Materials: Performance Criteria—Summary. *Concrete International*, Vol. 24, 2001, pp. 37–44.
4. Baluch, M. H., M. K. Rahman, and A. H. Al-Gadhib. Risks of Cracking and Delamination in Patch Repair, *Journal of Materials in Civil Engineering*, Vol. 14, No. 4, 2002, pp. 294–302.
5. Barde, A. D., S. Parameswaran, T. Chariton, W. J. Weiss, M. D. Cohen, and S. A. Newbolds. *Evaluation of Rapid Setting Cement-Based Materials for Patching and Repair*. Publication FHWA/IN/JTRP-2006/11. Joint Transportation Research Program, Indiana Department of Transportation and Purdue University, West Lafayette, Indiana, 2006. doi: 10.5703/1288284313392.
6. Deshpande, Y., and J. Olek. *Dowel Bar Retrofit Mix Design and Specification*. Publication FHWA/IN/JTRP-2012/15. Joint Transportation Research Program, Indiana Department of Transportation and Purdue University, West Lafayette, Indiana, 2012. doi: 10.5703/1288284314859.
7. Parameswaran, S. Investigating the Role of Material Properties and their Variability in the Selection of Repair Materials. M.S Thesis, Purdue University, Aug 2004.

8. Emberson, N. K., and G. C. Mays. Significance of Property Mismatch in the Patch Repair of Structural Concrete, Part I: Properties of Repair Systems. *Magazine of Concrete Research*, Vol. 42, 1990, pp. 147–160.
9. Fowler, D. W., G. P. Beer, and A. H. Meyer. A Survey on the Use of Rapid-Setting Repair Materials. In *Transportation Research Record: Journal of the Transportation Research Board*, No. 943, Transportation Research Board of the National Academies, Washington, D.C., 1983, pp. 33–37.
10. ASTM C 125. *Standard Terminology Relating to Concrete and Concrete Aggregates*. American Society for Testing and Materials, West Conshohocken, Pennsylvania.
11. Mehta, P. K. *Concrete: Structure, Properties, and Materials*. Prentice Hall, Inc., New Jersey, 1986.
12. Mangat, P. S. and F. J. O'Flaherty. Influence of Elastic Modulus on Stress Redistribution and Cracking in Repair Patches. *Cement and Concrete Research*, Vol. 30, 2000, pp. 125–136.
13. Concrete Construction Staff. Four Steps to Successful Concrete Repair. *Concrete Construction*, January 1983.
14. Shah, S. P., W. J. Weiss, and W. Yang. Shrinkage Cracking—Can it be prevented? *Concrete International*, Vol. 20, 1998, pp. 51–55.
15. Baluch, M. H., M. K Rahman, and A. H. Al-Gadhib. Risks of Cracking and Delamination in Patch Repair. *Journal of Materials in Civil Engineering*, Vol. 14, 2002, pp. 294–302.
16. Li, S., D. G. Geissert, G. C. Frantz, and J. E. Stephens. Freeze-Thaw Bond Durability of Rapid-Setting Concrete Repair Materials. *ACI Materials Journal*, Vol. 96, 1999, pp. 242–249.
17. Li, S., G. C. Frantz, and J. E. Stephens. Bond Performance of Rapid-Setting Repair Materials Subjected to Deicing Salt and Freezing-Thawing Cycles. *ACI Materials Journal*, Vol. 96, 1999, pp. 692–697.
18. Momayez, A., A. A. Ramezanianpour, H. Rajaie, and M. R. Ehsani. Bi-Surface Shear Test for Evaluating Bond between Existing and New Concrete. *ACI Materials Journal*, Vol. 101, 2004, pp. 99–106.
19. Momayez, A., M. R. Ehsani, A. A. Ramezanianpour, and H. Rajaie. Comparison of Methods for Evaluating Bond Strength between Concrete Substrate and Repair Materials. *Cement and Concrete Research*, Vol. 35, 2005, pp. 748–757.
20. Iowa DOT. *Method of Test for Determining the Shearing Strength of Bonded Concrete* (Test Method No. Iowa 406-C-2000). Iowa Department of Transportation, 2000.
21. Ram, V. P. Rapid-setting Materials for Transportation Infrastructure Repair Applications: Laboratory and Field Studies, MSCE Thesis (MSCE). Purdue University, West Lafayette, Indiana, 2008.
22. ASTM C 266. *Standard Test Method for Time of Setting of Hydraulic-Cement Paste by Gillmore Needles*. American Society for Testing and Materials, West Conshohocken, Pennsylvania.
23. ASTM C 143. *Standard Test Method for Slump of Hydraulic-Cement Concrete*. American Society for Testing and Materials, West Conshohocken, Pennsylvania.
24. ASTM C 39. *Test Method for Compressive Strength of Cylindrical Concrete Specimens*. American Society for Testing and Materials, West Conshohocken, Pennsylvania.
25. ASTM C 882. *Standard Test Method for Bond Strength of Epoxy-Resin Systems Used with Concrete by Slant Shear*. American Society for Testing and Materials, West Conshohocken, Pennsylvania.
26. ASTM C 109. *Standard Test Method for Compressive Strength of Hydraulic Cement Mortars (Using 2-in. or [50-mm] Cube Specimens)*. American Society for Testing and Materials, West Conshohocken, Pennsylvania.
27. ASTM C 157. *Standard Test Method for Length Change of Hardened Hydraulic-Cement Mortar and Concrete*. American Society for Testing and Materials, West Conshohocken, Pennsylvania.
28. AASHTO PP 34. *Standard Practice for Estimating the Cracking Tendency of Concrete*. American Association of State Highway and Transportation Officials, Washington, D.C., 2005.
29. ASTM C 666. *Standard Test Method for Resistance of Concrete to Rapid Freezing and Thawing*. American Society for Testing and Materials, West Conshohocken, Pennsylvania.
30. ASTM C 672. *Standard Test Method for Scaling Resistance of Concrete Surfaces Exposed to Deicing Chemicals*. American Society for Testing and Materials, West Conshohocken, Pennsylvania.
31. ASTM C 1202. *Test Method for Electrical Indication of Concrete's Ability to Resist Chloride Ion Penetration*. American Society for Testing and Materials, West Conshohocken, Pennsylvania.
32. ASTM C 928. *Standard Specification for Packaged, Dry, Rapid-Hardening Cementitious Materials for Concrete Repairs*. American Society for Testing and Materials, West Conshohocken, Pennsylvania.
33. Ramachandran, V. S., R. M. Paroli, J. J. Beaudoin, and A. H. Delgado. *Handbook of Thermal Analysis of Construction Materials*. Noyes Publication/William Andrew Publishing, Norwich, New York USA, 2003.
34. Sant, G., P. Lura, and W. J. Weiss. Measurement of Volume Change in Cementitious Materials at Early Ages: Review of Testing Protocols and Interpretation of Results. In *Transportation Research Record: Journal of the Transportation Research Board*, No. 1979, Transportation Research Board of the National Academies, Washington, D.C., 2006, pp. 21–29.
35. Schlitter, J. L., A. H. Senter, D. P. Bentz, T. Nantung, and W. J. Weiss. A Dual Concentric Ring Test for Evaluating Residual Stress Development due to Restrained Volume Change. *Journal of ASTM International*, Vol. 7, No. 9, 2010, 13 p.
36. Radlinska, A., J. H. Moon, F. Rajabipour, and J. Weiss. The Ring Test: A Review of Recent Developments. In *Proceedings of International RILEM Conference on Volume Changes of Hardening Concrete: Testing and Mitigation*, RILEM, Jensen, O., Lura, P., and Kovler, K. eds., Lyngby, Denmark, 2006, pp. 205–214.
37. Rudy, A., J. Olek, T. Nantung, and R. M. Newell. Evaluation of Ternary Concrete Mixtures with GGBFS and Fly Ash for Pavements. Presented at the International Conference on Optimizing Pavement concrete Mixtures and Accelerated Concrete Pavement Construction and Rehabilitation, 2007.
38. AASHTO T 277. *Standard Practice for Electrical Indication of Concrete's Ability to Resist Chloride Ion Penetration*. American Association of State Highway and Transportation Officials, Washington, D.C., 2005.
39. Peterson, K., L. Sutter, and M. Radlinski. The Practical Application of a Flatbed Scanner for Air-Void Characterization of Hardened Concrete. *Journal of ASTM International*, Vol. 6, No. 9, 2009, 15 p.

APPENDIX A. FIELD INSPECTION—SPRING 2008

This section presents the preliminary investigation of the field performance of the repair patches installed in October, 2007. The repair patches were inspected on April 9, 2008, approximately six months (one winter season) after installation. During these six months, the patches were exposed to the regular highway traffic as well as to deicing chemicals and freezing and thawing conditions. The ambient temperature history experienced by the patches since the installation is shown in Figure A.1 (Meteorological Data for Lafayette, IN; Source: http://www.wunderground.com). The temperature varied from +30°C to as low as -20°C. If the coefficient of thermal expansion for the repair material is considerably different (lower or higher) from that of the existing concrete, such variations in temperatures would result in major thermal-compatibility issues which can result in premature-failure of the patches.

A. 1 PERFORMANCE OF THE HD-50 PATCHES

Figure A.2 shows a view of the HD-50 patch-I after one winter season. No cracks were visible on the surface of the pavement but there were signs of minor scaling on the surface of the patch. There was also a minor abrasion along the edge, perpendicular to the approach of the traffic due to mismatch between the levels of the existing concrete and the repair patch.

A closer look at the patch shown in Figure A.3 reveals that the edges which had not been finished properly during the construction of the patch show signs of slight deterioration. Figure A.4 shows a view of the HD-50 patch-II. As in the case of the first patch, the edge perpendicular to the approach of the traffic is abraded.

Figure A.5 shows a close-up view of the HD-50 patch-III. This patch had very conspicuous edge deterioration and had also cracked perpendicular to the long edge and to the direction of the traffic. This patch was located along the boundary between the driving and passing lanes. The surface of the patch was not finished to the level of the existing concrete during the installation process. This patch may have undergone cracking purely due to fatigue as a result of the impact loading during the lane change operations.

A.2 PERFORMANCE OF THE SIKAQUICK-1000 PATCHES

Figure A.6 shows the view of the SikaQuick-1000 patch two days of placement. Due to severe bleeding, the top surface of the patch was very weak, which resulted in heavy abrasion of the surface. When the current condition of the patch (Figure A.7) was compared to the condition of the patch after two days after placement, it was observed that subsequent deterioration to the patch was minimal. There were no visible cracks on the surface.

A.3 PERFORMANCE OF THE SIKAQUICK-2500 PATCHES

Figure A.8 shows a close-up view of the SikaQuick-2500 patch-I. The patch had undergone moderate scaling and had multiple cracks on the surface.

The condition of the SikaQuick-2500 patch-II is shown in Figure A.9. The patch cracked within two days after placement. The cracks were located almost directly over the longitudinal rebars. The mixture in this particular patch was not compacted at all, which would have resulted in air pockets beneath the rebars and these cracking might be due to settlement of the patch upon repeated loading from traffic. There was also de-bonding along the edges due to improper finishing of the patch.

A.4 PERFORMANCE OF THE FX-928 PATCHES

Figure A.10 and Figure A.11 show the condition of the FX-928 patches on April 9, 2008. Both patches had cracked. Patch-I had two cracks on the surface while the second patch had undergone more severe cracking and its edges were de-bonding from the existing concrete due to improper finishing. As observed

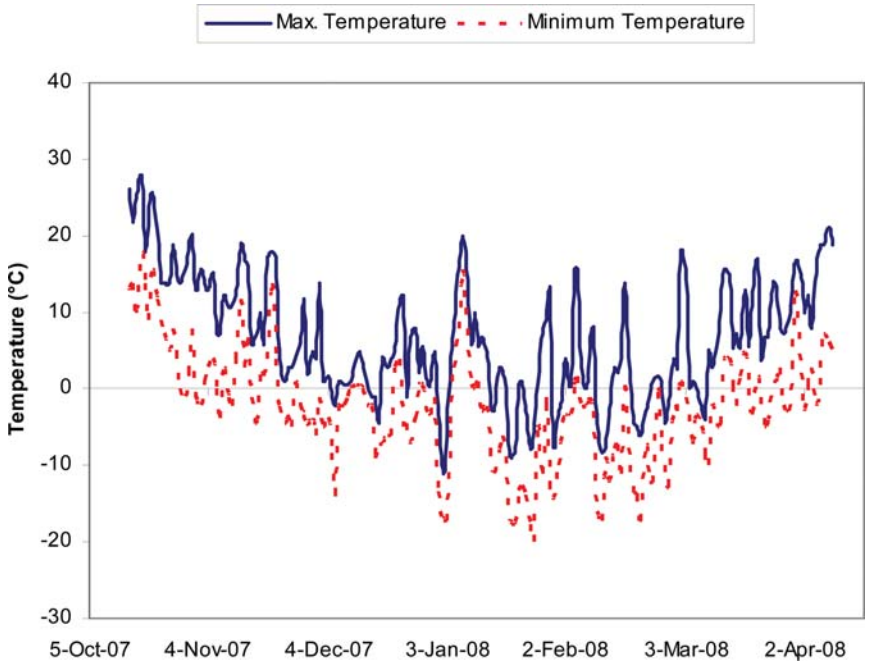

Figure A.1 Ambient temperature history.

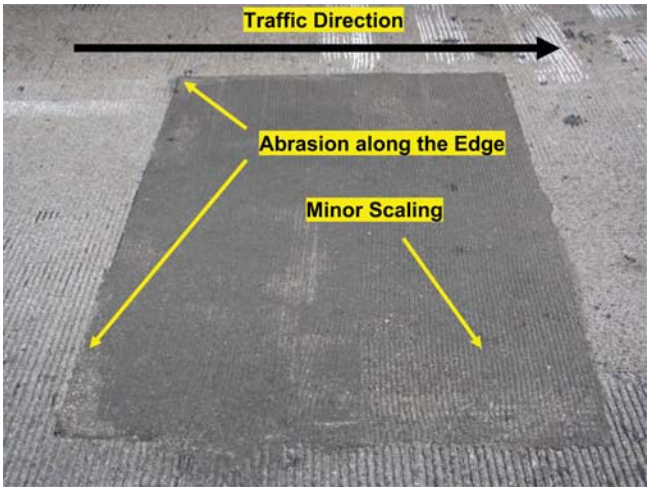

Figure A.2 HD-50 patch-I.

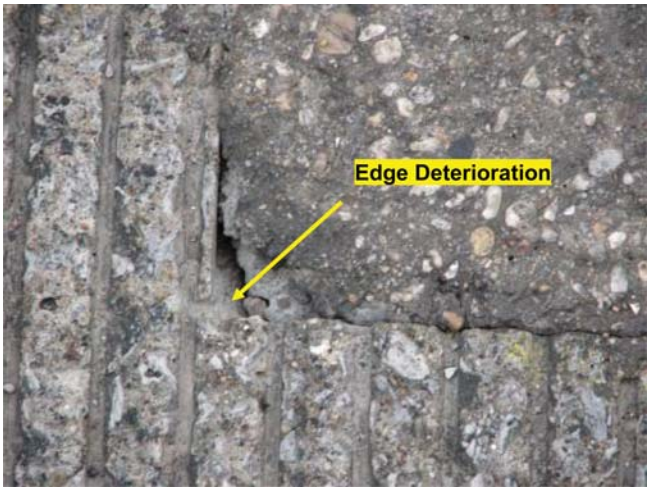

Figure A.3 HD-50 patch-I : close-up view of edge.

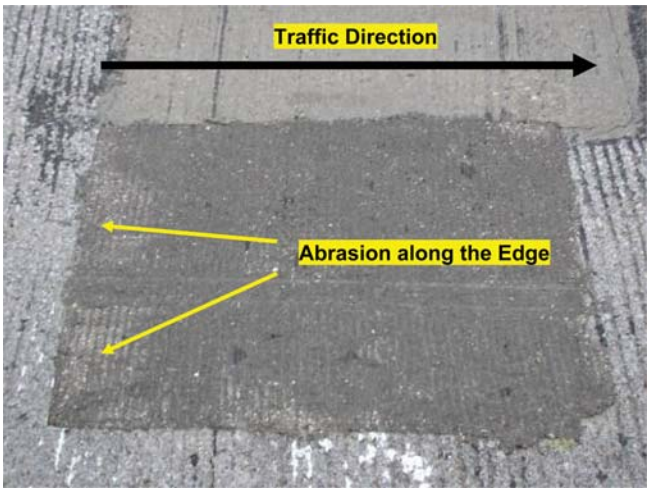

Figure A.4 HD-50 patch-II.

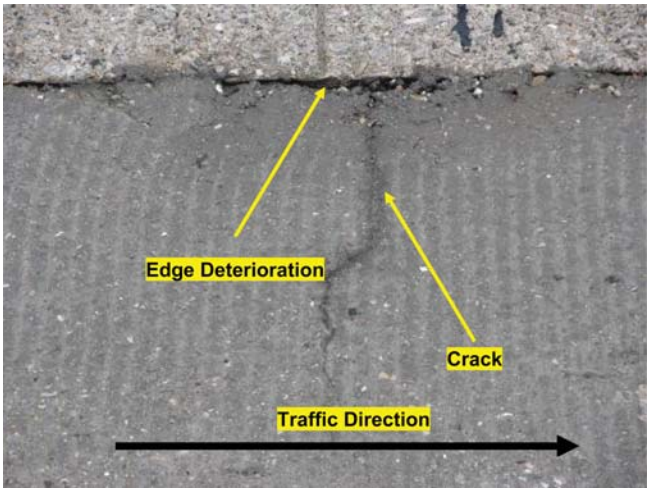

Figure A.5 HD-50 patch-III: close-up view of the edge.

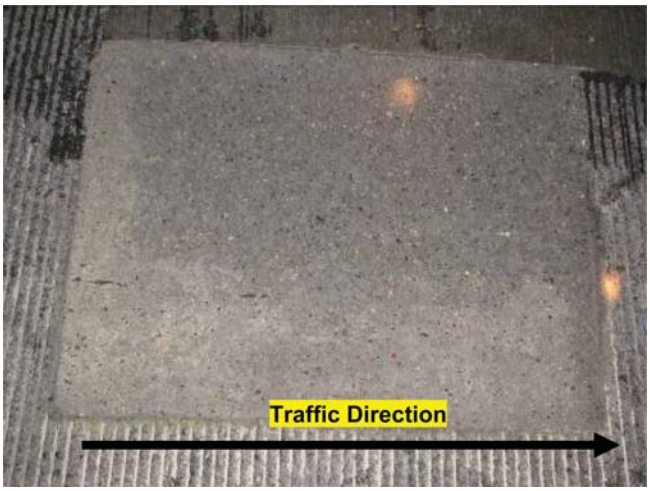

Figure A.6 SikaQuick-1000 patch condition two days

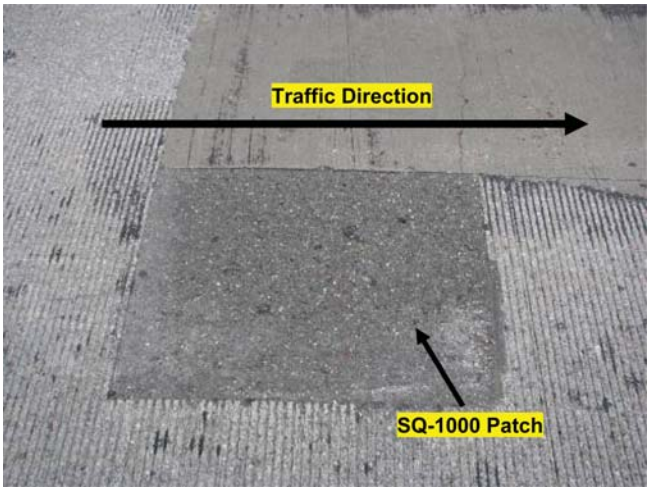

Figure A.7 SikaQuick-1000 patch: condition on April

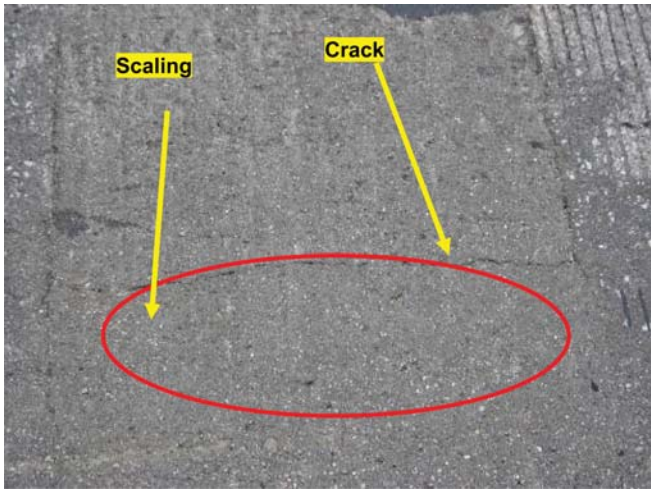

Figure A.8 SikaQuick-2500 patch: close-up view.

Figure A.9 SikaQuick-2500 patch-II: overview.

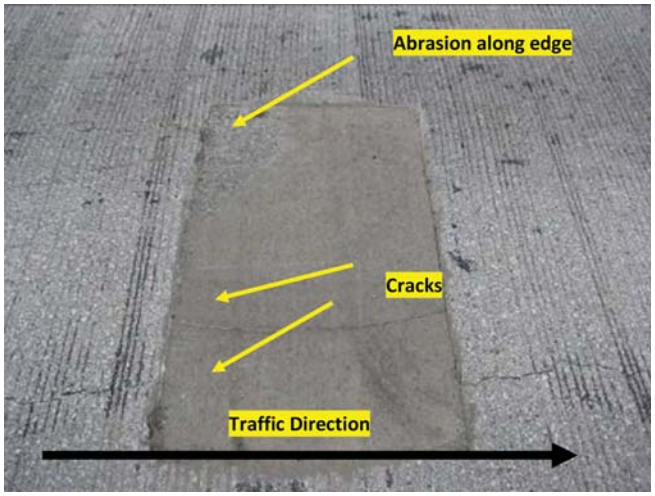

Figure A.10 FX-928 patch-I.

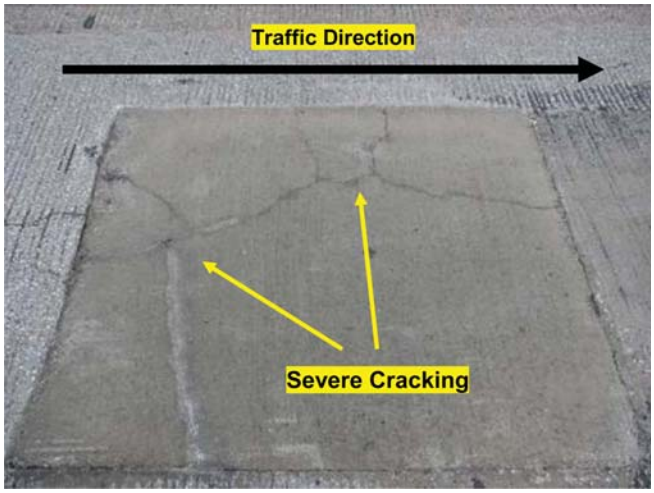

Figure A.11 FX-928 patch-II.

in earlier cases, these patches also underwent abrasion along the edge in the direction of the traffic.

A.5 PERFORMANCE OF THE THOROC 10-60 PATCHES

Figure A.12 shows the condition of the ThoRoc 10-60 patch. The patch had abraded along edge perpendicular to the approach of the traffic. The surface had one very conspicuous crack along the direction of the longitudinal rebars and a few other minor surface cracks.

A.6 PERFORMANCE OF THE SET 45 PATCHES

The SET 45 Regular patch (Figure A.13) had undergone the most severe deterioration. The eastern half of the patch had completely deteriorated in the freezing weather and an emergency closure was imposed on that section of the bridge-deck during the winter to patch the deteriorated section with asphalt concrete. The west-end of the patch was falling apart at the time of inspection and this patch will have to be replaced in the near future. It is very evident that the SET 45 Regular material does not work well with the locally available pea-gravel aggregate used for extension purposes.

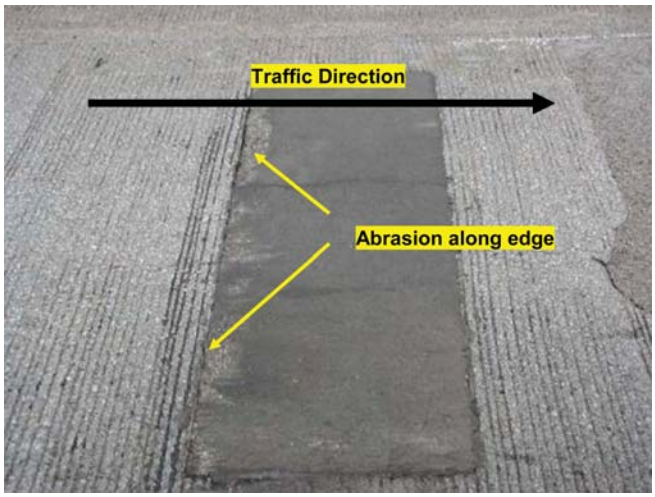

Figure A.12 ThoRoc 10-60 patch.

Figure A.13 SET 45 Regular patch.

Figure A.14 shows the condition of the SET 45 Hot Weather Patch. As mentioned earlier, this patch was installed without using the pea gravel extension. In addition to one crack on the surface, edge de-bonding was also observed.

Figure A.15 shows a view of the SET 45 50/50 Blend patch-I. Minor Edge cracking and edge de-bonding were observed. A view of the second SET 45 50/50 Blend Patch is shown in Figure A.16. This patch had one obvious surface crack and also showed signs of abrasion on the edge perpendicular to the approach of the traffic.

A.7 PERFORMANCE OF THE DURACAL PATCHES

The condition of the Duracal-AE and Duracal-AE-F patches (as on April 9, 2008 is shown in Figure A.17). There were no surface cracks. However the surface underwent considerable abrasion. This abrasion can be attributed primarily due to the improper finishing of the surface. Extra water was added to the surface of the patch after placement to produce a good finish, which would have resulted in a weak layer at the top of the patch.

A.8 SUMMARY OF PHASE-II STUDY: FIELD INSTALLATIONS AND PERFORMANCE VERIFICATION

This section provides some general comments regarding the general field installation procedures followed performance of the

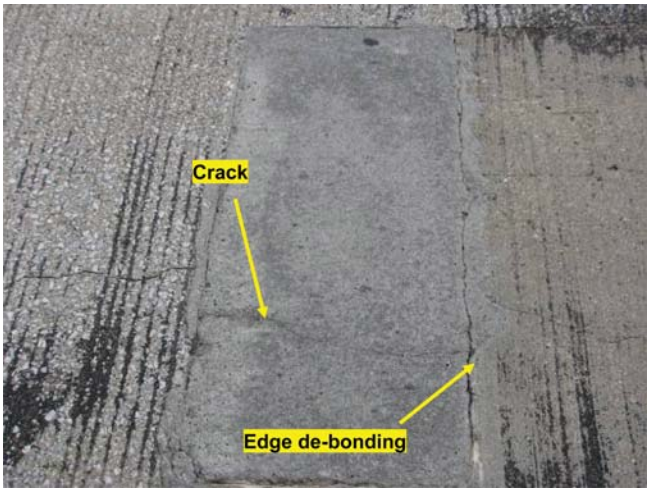

Figure A.14 SET 45 Hot Weather patch.

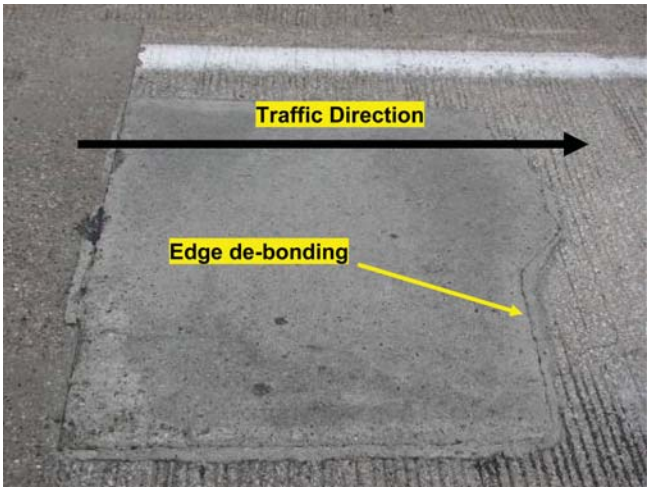

Figure A.15 SET 45 50/50 Blend patch-I.

patches based on the evaluation of patches conditions. These comments are as follows:

- Due to time constraints (the bridge-deck had to be open to traffic in 8 hours), none of the materials used to prepare repair mixtures were actually weighed. Instead, a volume-based approximation to the mass was used to proportion the mixtures.
- The water was added using 1 gallon containers. Depending on the results of visual observation of the consistency of the mix inside the mixer, extra water was added upon the recommendation of the material manufacturer representative. The amount of mix water varied from batch to batch.
- The consistency of mixes sometimes varied significantly from batch to batch due to the variations in the amount of aggregate extension and mix water used.
- The moisture content of the aggregates used was not taken into account when batching the materials.
- The ambient temperature at the time of placement was around 10°C and as a result, the setting time of the materials was extended compared to the laboratory mixtures. Some of the material manufacturer's recommend that the material and water be preconditioned to 23°C if the installations are to be carried out under cold weather conditions. However, these recommendations were not followed during this installation process.

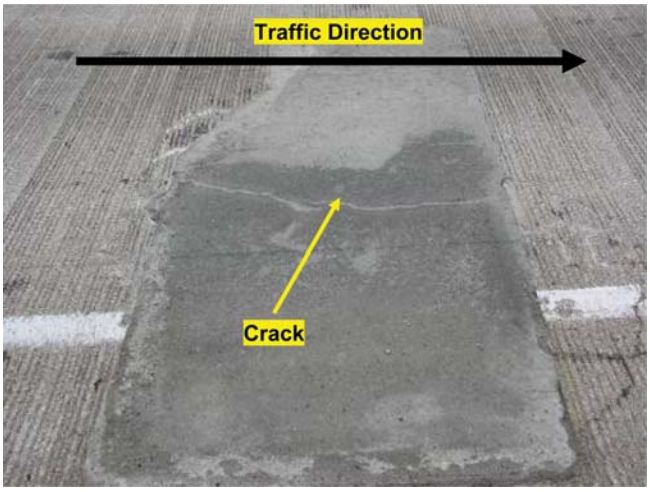

Figure A.16 SET 45 50/50 Blend patch-II.

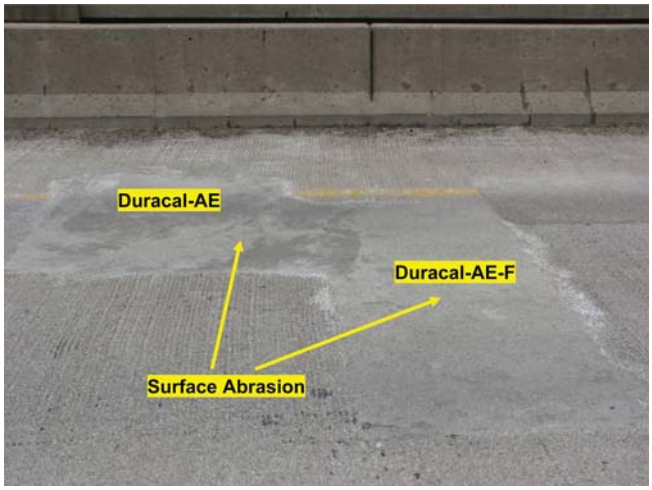

Figure A.17 SET 45 50/50 Blend patch-II.

A.9 SUMMARY OF THE SIX-MONTH FIELD PERFORMANCE

- HD-50, Duracal-AE and Duracal AE-Fibers were the only materials which exhibited good performance in the field. None of the Duracal patches cracked. Only one of the HD-50 patches cracked (which was due to construction related issues).
- The SQ-1000 and the SQ-2500 mixtures produced on site were over-watered, which resulted in excessive bleeding and poor surface finishing; this subsequently resulted in severe surface scaling and abrasion.
- The FX-928 patches developed multiple surface cracking.
- The SET 45-R patches deteriorated severely—possibly as a result of freeze-thaw related damage. The SET 45 HW and SET 45 50/50 patches performed relatively better showing only minor surface abrasion and cracking.
- The ThoRoc 10-60 patches developed minor cracking and surface abrasion.

APPENDIX B. FIELD INSPECTION—SPRING 2009

B.1 INTRODUCTION

This section presents the investigation of the field performance of the repair patches installed in October 2007 after two winter cycles. The repair patches were inspected on April 16, 2009, approximately 18 months (two winter cycles) after installation. During these 18 months, the patches were exposed to the regular highway traffic as well as to deicing chemicals and freezing and thawing conditions. Table B.1 has the stationing information of the patches. The stationing for patches 1 through 13 begin from the south-bound bridge deck approach and the stationing for patches 14 and 15 begins from the north-bound bridge deck approach.

B.2 PERFORMANCE OF THE HD-50 PATCHES

Figure B.1 shows a view of the HD-50 patch-I after two winter seasons. One small crack is visible on the surface of the patch. The overall condition of the patch is similar to that observed after one winter season and the material seems to be performing well.

Figure B.2 shows a view of the HD-50 patch-II. This patch is in good condition. No cracks were observed.

Figure B.3 shows a view of the HD-50 patch-III. The condition of the patch has not changed since the previous inspection. The crack that developed after one winter season (near the boundary between the driving and the passing lanes) has not deteriorated further indicating that the patch is structurally sound.

B.3 PERFORMANCE OF THE SIKAQUICK-1000 PATCHES

Figure B.4 shows a view of the SikaQuick-1000 patch. The surface of the patch has undergone severe weathering/scaling, most likely due to the use of extra water during mixing. No cracks were visible on the surface of the patch and the overall condition of the patch was similar to that observed during the previous inspection.

B.4 PERFORMANCE OF THE SIKAQUICK-2500 PATCHES

Figure B.5 shows a view of the SikaQuick-2500 patch-I. The patch had undergone moderate scaling and had developed multiple cracks on the surface. The poor performance of the

TABLE B.1
Stationing Information for the Patches on I-65 Bridge Deck

Patch No.	Repair Material	Start Station (ft.)	End Station (ft.)
1	HD-50 patch-I	79	83
2	SQ-2500 patch-I	88	90
3	SQ-1000	111	113
4	HD-50 patch-II	186	187
5	HD-50 patch-III	204	208
6	SQ-2500 patch-II	239	240
7	FX-928 patch-I	353	355
8	FX-928 patch-II	391	394
9	ThoRoc 10-60	440	441
10	SET 45 R	451	453
11	SET 45-50/50 patch-I	458	460
12	SET 45 HW	473	475
13	SET 45 50/50 patch-II	1076	1080
14	Duracal AE	15	19
15	Duracal AE-F	19	23

Figure B.1 HD-50 patch-I.

Figure B.2 HD-50 patch-III.

Figure B.3 HD-50 patch-III.

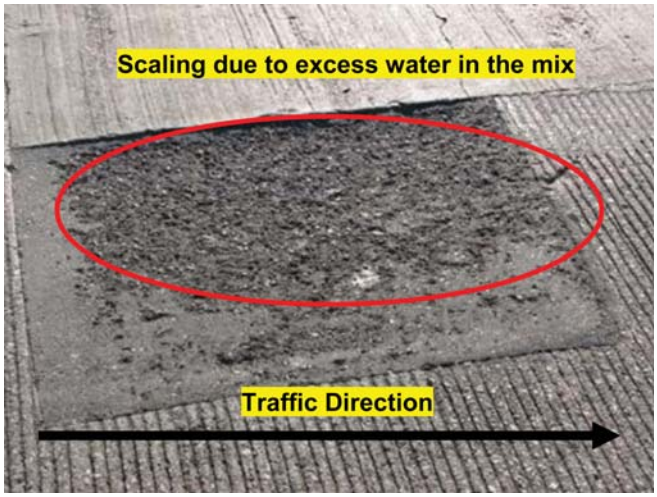

Figure B.4 SikaQuick-1000 patch.

patch can be attributed to the improper mix proportioning of the material during the installations. As in the case of SQ-1000, the SQ-2500 patches had extra water added at the time of mixing.

The condition of the SikaQuick-2500 patch-II is shown in Figure B.6. As noted during the previous inspection, the patch had developed cracks within two days after installation. This was attributed to improper compaction of the patch, which would have resulted in voids beneath the rebar. These general conditions of the patch have not visibly deteriorated since the previous inspection. The surface cracks were not clearly visible since they have been filled by salt deposits.

B.5 PERFORMANCE OF THE FX-928 PATCHES

Figure B.7 and Figure B.8 show the condition of the FX-928 patches on April 16, 2009. The condition of patch-I had not change since the time of previous inspection.

As noted in the previous inspection, patch-II had undergone more cracking and the deteriorated portion of the patch has been replaced by another repair material (potentially Duracal).

B.6 PERFORMANCE OF THE THOROC 10-60 PATCHES

Figure B.9 shows the condition of the ThoRoc 10-60 patch. The patch exhibited two cracks along the direction of the traffic.

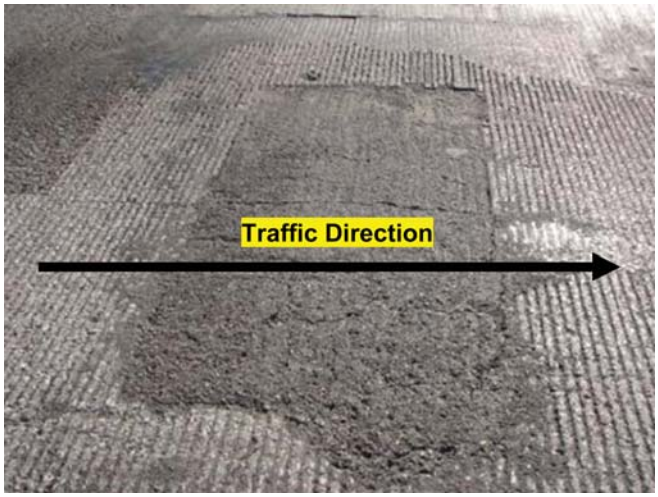

Figure B.5 SikaQuick-2500 patch-I.

Figure B.6 SikaQuick-2500 patch-II.

Figure B.7 FX-928 patch-I.

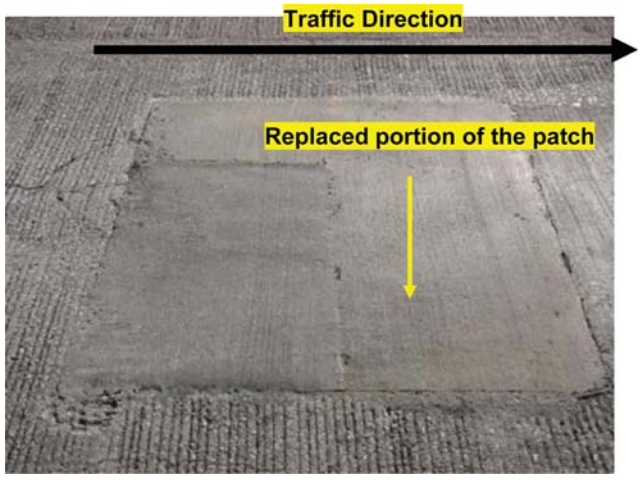

Figure B.8 FX-928 patch-II.

Figure B.9 ThoRoc 10-60 patch.

During the previous inspection, the patch contained only one crack. The overall condition of the patch has not changed much since the last inspection.

B.7 PERFORMANCE OF THE SET-45 PATCHES

The SET 45 Regular patch had undergone severe deterioration before the previous inspection and portions of the patch had been replaced by asphalt concrete. At the time of current inspection the patch has been completely replaced by another cementitious repair material (potentially Duracal). Figure B.10 shows the original SET 45 Regular patch area that has now been replaced by another repair material.

The Set 45 Hot Weather patch has also been completely replaced by the same material which was used to replace the Set 45 Regular patch. The Set 45 Hot Weather patch area that has been replaced by another material is shown in Figure B.11.

Figure B.12 shows a view of the SET 45 50/50 Blend patch-I. The condition of the patch has not visibly changed since the previous inspection. A view of the second SET 45 50/50 Blend patch-II is shown in Figure B.13. The condition of this patch has not changed much since the last inspection. The concrete around patch-II has deteriorated, which will potentially affect the performance of the patch in future years if that area is not repaired.

Figure B.10 SET 45 Regular patch that has been replaced.

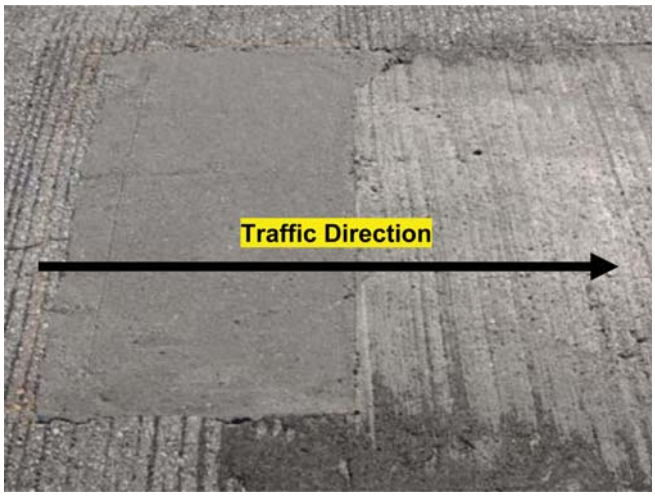

Figure B.11 SET 45 Hot Weather patch that has been replaced.

Figure B.12 SET 45 50/50 Blend patch-I.

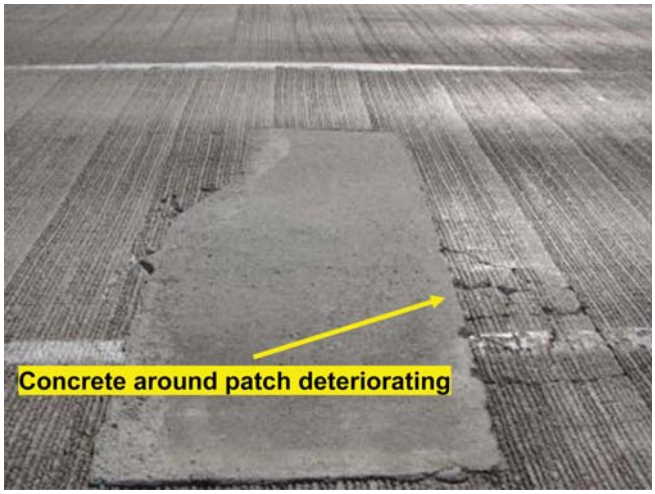

Figure B.13 SET 45 50/50 Blend patch-I.

Figure B.14 Duracal AE patch.

Figure B.15 Duracal AE-F patch.

B.8 PERFORMANCE OF THE DURACAL PATCHES

The condition of the Duracal-AE and Duracal-AE-F patches as on April 16, 2009 is shown in Figures B.14 and B.15, respectively. There were no surface cracks observed on either of these patches. As noted in the previous inspection, the surface of the patch has undergone moderate abrasion/scaling due to the excess water added to the surface during finishing. The condition of the patches has not visibly changed since the last inspection.

B.9 DISCUSSIONS ON PERFORMANCES

This appendix presented the review of field performance of the patches after two winter seasons. Some general observations are presented below:

- The condition of the HD-50 patches has not changed since the previous inspection. All patches appear to be performing in satisfactory condition.
- Though the conditions of the SQ-1000 and the SQ-2500 patches have not worsened since the previous inspection, these patches are in poor condition and may require replaced after the next winter season. The poor condition of the patches is attributed to the inconsistent mix-proportioning during placement. These mixtures used for these patches contained excessive amount of water.
- The condition of FX-928 patch-I has not visibly degraded since the previous inspection. Portions of the FX-928 patch-II have been replaced by another repair material, indicating that the patch had deteriorated further since the previous inspection.
- Out of the three Set 45 formulations used during the field installation, the Set 45 50/50 Blend is the only one which has not deteriorated since the previous inspection. Both Set 45 Regular and Hot Weather patches have been completely replaced.
- The performance of the ThoRoc 10-60 has not degraded much since the previous inspection. An extra crack has developed on the surface.
- The Duracal patches have not deteriorated since the previous inspection.

Based upon the inspection of the performance of the patches after two winter seasons, it appears that HD-50 and Duracal are the best performing materials. It is recommended that another set of field trials be arranged for SQ-2500, which appears to be a very promising material in terms of the laboratory performance. Rest of the materials have exhibited mediocre performances considering laboratory and field results and are not recommended for further testing.

APPENDIX C. FIELD INSPECTIONS—SUMMER 2010

This appendix describes the details regarding the field performance of the repair patches installed in October, 2007 and thus subjected to 3 winter cycles as well as the performance of only 2-weeks old patches installed in July 2010 (see Chapter 7). These repair patches installed in 2007 were approximately 34 months old at the time of inspection. During these 34 months, the patches were exposed to the regular highway traffic as well as to deicing chemicals and freezing and thawing conditions. Table C.1 has the stationing information for the 2007 patches (similar information for the patches installed in July 2010 is provided in Table C.2).

C.1 PERFORMANCE OF THE HD-50 PATCHES

Figure C.1 shows a view of the HD-50 patch-I. The overall condition of the patch is similar to that observed after 2 winter seasons and this material in general, seems to be performing well. The bond between the material and concrete is also in good condition.

Figure C.2 shows a view of the HD-50 patch-II. This patch is also in good condition and there were no sign of visible cracks.

Figure C.3 shows a view of the HD-50 patch-III. The patch has not deteriorated since the last inspection. The crack that developed after one winter season (near the boundary between the driving and the passing lanes) has not deteriorated further, indicating that the patch is structurally sound.

C.2 PERFORMANCE OF THE SIKAQUICK-1000 PATCHES

A patch of SikaQuick-1000 material which exhibited severe weathering/scaling during the previous (2009) inspections was removed and replaced with different material.

C.3 PERFORMANCE OF THE SIKAQUICK-2500 PATCHES

Figure C.4 shows a view of the SikaQuick-2500 patch-I. The patch had undergone moderate scaling and had multiple cracks on the surface. The poor performance of the patch can be attributed to the improper mix proportioning of the material during the installations. As in the case of SQ-1000, the SQ-2500 patches were installed using the materials with excessive amount of water in the mix. A new patch can be seen near this patch. It should be noted, however, the patch lasted 3 winter seasons, in spite of some cracking that developed during the last 2 years.

The condition of the SikaQuick-2500 patch-II is shown in Figure C.5. As noted during the previous inspection, the patch had developed cracks within two days of installation. This was attributed to improper compaction of the patch, which would have resulted in voids beneath the rebars. These general conditions of the patch have deteriorated further and some portion was replaced with new patching materials as can be seen from Figure C.5.

TABLE C.1
Stationing Information for the Patches on I-65 Bridge Deck

Patch No.	Repair Material	Start Station (ft.)	End Station (ft.)
1	HD-50 patch-I	79	83
2	SQ-2500 patch-I	88	90
3	SQ-1000	111	113
4	HD-50 patch-II	186	187
5	HD-50 patch-III	204	208
6	SQ-2500 patch-II	239	240
7	FX-928 patch-I	353	355
8	FX-928 patch-II	391	394
9	ThoRoc 10-60	440	441
10	SET 45 R	451	453
11	SET 45-50/50 patch-I	458	460
12	SET 45 HW	473	475
13	SET 45 50/50 patch-II	1076	1080
14	Duracal AE	15	19
15	Duracal AE-F	19	23

TABLE C.2
Patches Inspected After 2 Weeks of Installation

Patch No.	Repair Material	Start Station (ft.)	End Station (ft.)	Lane
1	MG-Krete	114	113	Driving lane
2	MG-Krete	133	137	Driving lane
3	Pro-Poxy 2500	253	240	Driving lane
4	Pro-Poxy 2500	263	355	Driving lane
5	Fastrak	331	394	Driving lane
6	Fastrak	339	441	Driving lane
7	Pro-Poxy 2500	376	453	Driving lane
8	Fastrak	394	460	Driving lane

Figure C.1 HD-50 patch-I.

Figure C.2 HD-50 patch-II.

Figure C.3 HD-50 patch-III.

Figure C.4 SikaQuick-2500 patch-I.

Figure C.5 SikaQuick-2500 patch-II.

C.4 PERFORMANCE OF THE FX-928 PATCHES

Figure C.6 and Figure C.7 show the condition of the FX-928 patches during the summer of 2010. Patch-I had not deteriorated since the previous (2009) inspection but some portions of the pavement located near the patch were replaced during 2010 with new material (potentially Pro-Poxy 2500). As noted during the previous inspection, patch-II had undergone more cracking and scaling as compared to 2008 inspection. At the time of current inspections the deteriorated portion of the patch (previously replaced by another repair material (potentially Duracal)) also exhibited some cracks.

C.5 PERFORMANCE OF THE THOROC 10-60 PATCHES

Figure C.8 shows the condition of the ThoRoc 10-60 patch. The patch exhibited two cracks along the direction of the traffic which were first observed during the 2009 inspection. No more cracks formed after that and the overall condition of the patch has not degraded much since the last inspection.

Figure C.6 FX-928 patch-I.

Figure C.7 FX-928 patch-II.

Figure C.8 ThoRoc 10-60.

C.6 PERFORMANCE OF THE SET 45 PATCHES

The SET 45 Regular patch has been completely replaced by another cementitious repair (potentially Duracal) material before 2009 inspection. Figure C.9 shows the patch area originally repaired using SET 45 repair material that has now been replaced by another material which shows some scaling compared to previous inspection.

The SET 45 HW Patch is shown in Figure C.10. Two cracks are visible on the surface but there is no scaling. As shown in Figure C.11 the portion near SET 40-50/50 patch-II is replaced with new patching material but the patch itself was not deteriorated much since the last inspection in 2009. The increased scaling of material is observed but overall the material seems to be holding up very good.

C.7 DURACAL PATCHES ON I-65 NB

Figure C.12 shows the Duracal AE patches which are in good condition.

Figure C.9 Patch area originally repaired with SET 45 Regular material which has been since replaced.

Figure C.10 SET 45 HW.

Figure C.11 SET 45 50/50 patch-II.

Figure C.12 Duracal AE Additional patches inspection.

C.8 NEW PATCHES INSTALLED IN SUMMER 2010

The additional patches which were installed during the summer of 2010 were also inspected at the time of inspection of the 2007 patches. At this time, these new patches were just two weeks old.

The listing of locations of these new patches is given in Table C.2.

Figure C.13 shows the MG-Krete patch which was installed in the summer of 2010. This material looks very good after 2 weeks since placement.

C.8.1 Fastrak Patches

Figure C.14 to Figure C.16 show patches installed using Fastrak material. It was observed that Fastrak material was very cohesive at the time of placement and was very easy to work with. Only one little crack was observed in patch-I during the current inspections of these 2 weeks old patches.

Patches II and III also exhibited some cracking but their overall condition was very good, even at the integrate with the old concrete.

Figure C.13 Mg-Krete patch-I.

Figure C.14 Fastrak patch-I.

Figure C.15 Fastrak patch-II.

Figure C.16 Fastrak patch-III.

C.8.2. Pro-Poxy 2500 Patches

Three patches placed using the Pro-Poxy 2500 material are shown in Figures C.17 through C.19. The finishing of this material was little difficult due to its lower workability and early stiffening tendencies. On the other hand, this material was very cohesive at the time of placement and relatively very easy to work with.

C.9 SUMMARY

This appendix presented the field performance of patches after three winter seasons (for those placed in 2007) and after 2 weeks of service (for those placed in 2010). Some of the general observations related to field performance of these patching materials are presented below:

- The condition of the HD-50 patches has not developed since the previous inspection. All patches appear to be performing well.
- The patches made using the SQ-1000 material were replaced. Although the conditions of the SQ-2500 patches have not worsened since the previous inspection, these patches are in poor condition and may require replaced after the next winter season.

Figure C.18 Propoxy 2500 patch-II.

- The FX-928 patch-I has not visibly degraded since the previous inspection. Portions of the FX-928 patch-II have been replaced by another repair material, indicating that the patch had deteriorated further since the previous inspection.
- As also observed during the previous inspections, patches made with Set 45 50/50 Blend were the only ones which have not deteriorated further. Patches from both, the Set 45 Regular and Set 45 Hot Weather material have been completely replaced.
- The performance of the ThoRoc 10-60 has not changed much from the last inspection.
- The Duracal patches have not deteriorated since the previous inspection.

Based upon the inspection of the performance of the patches after three winter seasons, it appears that HD-50 and Duracal are the best performing materials.

As expected patches installed during summer 2010 did not show any distress after 2 weeks of service except for patches from Zero-C material which was removed after initial installation due to having very low strength. Shortly, all patches made from remaining materials (Fastrak followed by MG-Krete and Pro-Poxy 2500) seemed to be performing well during the first two weeks after installation. However more definite conclusions with respect to performance of these patches can only be reached after they are subjected to at least 1 winter season exposure.

Figure C.17 Propoxy 2500 patch-I.

Figure C.19 Propoxy 2500 patch-III.

APPENDIX D. FIELD INSPECTIONS AFTER FOUR WINTERS (IN SUMMER 2011) OF PERFORMANCE OF REPAIR WORK DONE IN 2007

This appendix describes the details of visual observations to assess the field performance of the rapid-setting repair materials installed as patches in October, 2007. These repair patches were inspected on August 25, 2011, approximately 46 months (four winter cycles) after initial installation. During this period of 46 months, the patches were exposed to the regular highway traffic as well as to deicing chemicals and freezing and thawing conditions. In addition, the patches which were installed during summer 2010 (using four different rapid-setting materials) were also inspected at this time.

D.1 PERFORMANCE OF THE HD-50 PATCHES

Figure D.1 shows a view of the HD-50 patch-I after 4 winter seasons. One small crack is visible on the surface of the patch. The overall condition of the patch is similar to the one observed after 3 winter seasons and the material, in general, seems to be performing very well.

Figure D.2 shows a view of the HD-50 patch-II. This patch is in good condition and did not seem to have changed since the time of last inspections. No visible cracks were observed on the surface of the patch.

Figure D.3 shows a view of the HD-50 patch-III. The condition of the patch has deteriorated slightly since the last inspection. The crack seen in Figure D.3 was also observed during the inspection of 2010, and it does not appear to have changed.

D.1.1 Performance of the SikaQuick-2500 Patches

Figure D.4 shows a view of the SikaQuick-2500 patch-I. The patch had undergone scaling and developed multiple cracks on the surface but did not change significantly since the last inspection performed in 2010.

The condition of the SikaQuick-2500 patch-II is shown in Figure D.5. The deteriorated portion of the patch was replaced with Pro-Poxy 2500 in 2010 and the construction joint is visible in the figure.

D.1.2 Performance of the FX-928 Patches

Figure D.6 and Figure D.7 show the conditions of the FX-928 patches. The condition of patch-I (Figure D.6) has not changed since the previous inspection performed in 2010. The adjacent

Figure D.1 HD-50 patch-I.

Figure D.2 HD-50 patch-II.

Figure D.3 HD-50 patch-III.

Figure D.4 SikaQuick-2500 patch-I.

Figure D.5 SikaQuick-2500 patch-II.

Figure D.6 FX-928 patch-I.

Figure D.7 FX-928 patch-II.

portion, which was replaced with Pro-Poxy 2500 seem to have deteriorated. The concrete near this replaced section appears to have been replaced with asphalt concrete (Figure D.6).

As noted during the previous inspection patch-II (Figure D.7) had not undergone any more cracking and the deteriorated portion of the patch (which has been replaced with another repair material (potentially Duracal)) exhibited cracks.

D.1.3 Performance of the ThoRoc 10-60 Patches

Figure D.8 shows the condition of the ThoRoc 10-60 patch. The patch exhibited two cracks along the direction of the traffic. Since the previous inspection in 2010, these cracks did not deteriorate further. Also, the overall condition of this patch has not changed much since the last inspection in 2010.

D.1.4 Performance of the SET 45 Patches

The SET 45 Regular patch had undergone severe deterioration prior to the previous inspection, and portions of the patch had been replaced by asphalt concrete. By the time of the 2010 inspection this patch has been completely replaced by another cementitious repair (potentially Duracal). Figure D.9 shows the original SET 45 Regular patch area that has now been replaced by another material.

Figure D.10 shows SET 45 HW patch which did not deteriorated further since the last inspection. Also, these cracks which were observed during the last inspection appear to look the same. The condition of SET 45 50/50 patch-II also did not change since the last inspection (see Figure D.11).

D.2 Field Inspection of 2010 Patches

This section describes the visual observations of the patches which were installed during summer of 2010 with different rapid-setting materials. The patches are listed in Table D.1.

D.2.1 MG-Krete Patch I

Figure D.12 shows the patch-I with MG-Krete which was placed in summer 2010. This material has exposed to different weather conditions including exposure to deicing chemicals and looks very good after 1 winter cycle. Figure D.13 shows MG-Krete patch-II which exhibited some cracking but areas which have no cracks look good.

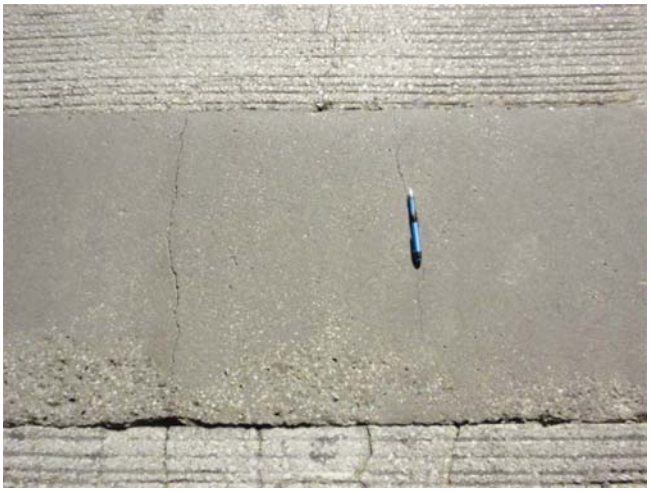

Figure D.8 ThoRoc 10-60.

Figure D.9 SET 45 R patch area.

Figure D.10 SET 45 HW.

D.2.2 Zero C Materials

The patch with Zero C material was replaced with asphalt concrete due to early deterioration of this material (see Figure D.14). This deterioration could be due to very low strength after 1 day of placement. This mixture did not gain sufficient strength in field as well as laboratory.

TABLE D.1
Patches Installed Summer 2010

Patch No.	Repair Material	Start Station (ft.)	End Station (ft.)	Lane
1	MG-Krete	114	113	Driving lane
2	MG-Krete	133	137	Driving lane
3	Asphalt patch	214	208	Driving lane
4	Propoxy	253	240	Driving lane
5	Propoxy	263	355	Driving lane
6	Fastrak	331	394	Driving lane
7	Fastrak	339	441	Driving lane
8	Propoxy	376	453	Driving lane
9	Fastrak	394	460	Driving lane

Figure D.11 SET 45 50/50 patch-II.

Figure D.12 MG-Krete patch-I.

Figure D.13 MG-Krete patch-II.

Figure D.14 Asphalt concrete in place of Zero C materials.

Figure D.16 Propoxy 2500 patch-II.

D.2.3 Patches with Propoxy 2500

Figure D.15 shows the patch-I with Propoxy 2500 after 1 year of placement and thus exposed to deicing chemicals and low temperatures during one winter season. It really looks excellent with no cracks. The little rough surface is observed which is due to early setting time of this material. Overall this patch looks good. Patch-II also looks good as can be seen from Figure D.16 The third patch of Propoxy is replaced partially with asphalt concrete (see Figure D.17).

D.3 SUMMARY

This appendix presented the details of field performance of the patches after four winter seasons for those patches which were placed in 2007 and after 1 year for those placed in 2010. Some general discussions about the performance of these patching materials are presented below:

- The condition of the HD-50 patches has not deteriorated even after 4 winter seasons indicating very good performance. All the patches appear to be performing in satisfactory condition.
- The conditions of the SQ-1000 worsened and therefore were replaced. The SQ-2500 patches have shown little more scaling as compared to the previous inspection. These patches are in poor condition and may require replacement before the winter season. The poor condition of the patches is attributed to the inconsistent mix-proportioning during placement. These patches had excessive water in the mix.
- The condition of FX-928 patch-I has not visibly degraded since the previous inspection.
- Out of the three Set 45 formulations used, the Set 45 50/50 Blend is the only one which has not deteriorated since the previous inspection. Both Set 45 Regular and Hot Weather patches have been completely replaced.
- The performance of the ThoRoc 10-60 has not degraded much since the previous inspection. An extra crack has developed on the surface.
- The Duracal patches have not deteriorated since the previous inspection.

Based upon the field inspection of the patches, the performance of HD-50 and Duracal materials appear to be the best after 4 winter cycles.

For the patches which were installed during the summer of 2010, the following conclusions can be made based on 1 year performance:

- Zero-C material from BASF which was removed after initial installations due to very low strength and even did not perform well during the second placement. This material does not have good early strength. Also it was difficult to mix it, especially, in larger quantities.

Figure D.15 Propoxy 2500 patch-I.

Figure D.17 Propoxy patch-III.

- The field performance of Fastrak materials was good after 1 winter. The ease of use as well as the testing of field specimens in laboratory indicated very good performance for this material.
- MG-Krete and Propoxy 2500 also exhibited good performance after one winter season as these patches were found to be in good conditions except one of the patches of Propoxy 2500 which was replaced with asphalt concrete.

About the Joint Transportation Research Program (JTRP)

On March 11, 1937, the Indiana Legislature passed an act which authorized the Indiana State Highway Commission to cooperate with and assist Purdue University in developing the best methods of improving and maintaining the highways of the state and the respective counties thereof. That collaborative effort was called the Joint Highway Research Project (JHRP). In 1997 the collaborative venture was renamed as the Joint Transportation Research Program (JTRP) to reflect the state and national efforts to integrate the management and operation of various transportation modes.

The first studies of JHRP were concerned with Test Road No. 1—evaluation of the weathering characteristics of stabilized materials. After World War II, the JHRP program grew substantially and was regularly producing technical reports. Over 1,500 technical reports are now available, published as part of the JHRP and subsequently JTRP collaborative venture between Purdue University and what is now the Indiana Department of Transportation.

Free online access to all reports is provided through a unique collaboration between JTRP and Purdue Libraries. These are available at: http://docs.lib.purdue.edu/jtrp

Further information about JTRP and its current research program is available at: http://www.purdue.edu/jtrp

About This Report

An open access version of this publication is available online. This can be most easily located using the Digital Object Identifier (doi) listed below. Pre-2011 publications that include color illustrations are available online in color but are printed only in grayscale.

The recommended citation for this publication is:

Ram, P. V., J. Olek, and J. Jain. *Field Trials of Rapid-Setting Repair Materials.* Publication FHWA/IN/JTRP-2013/02. Joint Transportation Research Program, Indiana Department of Transportation and Purdue University, West Lafayette, Indiana, 2013. doi: 10.5703/1288284315185.